NASA Contractor Report 189705

$p.95$

Aircraft IR/Acoustic Detection Evaluation

Volume 2 - Development of a Ground-Based Acoustic Sensor System for the Detection of Subsonic Jet-Powered Aircraft

Robert E. Kraft

General Electric Aircraft Engines
Cincinnati, Ohio

McDonnell Douglas Corporation
Douglas Aircraft Company
Long Beach, California

N95-28073

Unclas

0051307

G3/71

(NASA-CR-189705-Vol-2) AIRCRAFT IR/ACOUSTIC DETECTION EVALUATION. VOLUME 2: DEVELOPMENT OF A GROUND-BASED ACOUSTIC SENSOR SYSTEM FOR THE DETECTION OF SUBSONIC JET-POWERED AIRCRAFT (Douglas Aircraft Co.) 85 p

Date for general release December 31, 1994

TABLE OF CONTENTS

LIST OF ILLUSTRATIONS

NOMENCLATURE

AG	Array-gain, dB
AGL	Above Ground Level
A_j	Amplitude of jth background noise source
AVESPL	Average Sound Pressure Level, dB
BW	Array processing frequency bandwidth, Hz.
c	Speed of sound, m/sec
CSD	Cross-Spectral Density
d	Array sensor spacing, m.
d'	Detector performance index from Receiver Operating Characteristic curves
DI	Array directivity index, dB
DT	Detection threshold, dB
$D(\theta,\phi)$	Array directivity in θ,ϕ direction, dB
f	Frequency, Hz.
FFT	Fast Fourier Transform
$G(\phi,\omega)$	Angular distribution function of background noise sources
$J_0(x)$	Zero order Bessel function of first kind
k	wavenumber, ω/c, 1/m.
M	Summation limit for array cross-spectral density
NB	Number of beams
NL	Background noise level, dB
NS	Number of sensors in array
NSRC	Number of sources used in coherence computation

R	Horizontal range, meters
RS	Received Signal, dB
RSN	Required signal-to-noise-ratio for detection, dB
S/N	Signal-to-noise-ratio, dB
T	Integration time, seconds
T_c	Time for target to cross beam, seconds
V	Aircraft speed, meters/sec.
γ	Ratio of specific heats
$\delta(x)$	Dirac delta function
$\Delta\phi$	Beamwidth, radians
θ	Beam direction angle from vertical, radians or degrees
λ	Acoustic wavelength, m.
ρ_n	Background noise spatial coherence
ϕ	Beam direction azimuthal angle, radians or degrees
ω	Circular frequency, $2\pi f$, radians/sec.

Development of a Ground-Based Acoustic Sensor System for the Detection of Subsonic Jet-Powered Aircraft

1 Introduction

1.1 Acoustic Detection Systems

The use of electronic acoustic sensor arrays as passive detection devices for both underwater and atmospheric purposes has been known for well over 50 years. The art and technology of acoustic sensor array design is particularly well-developed for application to underwater detection purposes[1]. Although much of the technology and many of the concepts used for underwater acoustics are directly applicable to the atmospheric propagation case, atmospheric acoustic detection presents a number of unique problems requiring special design consideration.

In particular, the background noise environment, the acoustic propagation effects, and the nature of airborne targets are different in character from those considered in underwater acoustics. The effect of wind, in particular, must be considered in the atmosphere. Airborne targets have characteristic noise signatures and may have flight speeds that approach the speed of propagation of sound, requiring special processing and operational techniques for atmospheric acoustic detectors. Atmospheric sound absorption and ground effects, although having analogues in underwater acoustics, have different dependence on frequency.

1.2 Basic Equations of Acoustic Detector Performance

The purpose of this section is to provide a basic introduction to the parameters affecting acoustic detection system performance. Those already familiar with the Sonar Equation and its components may wish to skip forward to the next section.

A first order estimate of acoustic detector performance and a fundamental formula for design development and evaluation is the Sonar Equation, given, in dB units, by[2]:

$$RSN \equiv RS - NL = DT - DI \qquad (1)$$

where

RSN = required signal-to-noise-ratio for detection, dB

RS = received signal, dB

NL = ambient noise level at sensors, dB

DT = detection threshold, dB

DI = array directivity index, dB

Each of these terms can be split into several components. Each component has a particular effect on sensor system design and performance, and each will be considered in turn.

The received signal, RS, is composed of the signal level generated at the source (at a reference radius of 1 meter) minus the transmission loss suffered during propagation. The transmission loss is composed of spherical spreading, atmospheric absorption, and extra attenuation due to diffraction, refraction, turbulence, and ground effects. Perhaps the best understood of these extra attenuation effects, particularly for long range propagation, are those due to the presence of the ground surface.

The ambient noise level at the sensors depends upon the environmental conditions. This can generally have a wide variation, depending on weather conditions and the amount of noise-making activity in the vicinity (rural, suburban, urban, etc.). Data on typical ambient noise conditions is not as plentiful as might be expected, particularly in the form needed for adequate detector design.

The detection threshold, DT, depends on desired probability characteristics of the detector operation and the frequency bandwidth and integration time of the signal processing. The detection process is assumed to be an unknown broadband signal in a gaussian noise background. The detection threshold can be expressed in dB units as

$$DT = 5 \log_{10}(d') - 5 \log_{10}(BW*T) \qquad (2)$$

where d' is the detector performance index obtained from the Receiver Operating Curves[3], BW is the frequency bandwidth, and T is the integration time. It is assumed that the signal bandwidth has been chosen such that it is equal in width to the background noise bandwidth and that the signal endures for the entire integration time T. The time-bandwidth product term can be considered as a signal processing gain for the detector, as distinguished from the array processing gain to be discussed below.

The value of detector performance index depends on the desired probability of detection and probability of false alarm for each detection event. For instance, if a probability of detection of 50% and a probability of false alarm of 0.1% is desired, then d' = 10.1, and 5*log(d') = 5.02. This means that an additional 5.0 dB must be included in the level that gives a positive detection to guarantee the desired probabilities of detection and false alarm.

The array directivity index is generally a complicated function of the array signal processing algorithm, the nature of the received signal itself, the nature and level of the background noise, the array geometry, and the array beam directivity in a given direction. It is thus impossible to calculate precisely in the general case. An approximate formula for directivity index, adequate for preliminary design, is

$$DI = AG - D(\theta,\phi) \qquad \textbf{(3)}$$

where AG is the array gain and $D(\theta,\phi)$ is the directivity in the (θ,ϕ) direction, where θ is the elevation angle and ϕ is the azimuthal angle. $D(\theta,\phi)$ is normalized such that it is zero in the direction of maximum gain.

The array gain, AG, is, to a first approximation, a function of the number of sensors in the array, the sensor-to-sensor coherence of the received signal, and the sensor-to-sensor coherence of the background noise. If we assume the coherence of the received signal across the array is 100%, the array gain is given by

$$AG = 10 \log_{10}\left[\frac{NS}{1 + (NS-1)\rho_n}\right] \qquad \textbf{(4)}$$

where NS is the number of sensors and ρ_n is the background noise coherence.

Little is known about the nature of the coherence of the background noise. It should be a function of frequency, spatial separation, and environmental conditions. Very little useable data was found. An analytical evaluation, based on some previous work in underwater ambient noise, will be presented below.

The foregoing relationships will be used as the basis for the detection system design and its performance evaluation. More detailed discussions of the Sonar Equation and its constituents can be found in Reference 2 or in Kinsler and Frey[4].

1.3 Importance to Detection Range Study

In order to predict the acoustic detection range of a jet-powered aircraft at a given flight condition it is necessary to postulate the performance characteristics of the acoustic sensor system that will be doing the detection. Although it would have been preferable that the detection system definition be provided as input to the detection range study, accepted standard definitions of acoustic detection systems are not yet available. Therefore, it is necessary to develop this definition as part of the overall study.

The performance of the detection system contributes directly to the determination of the signal-to-noise ratio at which a detection of the target occurs. Given a background noise level, the received target signal level is a function of the range from the target to the receiver. The received signal level decreases (suffers transmission loss) due to spherical spreading, atmospheric absorption, and effects of excess attenuation. If the ray path is close to grazing incidence to the ground, then the ground effects become significant over long ranges.

1.4 Operational Objectives

The operational objective of the acoustic detection system is, most simply, to provide an alert to an area defense system that a target has been detected within the detection range from the known sensor location. The particular use made of this information to intercept and neutralize the target is subsequent to the acoustic detection and not considered specifically in the acoustic detection system design (although a proper and complete design procedure would certainly do so). It is assumed that the acoustic system is a *cuing* system, as opposed to a tracking or weapon terminal guidance system.

Although a simple detection is the most fundamental manifestation of the acoustic detection system, further information such as rough bearing to the target is both feasible and desirable. Given multiple sensor sites of known geographical location and orientation, target tracking is possible through triangulation.

The key operational objective of the postulated acoustic detection system design is that it be *reasonable, practical, and technically defendable*. Since the performance of the proposed design will not be field-demonstrated, the performance estimates will tend to be conservative. If the predicted performance of the acoustic detection system is not accepted, the results of the detection range predictions for the overall study will also be open to question.

1.5 Design Ground-Rules and Guidelines

The acoustic detection system is assumed to be ground-based, that is, part of an area defense system set up to guard a region of friendly territory. Each sensor array will most likely be permanently situated, although mobile (portable) array systems are not implausible. Each individual sensor array site may be part of a larger network of arrays providing wide-area coverage. It is assumed that each array site is in continuous and immediate communication with a Command and Control Center.

An alternative use of the acoustic detector would be as a localized, autonomous, isolated system. The acoustic detection would provide a rough bearing, which would then be handed over to a visual or IR system for improved weapon lock-on and launch.

The detection system will be assumed to operate in passive mode, due to the extreme energy and large inherent time delays associated with active acoustic systems in the atmosphere. Since the detection system is passive, and can easily be camouflaged, it is assumed that the target is unaware of its state of detection.

The system will be designed specifically for the purpose of detecting low or high altitude subsonic jet aircraft. Although it may successfully detect other vehicles, such as helicopters or ground vehicles, it will not be optimized for this purpose. The system as designed, however, will not distinguish between a jet aircraft or any other type of target vehicle that may generate sufficient energy in the same detection passband to be detected.

A strong driver in the design is simplicity. Large numbers of sensors and complex, unproven signal processing algorithms are avoided. A goal is to achieve the design with about five sensors in the array. The signal processing must be well within the capability of current off-the-shelf solid-state devices. By keeping the design simple, it will be practical, deployable, and inexpensive.

Compactness of the array overall dimensions is a desirable trait. Design goals are to achieve less than about two meters in maximum extent. A system of this size could be pre-assembled and self-contained, with built-in electronics and communications. Installation would consist of preparing the site, aligning the device on and fixing it to the mounting pad, and turning it on.

It is assumed that the detection system designer has a fairly sophisticated knowledge of the character of source noise signatures of "typical" attack or penetration jet aircraft and the relevant propagation phenomena. This knowledge is available in the open literature, and may be enhanced by test data acquired from friendly aircraft of similar design.

The detection system will be designed to attempt to meet the following objectives:

1) Provide 100% area coverage over protected territory.

2) Provide target localization within a desired 10 km detection range radius for each sensor array.

3) Provide detection updates over the entire spatial range of coverage for each array at least every five seconds, preferably every second.

4) A hemispherical directivity pattern is desired, with only small decreases in directivity at grazing angles to the ground.

1.6 Issues Not Considered in Detector Design

Due to the limited scope of the study, certain assumptions, simplifications, and restrictive conditions had to be invoked. Some of these are:

1) The effects of acoustic refraction due to atmospheric wind or temperature gradients are ignored. Effects of atmospheric turbulence are ignored.

2) Standard day atmospheric conditions are assumed. No studies are made of the effects of different weather conditions.

3) The logistics and cost of deploying, maintaining, and protecting a network of acoustic sensor systems is not considered.

4) Effects of variable terrain or foliage are not considered. The ground surrounding the array is assumed to be flat and of constant acoustic impedance.

5) Deterioration of effectiveness when some sensor sites become inoperative is not considered. Likewise, effects of loss of individual sensors in an array is not considered. Adequate reliability or redundancy is assumed.

6) The engineering issues of providing electrical power to the device, weather-proofing, protection from animals or vandalism, wind noise protection, monitoring system operational state, sensor calibration procedures, and maintenance are not considered here.

2 Representative Aircraft Target Definition for Design

2.1 Aircraft Performance and Mission Assumptions

The aircraft target is modelled after a lightweight, single-engine attack aircraft, roughly representative of the F-16 class. A high-performance engine with no acoustic suppression features is assumed. The jet exhaust nozzle is of variable area converging-diverging type. The primary mission considered is low-altitude penetration, 61 meters AGL, at Mach 0.8, straight and level flight.

The following list of conditions is assumed to hold:

<u>Atmosphere</u>:

   Ambient Temperature = 287.8 °K (14.6 °C)

   Ambient Pressure = 100,580 nt/m²

   Relative Humidity = 70.0%

   Speed of Sound = 340.3 m/sec

<u>Aircraft</u>:

   Speed = Mach 0.8 (252.9 m/sec)

   Physical Nozzle Throat Area (A8) = 0.28 m²

   Nozzle Exit Area (A9) = 0.33 m²

   Exhaust Gas Total Temperature = 833.3 °K

   Nozzle Pressure Ratio = 4.0

   Fuel-Air-Ratio = 0.015

   Exhaust gas γ = 1.37

It is assumed that jet exhaust noise is the dominant noise source, and that the jet noise directivity is unaffected by the airframe (no installation effects). For ranges of propagation in excess of several kilometers, the higher frequency turbomachinery noise will be absorbed to a much greater extent than the low frequency jet noise; thus, the jet noise will dominate the received signal.

The jet noise is assumed to exceed the airframe noise, although this may not be true at all radiation angles at this aircraft speed. As a conservative estimate, airframe noise is omitted for purposes of detection system design.

2.2 Representative Target Acoustic Signature

The jet noise signature at the source was obtained using the jet exhaust noise prediction procedure due to Stone[5]. This is a semi-empirical model that includes the spectra and directivity for both jet mixing and jet shock noise sources. It incorporates the effects of forward motion on radiated noise spectrum and directivity, although the forward motion effects model may be extended beyond the model's empirical range of validity. Doppler shifts due to relative motion between source and receiver are included.

Based on the parameters listed in the previous section, the jet noise spectrum (at the source) was calculated. The spectrum at an equivalent distance of 1 meter from the source, radiated at 90 degrees to the jet forward axis is shown in Figure 1. This is the source spectrum used for the sensor system design.

Take note that the aircraft noise spectrum is being used as a representative target signal for sensor system design. When the sensor system is designed and its performance is specified, more accurate noise source models may be used to determine detection ranges for particular targets. Holding the detection system performance parameters constant, studies can be made of detection range sensitivities to variations in source level or propagation effects.

3 Atmospheric Propagation and Ground Effects Models

3.1 Atmospheric Propagation Model

Two effects included in the atmospheric propagation other than ground effects are spherical spreading and atmospheric absorption. Atmospheric absorption, a function of frequency, temperature, and relative humidity, is based on the model of ANSI S1.26-1987[6].

3.2 Ground Effects Propagation Model

When the sound wave propagates from source to receiver at near grazing incidence angle to the ground (below roughly 15 degrees angle of elevation), additional transmission loss (or amplification) effects occur due to the presence of the ground surface. The ground surface will normally have a finite, but relatively high, complex value of surface impedance. A locally reacting surface is assumed.

For propagation over long ranges with the receiver sensors close to or on the ground surface, the ground effect can be significant. Little measured data exists for the development of empirical models or substantiation of theoretical models for this effect. A theoretical model was used for this study, under the assumption that the inclusion of at least an approximate correction for ground effects was important. It should be remembered that the model is not validated by test data for long range propagation.

The ground effects analysis due to Chien and Soroka[7] was coded for this purpose. Figure 2 shows a sample computation from the program, showing the "extra ground attenuation" as a function of frequency for source at 61 meters altitude, receiver on the ground surface, and ground impedance typical of grassland, for various propagation ranges. Figure 3 shows results similar to Figure 2 but with the receiver 1.8 meters above the ground surface. Note the rapid increase in attenuation in both cases above a frequency of about 30 Hz.

The acoustic impedance used in these calculations, taken from a model by Thomasson[8], is shown in Figure 4. The parameters used in the model are those for a typical grass surface. No studies were made in which surface impedance was varied.

4 Preliminary Design of Detection Sensor System

4.1 Acoustic Detection System Design Alternatives

An almost unlimited range of alternatives exist for the design of an acoustic detection system, ranging from extremely simple to highly complex. A brief review of these choices will be presented to motivate the design path finally selected.

Probably the simplest choice, and that requiring no hardware at all, would be to station a human listener at the detection site. Aural detection is amazingly effective, but subject to numerous human factor and psychoacoustic effects that tend to deteriorate system performance or at least make the performance level highly variable. Human listeners are subject to lapses in concentration, confusing effects such as echoes, and would require training to increase efficiency. Maintenance of a continuously manned detection site might cost more than if it were a simple electronic system.

A single, isolated microphone is the simplest electronic system imaginable. The electronic microphone would have the edge over a human listener in continuous reliability of performance (assuming a reliable power source). Both are subject to the effect of background noise variations.

A small, compact array of microphones is the design approach selected for this study. It offers relative simplicity, steady performance, and an improvement in required S/N over aural detection.

At the other extreme are large, possibly three-dimensional, arrays of microphones in complex geometric patterns that can form narrow beams in arbitrary directions and sweep these beams through space. Special high-resolution beamforming can be used to further increase the array gain in specified direction, at the expense of processor time and power. Adaptive array processing could be used to reject extraneous known noise source coming from specific directions.

Not only is the design of the more complex systems beyond the scope of this study, the predicted but unverified performance of such a system would be subject to controversy. The more complex system would be more expensive to procure and maintain, thus inhibiting its widespread deployment. Such systems, however, are within the current state-of-the-art, and await development.

4.2 Initial Design Goals and Assumptions

Design objectives for the initial acoustic sensor system design were the following:

1) Aim for detection ranges on the order of 10-20 km. in median background environments.

2) Use at most five sensors in the array in an arrangement that provides spatial coverage that is nearly omnidirectional (hemispherical), with small directivity loss at grazing angle.

3) Use an extremely simple data processing algorithm---square law detector with at most a single, vertically-oriented beam.

4) Design an array of one meter or less in extent.

In retrospect, these design goals were slightly over-ambitious. The primary shortcoming of the design, it will be seen, is an inability to provide the desired detection range. The primary reason for this deficiency turns out to be array gain losses due to background noise sensor-to-sensor coherence at the necessarily close sensor spacing (0.1 wavelength).

For this initial design, some of the input parameters were slightly different from those adopted for the final, more refined, design. Aircraft jet noise parameters that are different in the preliminary case are C-D nozzle exit area A9, taken to be 0.29 m^2, aircraft altitude, taken to be 300 meters, and exhaust total temperature, taken to be 1111 °K. These were later refined to 0.33 m^2, 61 meters, and 833 °K, respectively, for the final design.

The sensor-to-sensor coherence of the background noise was initially estimated to be 25%, which was later shown very likely to be too low. Assumptions for standard background levels were also refined based on additional data acquired after the preliminary design was completed.

4.3 Array Design Procedure

A rough procedure for the preliminary design of a detection array consists of the following steps:

1) Choose the number of sensors in the array.

2) Choose the array geometric configuration.

3) Estimate the received signal at different ranges.

4) Assume background noise levels and spatial coherence.

5) Determine the "optimum" detector bandwidth.

6) Determine the sensor spacing for adequate grazing angle directivity.

7) Choose an integration time based on expected event duration, maximizing gain, and desired detection repetition rate.

8) Choose the signal processing algorithm.

11

9) Determine the detection threshold from the desired Receiver Operating Characteristic (ROC) curves, bandwidth, and integration time.

10) Determine the Signal-to-Noise-Ratio (S/N) using the detection threshold and array gain.

It is assumed that the signals from all sensors are processed simultaneously, to form a single beam, the objective being to make the beam as omnidirectional as possible. Various other secondary parameters, such as the height of the array above the ground, may also be considered in the design process.

Several iterations of the above steps may be required to achieve an acceptable design. Detection system design is, in fact, an extremely complex process, with many interacting variables. Although it will not be explained in detail, Figure 5 is an attempt to produce a flow chart of the detector design process, illustrating this complexity.

4.4 Five-Sensor Planar Arrays

A planar array is such that all sensors are located in the same two-dimensional plane, but not necessarily in a linear arrangement. Planar arrays have been the subject of extensive study in underwater acoustics[9,10]. In particular, we will consider 5-sensor planar arrays arranged in either of two patterns: Mills Cross or Pentagon (Circular), as shown in Figure 6.

The directivity patterns of the Mills Cross and Pentagon Array arrangements as a function of sensor spacing to wavelength ratio (d/λ) are very similar, with the Mills Cross having a slight advantage. The directivity pattern for the Mills Cross can be expressed in functional form as

$$D(f,\theta,\phi) = 2 \cos\left(2\pi \sin(\theta) \cos(\phi) \frac{d}{\lambda}\right) + 2 \cos\left(2 \sin(\theta) \sin(\phi) \frac{d}{\lambda}\right) + 1 \tag{5}$$

Figure 7 illustrates the directivity pattern for a Mills Cross in the vertical angle, θ, and azimuthal angle, ϕ, for several values of d/λ. Note that for d/λ = 0.25, the pattern is nearly azimuthally symmetric, and the loss in directivity at grazing angles is less than 5 dB. (The vertical angle θ is the angle from the normal to the surface to the desired direction, and is the complement of the elevation angle, the angle up from the ground plane to the specified direction.)

The next step is to choose an optimum signal processing bandwidth. Two opposing effects are in confrontation here. First, the wider the bandwidth, the higher the array gain (assuming equal signal and noise bandwidths). But, the wider the bandwidth, the more the deviation from the design value of d/λ. The quantity to be maximized is the signal-to-noise-ratio, (S/N), which must be obtained by comparing the received signal at a given range to the assumed background noise spectra.

The first component in the received signal, RS, is the source spectrum. Figure 8 shows the jet mixing, jet shock, and overall jet noise levels at 1 meter from the source at 90 degrees to the inlet. Note that the jet mixing noise is the dominant component in the 50 to 200 Hz. range.

The second component of RS, the transmission loss TL is composed of spherical spreading, atmospheric absorption, and ground effects. Spherical spreading follows the standard inverse square law. The effect of atmospheric absorption (alone) on the transmitted source spectrum is illustrated in Figure 9, which shows the remaining SPL after propagating over various distances. Note that the atmosphere acts like a very effective low-pass filter above about 200 Hz.

The final transmission loss effect is that of ground attenuation, which must be included because of the low elevation angle of propagation (angle from the vertical of nearly 90 degrees). Figure 10 give an indication of the magnitude of the ground effect over grassland for three different ranges. Note that the signal is amplified below about 40-60 Hz.

The next step is to compare the received signal to the ambient background level. The signal spectra received at 10 km. and 20 km. ranges are compared to three background levels[11] in Figure 11. By inspection, it is obvious that the maximum S/N for all combinations of received signal and background level will occur somewhere near the 50-200 Hz. band.

In order to find the passband that optimizes the S/N over various combinations of range and background level, the S/N was calculated while the upper and lower band edges were varied parametrically. The results of this study indicated that the passband that includes the 100 Hz. and 160 Hz. 1/3 octave bands gives a useful compromise in maximizing S/N over the variety of conditions. Thus, a narrowband bandwidth of 90 Hz., between a lower frequency of 90 Hz. and an upper frequency of 180 Hz. was chosen for detector design.

At this point, a sensor spacing, d, can be selected. The array geometry has been chosen as a 5-sensor Mills Cross, and the median frequency for the design bandwidth is 125 Hz. At this frequency, the wavelength, λ, is 2.7 meters. Choosing a d/λ of 0.1 gives a directivity loss of only 0.7 dB at grazing elevation angles. Thus, we have d = 0.27 meters, and a total array extent of about 0.62 meters. A probability of detection of 50%, a probability of false alarm of 0.1%, and an integration time of 1 second were chosen to characterize detector operation.

The choice of 1 second integration time is based on several considerations. First, the integration time must be short enough that the signal remains relatively steady over its duration. Examination of time histories of long propagation range aircraft noise show amplitude envelope modulations with a period on the order of 1-5 seconds. Second, the integration time should be as long as possible to obtain the maximum time-bandwidth gain. Finally, the Command and Control Center may require regular detection updates at intervals that best integrate the acoustic system into the overall threat interdiction network.

Given the chosen parameters, we can determine the acoustic detection system performance as follows:

$$AG = 4.0 \text{ dB (for 5 sensors and 25\% background coherence)}$$

Directivity loss at grazing angle $= -0.7$ dB

$$DI = 4.0 - 0.7 = 3.3 \text{ dB}$$

$$5*\log(d') = 5.0 \text{ dB}$$

$$5*\log(BW*T) = -9.8 \text{ dB}$$

$$DT = 5.0 - 9.8 = -4.8 \text{ dB}$$

and, thus, the required S/N for detection is

$$RSN = DT - DI = -4.8 - 3.3 = -8.1 \text{ dB}$$

Based on the background noise data shown in Figure 11, in the 90-180 Hz. band the following background noise levels are obtained:

Low suburban: NL = 31.3 dB

Median suburban: NL = 45.6 dB

High suburban: NL = 61.8 dB

Therefore, the required received signal level for a positive detection in the 90-180 Hz. frequency band with 1 second integration is:

Low background: RS = 23.3 dB

Median background: RS = 37.6 dB

High background: RS = 53.7 dB

These values provide the criteria needed to determine detection range.

4.5 Estimated Detection Range Performance

The detection ranges predicted under these conditions for the aircraft source for the three background levels are shown in Figure 12. Note the extreme variation in detection range with background level. The desired 10 km. detection range is achieved over a range of aft angles of about 40 degrees for the median background level, but the detection range never exceeds 5 km. at the high background levels.

Figure 13 shows an analysis of the detection range in the form of a detection footprint in the horizontal plane for median background level. Note that at a closest approach distance to the array of 9 km, the aircraft will remain detectable for about 10.5 seconds.

Also noted on this chart are the positions of the aircraft relative to the location at which the sound was emitted for sound rays radiated at the 40 degree azimuth angle (received at time t_1) and the 120 degree azimuth angle (received at time t_2). This illustrates the effect of the propagation distance time lag.

4.6 Problems with the Preliminary Design

One very serious flaw exists with the foregoing development. It was assumed, without data to verify the assumption, that the sensor-to-sensor coherence of the background noise would be about 25%. Subsequent analysis, to be examined in the next section, shows that, at a d/λ of 0.1 at 125 Hz., the coherence is likely to be much higher than this value, probably above 90%. The array gain will deteriorate by about 4 dB, cutting the detection ranges roughly in half.

Considering that the detection ranges were already at the lower end of the desired values, it was decided to pursue an improvement to the design. First, however, an acceptable model for background noise coherence is required.

In addition to this change, several other refinements in noise source modelling and background noise were incorporated.

5 Ambient Noise Environment Studies

5.1 Availability and Validity of Background Noise Data

The extreme sensitivity of the acoustic detector performance to the background noise level has been illustrated in Figure 12, where the peak detection ranges were shown to vary from 5 to 25 km. from low to high background environments. There is surprisingly little measured background noise data available for various environments, and that which is available is not completely useful in that the conditions under which the measurement was performed are not documented (or reported) with the thoroughness required for this study.

A key parameter not usually recorded is the wind velocity. Wind noise can be a dominant contributor to background noise at low frequencies, either through self-noise of the microphone or from wind noise generated on nearby foliage or structures. The variability in the effectiveness of wind screens makes different measurements under the same environment not comparable. More experimental control and understanding of wind noise is required.

The exact nature of the environment itself is seldom thoroughly documented. The same "environment" is likely to undergo wide variations in level with time of day, weather conditions, etc. Although a "mean" level may be defined for such an environment, it is also necessary to provide some of the statistics of variation of the noise levels over time, as a function of frequency.

Background noise is usually measured in 1/3 octave bands, under the assumption that it is broadband in nature. These measurements may hide tones which are more properly associated with interfering sources than with background noise. Special adaptive array processing techniques could be used to extract relatively stationary discrete interfering sources, thus improving array performance. For this reason, background noise measurements should be made in narrowbands so that tones may at least be identified, if not extracted.

A key background noise parameter not usually measured is the spatial coherence of the sound field. This, however, is a critical parameter for array design. This is not a simple measurement, requiring deployment of an array of variably-spaced microphones and a fair amount of data-processing. Analytical models of background noise spatial coherence are in acute need of experimental verification.

A thorough and more useful measurement of background noise would require the following test procedures:

1) Continuously monitor the wind velocity and provide means of correlating wind velocity with measured level.

2) Describe the design and performance of any microphone wind screens used.

16

3) Provide a continuous monitoring of environmental conditions along with time of day, including occurrence of identifiable noise sources (vehicles, machines, etc.)

4) Reduce the data in narrow bandwidths. Examine the data for recurrent tonal content. Examine the standard deviation of the measured levels over periods of time. Separate random variation from identifiable trends.

5) Measure background noise using arrays with variable sensor spacing to obtain spatial correlation properties of the noise field. This will also assist in the identification of tonal interfering noise sources.

Information from tests adhering to the above procedures is critical for the accurate prediction of acoustic detector performance potential, as well as for system design. The testing, although extensive, is relatively simple and inexpensive in nature.

5.2 Existing 1/3 Octave Band Background Noise Data

Incompletely documented 1/3 octave band ambient noise measurement data, although not abundant, is available from several sources. In addition to the Lockheed report, Reference 11, test data has been provided to the author by Arnold Mueller of NASA Langley, some curves are published in Harris[12], and GEAE has made ambient noise measurements during static engine testing at Edwards Air Force Base and at the Peebles Test Operation Site.

Figure 14 shows unclassified data extracted from the Lockheed report, and Figure 15 shows data from the U.S. Army Air Mobility Research and Development Laboratory (USAAMRDL)[13]. For the 125 Hz. 1/3 octave band, levels range from a low of about 27 dB to a high of 75 dB.

As an alternative means of examining the existing data, 38 different sets of 1/3 octave band measurements were accumulated from the sources mentioned above, without regard to whether the data was from "low", "median", or "high" environments. Using this data, averages and standard deviations were calculated from the data in 1/3 octave bands from 100 Hz. to 200 Hz. The table in Figure 16 shows the results of this analysis.

Note that the average levels decrease from 100 to 200 Hz., but that the standard deviation remains nearly constant at around 9 dB. This might provide a better means of determining low, median, and high levels, based on going a set number of standard deviations above and below the mean. The 1/3 octave bands can be converted into a fixed bandwidth within the range by assuming a smooth broadband spectrum.

5.3 Sensor-to-Sensor Coherence Models

5.3.1 Underwater Acoustics Experience

Although no available information was found regarding the nature of spatial coherence of background noise in atmospheric environments, it has long been a topic of interest in underwater acoustics[13,14]. Its importance derives from the critical role the spatial coherence properties play in the design and performance of underwater sonar arrays. Urick[15] and Horton[16] devote entire chapters to the nature and sources of underwater ambient noise.

Various analytical models have been developed to predict the spatial correlation properties of ambient noise in the ocean. The general approach is:

1) postulate a distribution of mutually uncorrelated sources in two- or three-dimensional (underwater) space,

2) locate a pair of sensors at known positions,

3) propagate the sound from each source to each sensor,

4) sum the signals at each sensor (assuming linear superposition), and then

5) calculate the cross-correlation or coherence of the overall output signals at the two sensors.

In the idealized case of an isotropic noise field, such that the sound arrives at the sensors equally from all directions, the formulas for the cross-spectral density between two sensors separated by distance d reduces to a simple functional form[17]. For the case of a three-dimensional isotropic noise field, the cross-spectral density becomes

$$CSD_{3D} = \frac{\sin\left(2\pi\frac{d}{\lambda}\right)}{2\pi\frac{d}{\lambda}} \tag{6}$$

and for a two-dimensional isotropic noise field, it becomes

$$CSD_{2D} = J_0\left(2\pi\frac{d}{\lambda}\right) \tag{7}$$

where λ is the wavelength and J_0 is the zero order Bessel Function of the first kind. Plots of these functions for d/λ values between 0 and 1 are shown in Figure 17.

18

More complex models have been developed to describe non-isotropic directivities of underwater noise with receiving arrays of various geometries. These models have been compared to measured data to provide some understanding of the nature of underwater ambient noise under a variety of conditions[18,19,20,21] A significant source of noise is found to be wave motion due to wind effects on the surface of the sea, giving a roughly two-dimensionally distributed sound source. Studies have been made to attempt to determine the directionality of each source at the surface.

5.3.2 Atmospheric Ambient Noise Coherence Model

In the case of atmospheric sound, no immediately available ambient noise data was found to exist in a form readily comparable to spatial coherence noise models. One might hypothesize that the situation is analogous to that of the ocean surface sources, except turned upside down so that the sources are radiating upward into the medium. If the source of the atmospheric noise is aeroacoustic interaction with the wind, then whether the source field is isotropic or not might depend upon the local distribution of foliage or other protuberances with which the wind can interact.

An atmospheric ambient noise sensor-to-sensor coherence model was developed and studies were conducted in an attempt to provide design criteria for array sensor spacing. The model is two-dimensional, and assumes that the discrete noise sources can be distributed randomly around a sensor-pair position. Each source can be assigned an arbitrary amplitude and phase, and is statistically independent of all other sources.

In the case being modelled, each random source will be located a radial distance from the array at some azimuthal angle, and will generate broadband noise under wind action. At a selected narrowband frequency, a random phase can be assigned to the source signal, uniformly distributed between 0 and 2π. The amplitude of the sound source will vary randomly with some unknown distribution (probably depending on wind speed), and the level (and phase) at which it arrives at the sensors will depend on the propagation effects between source and receiver.

To avoid modeling the propagation effects on a large number of sources, it will be assumed that the sources can be modelled as having randomly distributed azimuthal locations around a 360 degree arc with randomly distributed signal amplitudes (as received). The amplitude distribution of the arriving signals will be simulated using a normally distributed random process with a given mean and standard deviation. The number of sources will be varied as a parameter. As the number of sources chosen gets very large, the results should tend toward that of an isotropic two-dimensional noise field.

The coherence statistics for a given number of noise sources is derived using a computer simulation experiment. The azimuthal position of each sensor is chosen from a uniform random distribution. The amplitude of the signal from each sensor is chosen from a normal distribution given mean and standard deviation, and the phase of the signal is chosen from a uniform distribution between 0 and 2π.

19

From Cox[22], the cross spectral density at circular frequency ω between two sensors spaced at distance d, in the presence of a noise field in which plane waves arrive with angular distribution $G(\phi,\omega)$, is given by

$$CSD(d,\omega) \; = \; \frac{1}{2\pi} \int_{-\pi}^{\pi} G(\phi,\omega) \; e^{i\frac{\omega}{c}d\cos\phi} d\phi \qquad (8)$$

In our case, we have NSRC sources, each source located at a discrete angle ϕ_j. Assign a complex amplitude A_j to each source. Then the distribution becomes

$$G(\phi,\omega) \; = \; \sum_{j=1}^{NSRC} A_j \; \delta(\phi - \phi_j) \qquad (9)$$

where $\delta(\phi)$ is the Dirac Delta Function. Substituting Equation (9) into Equation (8) and using the definition of the wavenumber $k = \omega/c$, we get

$$CSD(d,\omega) \; = \; \frac{1}{2\pi} \sum_{j=1}^{NSRC} A_j \; e^{ikd\cos\phi_j} \qquad (10)$$

If the A_j are normalized such that

$$\sum_{j=1}^{NSRC} A_j \; = \; 2\pi \qquad (11)$$

then the coherence is just

$$\rho_n \; = \; \sqrt{CSD \cdot CSD^*} \qquad (12)$$

where the asterisk implies complex conjugate. The equations can be written in terms of the non-dimensional parameter d/λ. For a given sensor number, then, a statistically averaged value of coherence and its standard deviation can be found as a function of d/λ using the computer experiments.

5.3.3 Results from Ambient Noise Coherence Model

The key results from a large number of computer runs are shown in Figure 18. For each run, 30 samples were run in which the source angles, amplitudes, and phases were varied

randomly as described above. The standard deviation of the background noise was arbitrarily chosen to be 5 dB. As the assumed standard deviation of the background noise increases, the sensor-to-sensor coherence increases, as might be expected.

Note that the minimum value of coherence occurs for d/λ of about 0.35-0.4, for all NSRC values. Note also that as the number of sources increases, the curve converges on the continuous isotropic noise source distribution case, as expected.

Figures 19 through 22 show the coherence standard deviation as a function of d/λ for source numbers of 2, 5, 10, and 100, respectively. Note the wide expected variation with few sources but the small standard deviation with many sources.

None of this, of course, explains what an actual atmospheric ambient noise environment is really like. Which set of parameters, if any, best describes an environment requires correlation with a set of carefully measured test data, which is at present non-existent. If the analysis is accepted, however, it does indicate that, no matter what the number of sources, the sensor-to-sensor coherence is minimized in the neighborhood of $d/\lambda = 0.35$-0.4, and it rises rapidly as d/λ becomes smaller.

Thus, the array design criteria for sensor spacing will be to set $d/\lambda = 0.35$. It is still necessary to chose a representative coherence value in order to evaluate array gain. Based purely on intuition, it is felt that a source number of around 10 might be reasonable. More sources than this may be in the vicinity, but possibly the nearest 10 or so may make the greatest contribution. This would give an ambient noise coherence estimate of around 0.3, which will be used in subsequent analysis.

The foregoing analysis also provides some conjectures about site preparation in the vicinity of the array. Ideally, of course, there would be no noise sources (such as bushes, trees, fences, structures, machines, etc.) anywhere near the array that would create wind noise in the critical band. Given the impracticality of this, the analysis would say that it might be better to locate the array such that a large number of small sources were roughly equidistant from the array, fairly evenly spaced in azimuth. If there are one or two close-in wind noise sources, they should probably be removed. The subject invites further investigation.

21

6 Detection System Redesign

6.1 Upgraded Parameter Set Used in Array System Definition

Upon completion of the preliminary detection system design, it was felt that various refinements and improvements should be incorporated for a final design. The upgrades reflect both the adoption of more realistic conditions and the need for at least a slight improvement in performance. It should be remembered that the objective was not to design the "best possible" acoustic detection system, but to achieve a design that would be representative of what could be accomplished within the current state-of-the-art.

The revised set of parameters used to predict the source noise levels are the following:

Altitude = 61 meters (AGL)

Aircraft Mach Number = 0.8

Aircraft Velocity = 252.9 m/sec

Nozzle Throat Area (A8) = 0.28 m^2

Nozzle Exit Area (A9) = 0.33 m^2

Exhaust Gas Total Temperature = 833.3 °K

Fuel-Air-Ratio = 0.015

Nozzle Pressure Ratio = 4.0

Ratio of Specific Heats γ = 1.37

Three parameters revised from the previous set are the altitude, nozzle exit area, and exhaust gas temperature. Atmospheric conditions at 200 ft. altitude are:

Ambient Temperature = 518 °R (14.8 °C)

Ambient Pressure = 2101.1 lb/ft^2

Relative Humidity = 70%

Speed of Sound = 1116.1 ft/sec

Using this revised set of parameters and some of the additional ambient noise data acquired after the preliminary design, the jet noise was calculated, propagated over three ranges, and compared to various low and median suburban background levels. These comparisons are

shown in Figure 23. The background level curves marked "USAAMRL" in Figure 23 are due to the United States Army Air Mobility Research and Development Laboratory (Reference 13), and were among the data provided by NASA Langley.

Under the revised conditions, appreciable S/N appears to remain in the 100-200 Hz. frequency band. At very long ranges, detection at frequencies below 50 Hz. might be worth considering. These comparisons will be examined further in the revised array design.

6.2 Potential Array Concepts Considered

A number of array concepts were considered as alternatives to the original design. All concepts operate in a bandwidth optimized for estimated received target spectral characteristics based on source signature and propagation transmission loss. The bandwidth must be wide enough to maximize S/N for received energy and narrow enough to design for an average d/λ.

Original Design

● The preliminary design consisted of a planar array on the ground with five closely-spaced sensors (d/$\lambda \approx 0.1$). This gave a hemispherical directivity pattern for both low and high altitude detection, and provided no bearing information.

Some Alternative Designs Considered

1) Vertically-oriented 5-10 sensor linear array, first sensor on the ground, the rest spaced with d/$\lambda \approx 0.3$-0.4 upward. Designed to give azimuthally symmetric beam oriented along the ground surface, aimed at low altitude detection with no bearing. Subject to variable levels of wind self-noise along the array. Could give an upward beam using endfire mode for some or all sensors.

2) Horizontal 2-D 5-10 sensor array with d/$\lambda \approx 0.3$-0.4, with fixed major lobe oriented vertically but with wide angle, aimed mainly at high altitude detection. Optimize beam width based on estimate of detection range. No bearing information. Must be combined with another array to cover low angles.

3) Horizontally-oriented array with electronically swept narrow beam, such as that considered by Gerhold and Wiese[24]. Number of sensors and spacing depend on desired beam width at operating frequency. Provides extra array gain from beamforming with increased detection range, and provides bearing information. Analysis of probability of detection complicated by operational problems of sweeping through space combined with intruder time-line.

A narrow beam could, of course, be mechanically-swept by rotating the array on a platform. The ease and well-developed technology of electronic beam sweeping, combined with the advantage of a system with no moving mechanical parts, would seem to rule in favor of the purely electronic system, even if it required extra sensors compared to the mechanical system.

Consider, for a moment, the kinematics involved in detecting a fast-moving aircraft in a swept acoustic beam. If the beam width, defined by the 3 dB down points, is $\Delta\phi$ radians, the number of beams required to cover 360 degrees of azimuth is

$$NB = 2\pi/\Delta\phi$$

The beam must remain stationary in direction long enough to acquire the signal. Assume that this combined signal acquisition and integration time is about 1 second.

The time required for an aircraft to cross the beam traveling perpendicular to the beam center line (thus the minimum time to cross) is given by

$$T_c = \frac{2R}{V} \tan\left(\frac{\Delta\phi}{2}\right) \qquad (13)$$

where R is the horizontal range to crossing and V is the aircraft speed. If the time to cross the beam is appreciably less than one second, the aircraft may not be detected.

Assume, for example, that the array is designed to have a beam width of 30 degrees. For an aircraft travelling at Mach 0.8, the minimum range for which the aircraft will remain within the beam for at least one second is 507 meters. Assume that the beam is rotating in a direction opposite to the direction in which the aircraft crosses it. This provides a single detection event, and another event won't occur until about 9 seconds later, when the aircraft is about 2.5 km. past closest point of approach.

Thus, a beamformer will have a *minimum* range of effectiveness, and alternative (simpler) detection means may be required when the aircraft passes too closely. In addition, to get multiple detections in a single beam, the beam will have to remain stationary for multiple integration time intervals, thus further increasing the time to cover a full 360 degree arc with a single swept beam. Parallel processing could be used to form simultaneous beams from the same sensor signals.

6.3 Crossed-Endfire Array Design

The crossed-endfire array design arose in response to the perceived performance deficiency in the initial Mills Cross array. The Mills Cross provides a single, nearly hemispherical, vertically-oriented major lobe, but this requires a sensor spacing of 0.1 d/λ. At this sensor spacing, the ambient noise sensor-to-sensor coherence is predicted to be over 90%, thus negating most of the array gain. An increase in sensor spacing will lead to directivity losses at grazing angles by decreasing the beamwidth of the major lobe.

The crossed-endfire design to be described uses the same five-sensor geometry as the Mills Cross, but processes the data with a different algorithm. The crossed-endfire will be shown to provide the required grazing angle directivity gains at the expense of the simplicity of

24

data processing afforded by the Mills Cross. The crossed-endfire does, however, give the added advantage of providing target bearings to within 90 degrees beamwidth that probably compensate for the added data processing complexity.

6.3.1 The Linear Endfire Array

For this design the additional constraint is imposed that the array spacing be $d/\lambda = 0.35$ to take advantage of the minimum in ambient noise coherence. Under this condition, it is assumed that the sensor-to-sensor ambient noise coherence is $\rho_n = 0.3$ (30%). The integration time is set at 1 second in order to decrease detection threshold and assure achieving the benefits of low background noise coherence.

An endfire array is a linear array for which the sensor outputs are phased to steer a beam along the array axis[24,25]. Definitions of the array geometry and the spherical coordinates θ and ϕ are shown in Figure 24. The expression for the beam directivity pattern when steered along an axis is

$$D(\theta,\phi) = 1 + 2 \sum_{n=1}^{M} \cos\left(2\pi n \frac{d}{\lambda}(\sin\theta \sin\phi - 1)\right) \tag{14}$$

where, if NS is the number of sensors (NS must be odd)

$$M = \frac{NS - 1}{2} \tag{15}$$

Figure 25 shows the horizontal directivity pattern for a three-sensor endfire array with $d/\lambda = 0.35$. Figure 26 shows the vertical directivity pattern for this array in the plane aligned with the array axis.

6.3.2 Design of Crossed-Endfire Array

By suitable signal phasing, the endfire array can be steered in either axial direction. By sending the sensor outputs to two independent processors, the beams in both directions can be formed simultaneously. By aligning two more sensors in a direction perpendicular to the linear array axis, such that the center sensor is common, as shown in Figure 27, the crossed endfire array may be formed. Note that the resulting geometry is the same pattern as that for a Mills Cross five-sensor array.

The crossed endfire detection array operates by forming five simultaneous receiving beams that effectively cover a hemisphere centered on the array. The beams are formed by five independent parallel data processors that each use a different subset of the five sensors. Each

of four horizontal beams covers a 90 degree quadrant in the horizontal plane, with an elevation angle coverage up to about 45 degrees above the horizontal.

Using the Mills Cross algorithm and all five sensors, a vertical beam is formed that points upward and is nearly symmetric about the vertical axis. The five beams overlap to provide the hemispherical coverage, as illustrated in Figures 28 and 29.

Since each beam is processed as an independent detector, a rough bearing to the target can be obtained, at least to within a 90 degree sector. Since the beams are formed simultaneously using parallel processors, the time delay and loss of coverage in "sweeping" a single beam is avoided, which is an added advantage of this design.

The horizontal beams are formed by combining the signals from three sensors at a time in a linear array pattern using endfire array beamforming. The three sensors in the cross direction (with the center sensor in common) are used to form two beams at 90 degrees to the first two horizontal beams. Figure 30 illustrates the beam overlap in the horizontal plane for the four simultaneous endfire beams.

The vertical beam is formed by using signals from all five sensors, with zero relative phasing, forming a Mills Cross. This pattern is nearly azimuthally symmetric about the array vertical axis for the prescribed sensor spacing. With the $d/\lambda = 0.35$ sensor spacing, the width of the vertical beam is about 35 degrees. The overlap of the vertical lobe with the vertical component of the endfire array is shown in Figure 31.

The five beams, which are formed simultaneously, provide nearly omnidirectional coverage, except where directivity is reduced along beam overlap lines. Thus, a detector with improved performance is obtained using the same number of sensors as the original design, at the expense of an increased array extent dimension (about 6.5 ft vs. 2 ft.) and a more complex signal processing algorithm.

6.3.3 System Design

With the array geometry and basic operation determined and with the sensor spacing constrained to $d/\lambda = 0.35$, it remains to choose the frequency bandwidth for the revised design. The comparison of received signal and background levels in Figure 23 seems to indicate the advisability of going to much lower frequencies than the previous 90-180 Hz. bandwidth.

However, designing for a low frequency bandwidth, say 30-50 Hz., was not done for several reasons:

1) Maintaining d/λ at 0.35 would require an array extent of about 12.2 meters at 40 Hz. mean frequency. This is conceivable, but it borders on the impractical, especially if some array portability is desired.

2) Little is understood about the background noise coherence at these low frequencies. It is postulated that wind noise, large scale turbulence, or other effects may increase coherence even at wide sensor spacing.

Designing for a very wide bandwidth, say 25 Hz. to 175 Hz, is not possible due to the wide range of d/λ from one end of the band to the other. Even the original 90-180 Hz. band gives a variation of 0.25 < d/λ < 0.5 from lower to upper band edge. For these reasons, a compromise bandwidth of 100-150 Hz. was chosen as the design bandwidth. For this bandwidth, the variation in d/λ is 0.28 < d/λ < 0.42. Refinement of this choice of bandwidth calls for additional, more detailed, knowledge of the expected background noise levels and the background noise coherence properties.

The new set of acoustic array design parameters are the following:

- Design bandwidth 100-150 Hz., giving mean frequency of 125 Hz.

- Five-sensor Crossed-Endfire Geometry

- Sensor spacing to give d/λ = 0.35, giving sensor spacing of 0.95 m., array extent of 1.90 m.

- Integration time set to 1.0 seconds

- Assumed background noise coherence of 30%

The array gain for each 3-sensor endfire array is AG = 2.7 dB. Assuming a nominal 0.5 dB directivity loss due to beam overlap, this gives the directivity index as

$$DI = AG - D(\theta,\phi) = 2.7 - 0.5 = 2.2 \text{ dB}$$

Assuming the same 50% probability of detection and 0.1% probability of false alarm as the preliminary design, and with a 50 Hz. bandwidth and 1 second integration time, the detection threshold becomes

$$DT = 5\log(d') - 5\log(BW*T) = 5.0 - 8.5 = -3.5 \text{ dB}$$

The required signal-to-noise-ratio for detection then becomes

$$RSN = DT - DI = -3.5 - 2.2 = -5.7 \text{ dB}$$

so that the required signal level for detection can be written

$$RS = NL + RSN = NL - 5.7 \text{ dB}$$

Using the averages of the 38 separate noise measurements described in Section 5.2, the average background noise value in the 100-150 Hz. bandwidth is obtained as

27

$$AVESPL_{100-150} = 47.7 \text{ dB}$$

The standard deviation for this bandwidth is taken to be $\sigma = 8.8$ dB. Assuming a variation of 1σ, three background levels are defined as

$$NL_{high} = 56.5 \text{ dB}$$

$$NL_{med} = 47.7 \text{ dB}$$

$$NL_{low} = 38.9 \text{ dB}$$

The required signal levels for detection under these three conditions, which will be used to determine detector performance, are, then,

$$RS_{high} = 50.8 \text{ dB}$$

$$RS_{med} = 42.0 \text{ dB}$$

$$RS_{low} = 33.2 \text{ dB}$$

One might question whether, if three sensors in a linear endfire array give a gain of 2.7 dB with $d/\lambda = 0.35$, why not add just one more sensor at each end, giving a 9-sensor, 5X5 crossed endfire configuration, which would provide an increase in array gain to 3.5 dB. For one thing, the 5-sensor endfire array at $d/\lambda = 0.35$ gives about a 20 degree narrower beamwidth than the 3-sensor array. To avoid losses at beam overlap points, this might require an additional line of sensors, with 60 degree spacing between lines. The four additional sensors in the third line would then mean 8 additional sensors in the entire array. This is a feasible upgrade of the original design, but it was judged to be bordering on excessive complexity for the present purposes.

6.3.4 Array Signal/Data Processing Algorithm

Before proceeding to the analysis of detection range performance, we shall examine the possible digital signal processing parameters that might be used to process the signal, to be assured of their practicality. The array system is envisioned to be composed of the sensors and mounting system, cabling from the sensors to the processor, an electronics enclosure for the signal processing electronics, power supply and conditioner, and transmitter, and an antenna for radio transmission of data, as shown in Figure 32. (If open communications are undesirable, a phone line could be used instead of radio transmission).

An overview of a proposed implementation of the signal acquisition/conditioning/processing system is shown in Figure 33. Each sensor output is analog-bandpass-filtered, digitized, windowed, and Fourier transformed. It is important that these parallel processes be synchronized and phase-matched.

28

The sensor outputs go to the appropriate beamformer circuits as shown in the figure. The beamformer outputs, in the form of energy levels, are then passed to a comparator, which performs the square-law detection decision. If any beam produces a positive detection, the transmitter is triggered and a Command and Control Center is alerted with a code that indicates which beams are detecting.

The objective of the digital signal processing is to obtain the maximum number of frequency averages within the desired detection output repetition time. The total averaging time is equivalent to the system integration time. This is accomplished by choosing the highest possible sampling rate along with the minimum block size, all commensurate with a frequency resolution that matches the detection bandwidth.

For example, with an optimum signal bandwidth from 100 to 150 Hz., assume that a detection update is desired at intervals of one second. The following set of digital signal processing parameters will accomplish this task:

Sampling rate = 1600 Hz.

Block size = 32

Record length per data sample = 0.02 seconds

Anti-aliasing frequency = 800 Hz.

With this choice of parameters, the frequency resolution of the FFT is 50 Hz. Thus, the third spectral element, centered at 125 Hz., covers the 100 to 150 Hz. bandwidth very closely. Subsequent data processing calculations, including the frequency averaging, beamformer phase shifting, and detection, are performed on only the single numerical value per beamformer.

Neglecting data processing time (i.e., assuming 100% duty cycle), up to 50 frequency averages can be accomplished in 1 second. Maximizing the number of frequency averages is critical for extracting the signal from the noise.

It is likely that the above sampling rate and block size can be obtained with off-the-shelf components. Thus, it appears that the detection system design is not only practical, but achievable at relatively low cost.

One additional parameter is required, the height at which the array is mounted above the ground surface. This depends on the ground effects on the propagation, which are calculated from the Chien and Soroka model assuming a ground impedance characteristic of grassland. Figure 34 shows the variation in received signal level for various ranges as a function of receiver height above the ground. It is assumed that the plane of the array remains horizontal.

A minimum in received signal is predicted at around 1.85-7.6 meters receiver height. Appreciable increases above the level received with the receiver flush to the ground occur for receiver heights above about 15 m. Since the difficulty and expense of mounting and

maintaining the array on say, 30-45 meter towers is likely to be quite high, the flush surface mounting is chosen as a compromise. In addition, wind levels are likely to be higher above 30 meters, possibly reducing array performance due to wind self-noise. The possibility and ramifications of higher altitude deployment are worth further investigation, however.

6.4 Estimated Detection Range Performance

The source noise prediction, propagation effects, and detection criteria are now assembled into an analytical model to predict detection range. An initial use of the model is to predict the "footprint" of contours of constant received signal levels in the horizontal plane, as shown in Figure 35. An interesting observation that can be made from Figure 35 is that noise levels are decreasing at about the rate of 14 dB per doubling of distance. This is due to the combined attenuation effects of spherical spreading, atmospheric absorption, and ground effects. Spherical spreading alone would account for 6 dB per doubling of distance.

In any region where the received level exceeds the detection criteria for a duration of one second or longer, a positive detection will occur. The detection range is defined as the horizontal distance from the point of emission to that contour where the received level just equals the detection criteria.

Figure 36 shows the detection range under median background level conditions as a function of azimuth angle from the aircraft heading. Note the peak in detection range at the radiation angles where the jet noise is at a maximum. The detection range varies from slightly over 3 km. at the forward angle to over 18 km. at the 150 degree azimuth.

Figure 37 shows the detection ranges versus azimuth angle for all three background environments. Note that at an azimuth angle of 150 degrees the peak value of detection range varies from about 12 km. to over 27 km. with the expected variation in background noise. Figure 38 shows the same data in detection contour (footprint) format.

Figure 39 shows a "circle of detection" superimposed on the median background footprint. The radius of the circle is about 9.5 km. and it is centered about 6 km. behind the aircraft signal emission point. This is an estimate of the radius of effectiveness of an individual array, and can be used to determine array site spacing to provide complete area coverage.

For instance, Figure 40 shows a staggered, "closest packing" approach to site deployment. Assume the distance from the site center to the corner of a hexagon that encloses the circles that defines site spacing is 9.5 km. The radius of the circles, then, is 8.2 km. This gives detection range overlap (for median background) along the lines connecting the sites with no uncovered area between detectors. With this spacing, each sensor site is responsible for about 234 square km. of coverage. Thus, to cover a region 50 km. deep and 500 km. wide would require about 107 sensor sites.

6.5 Adaptive Background Noise Level Accommodation

An operational problem would be anticipated for an acoustic detection array in an environment where the background noise level varied widely over a period of time. If the detection threshold were set for the highest background level expected, the array would be operating sub-optimally for an appreciable percentage of the time. On the other hand, if the detection threshold were set at the mean expected level, a large number of false alarms would result when the high background level exceeded the mean.

If the background level could be monitored continuously, the detection threshold could be continuously adjusted to adapt. The problem with this is that there must be some way to distinguish the background level (in the 100-150 Hz. band) from the signal, which is precisely the purpose of the detector.

An algorithm that might possibly accomplish this adaptive control might monitor the background noise levels in some band of frequencies higher than the 100-150 Hz. detection band. If it could be shown that the background noise level in the 100-150 Hz. bank were highly correlated with the level in the higher frequency band, this could be used to actively control the detection threshold level. The signal from the aircraft, being highly attenuated in the higher frequency band, could be guaranteed not to contribute to the control signal.

Studies are needed to determine how reliably the background noise levels in the 100-150 Hz. band could be predicted from measurements in higher bands. The signal integration time, as well as the frequency bandwidth, would be parameters of variation. Kalman filtering techniques might be employed to advantage.

7 Summary and Conclusions

An acoustic detection system has been designed that is predicted to give about a 10 km. detection range, depending strongly on background noise conditions. The system is simple, practical, and well within the technological state-of-the-art for both hardware and software.

Since the design is purely analytical, one must question the assumptions upon which the design is based. Although every attempt was made to be conservative in choice of assumed parameters, some assumptions require experimental substantiation before achieving acceptable credibility.

In particular, the assumption of background noise coherence properties require validation by measurement. More complete data is needed on typical background environment levels. The ground effect model needs to be substantiated for long range propagation. Refraction effects, neglected here, may be another important source of variation for grazing angle propagation.

For design and evaluation purposes, it is assumed that the background noise levels attain a constant value. In actual operation, it is likely that temporal variations in background noise level will give a large variability in the performance of the detection array. The consequences of this expected variability on the effectiveness of the detection system have not been examined. This is expected to be the largest source of variability in system performance, so that the biggest design problem in practice may be how to accommodate the variability in the background levels.

The detection system design resulting from this study should give a reasonable and achievable level of performance, and thus be representative of an "average" acoustic detection system. More complete understanding of the operating environment and developmental experience with actual hardware would undoubtedly lead to improved performance versions of the system. The performance criteria developed here will be used to define the acoustic system standard for subsequent detection range studies.

8 Further Development Needs

8.1 Experimental Validation of Design Assumptions

The most effective means of sensor system design validation would be to build it and use it to perform flight tests. A separate target vehicle tracking system, vehicle performance and engine cycle parameters, and weather data would be required for a successful test.

Much additional data is needed to characterize background noise environments. The ambient environment should be characterized continuously and wind data recorded. Background noise coherence should be a measurement objective, as this is a critical parameter in the array design. Universally acceptable testing criteria need to be established.

Long-range propagation measurements are needed to validate the ground effects model. This will be a difficult measurement, due to the need to separate the ground effects from other atmospheric propagation effects. Further studies should incorporate the effects of refraction, particularly for the low altitude target case.

The effects of high subsonic aircraft Mach numbers on source strength and radiation angle require validation. Very possibly at these high Mach numbers airframe noise becomes a significant contributor at certain angles, and should be included as a factor in future design studies. The addition of airframe noise, however, would only serve to increase the detection range of the current design.

8.2 Design Optimization

Studies are needed to examine the feasibility, coverage effectiveness, and cost of the proposed sensor site deployment scheme. Losses in effectiveness by increasing the detector site spacing should be examined. Other schemes such as random deployment locations should be studied using operations research methods (sort of an inverted screen and search scenario where the sensors are stationary and the source moves[26]).

Further studies are needed on the practicality and effectiveness of narrow beam sweeping techniques. Again, operations research methods must be applied to determine the effectiveness of this method in terms of technical feasibility and cost versus probability of interception for various penetrator scenarios.

Studies to define measures of and ways to accommodate expected variability in system performance under changing operating environment conditions are highly recommended. In particular, development of a method for automatic adaptation of detection threshold to variability in background noise level would be extremely useful.

9 References

1. Urick, Robert J., <u>Principles of Underwater Sound</u>, McGraw-Hill, 1983.

2. Urick, Robert J., <u>Principles of Underwater Sound</u>, McGraw-Hill, 1983, pp. 17-30.

3. Urick, Robert J., <u>Principles of Underwater Sound</u>, McGraw-Hill, 1983, pp. 381-383.

4. Kinsler, Lawrence E., Frey, Austin R., Coppens, Alan B., and Sanders, James V., <u>Fundamentals of Acoustics</u>, John Wiley, 1982, pp. 409-411.

5. Stone, James R. and Montegani, Francis J., "An Improved Prediction Method for the Noise Generated in Flight by Circular Jets", NASA TM-81470, April, 1980

6. Acoustical Society of America, "American National Standard Method for the Calculation of the Absorption of Sound by the Atmosphere", ANSI S1.26-1978 (ASA 23-1978), 1978.

7. Chien, C. F. and Soroka, W. W., "A Note on the Calculation of Sound Propagation Along an Impedance Surface", Journal of Sound and Vibration, 69(2), 1980, pp. 340-343.

8. Thomasson, Sven-Ingvar, "Sound Propagation Above a Layer with a Large Refraction Index", J. Acoustical Soc. America, Vol. 61, No. 3, March, 1977, pp. 659-674.

9. Urick, R. J., <u>Principles of Underwater Sound</u>, McGraw-Hill, 1983, Chapter 3

10. Ziomek, Lawrence J., <u>Underwater Acoustics: A Linear Systems Theory Approach</u>, Academic Press, 1985, Chapters 3 and 4

11. Revell, James D. and Lackey, David F., "Aircraft Acoustic Detection and Suppression", AFWAL-TR-86-3103, 30 January, 1987. ', pp. 2-6 to 2

12. Harris, Cyril M. (ed.), <u>Handbook of N̄   ̄ntrol</u>, McGraw-Hill, 1957 (Section 35).

13. Blewitt, S. J., Harding, D. G., Laughead, R. W., and spencer, R. H., "Analysis of the Effects of Aural-Detection Range on Helicopter Operations", USAAMRDL Technical Report 73-80, March, 1974.

14. Cron, Benjamin F. and Sherman, Charles H., "Spatial-Correlation Functions for Various Noise Models", J. Acoustical Society of America, Vol. 34, No.11, November 1962, pp. 1732-1736.

15. Talham, Robert J., "Ambient-Sea-Noise Model", J. Acoustical Society of America, Vol. 36, No. 8, August 1964, pp. 1541-1544.

16. Urick, Robert J., <u>Principles of Underwater Sound</u>, McGraw-Hill, 1983, Chapter 7.

17. Horton, C. W., Signal Processing of Underwater Acoustic Waves, U.S. Government Printing Office, November 1969, Chapter 9.

18. Cox, Henry, "Spatial Correlation in Arbitrary Noise Fields with Application to Ambient Sea Noise", J. Acoustical Society of America, Vol. 54, No. 5, 1973, pp. 1289-1300.

19. Fox, George R., "Ambient-Noise Directivity Measurements", J. Acoustical Soc. America, Vol. 36, No. 8, August 1964, pp. 1537-1540.

20. Arase, Elizabeth M. and Arase, T., "Correlation of Ambient Sea Noise", J. Acoustical Soc. America, Vol. 40, No. 1, 1966, pp. 206-210.

21. Cron, Benjamin F., Hassell, Beverly C., and Keltonic, Frank J., "Comparison of Theoretical and Experimental Values of Spatial Correlation", J. Acoustical Soc. of America, Vol. 37, No. 3, March 1965, pp. 523-529.

22. Cox, Henry, "Spatial Correlation in Arbitrary Noise Fields with Application to Ambient Sea Noise", J. Acoustical Soc. America, Vol. 54, No. 5, 1973, pp. 1289-1301.

23. Cox, Henry, "Spatial Correlation in Arbitrary Noise Fields with Application to Ambient Sea Noise", J. Acoustical Society of America, Vol. 54, No. 5, 1973, pp. 1291-1292.

24. Gerhold, C. and Wiese, M., "Application of Beamform to Sound Propagation in the Atmosphere", AIAA-90-3990, October 1990.

25. Urick, Robert J., Principles of Underwater Sound, McGraw-Hill, 1983, p. 57.

26. Ziomek, Lawrence J., Underwater Acoustics: A Linear Systems Approach, Academic Press, 1985, p. 62 ff.

27. Koopman, Bernard O., Search and Screening: General Principles with Historical Applications, Pergamon Press, 1980.

10 Figures
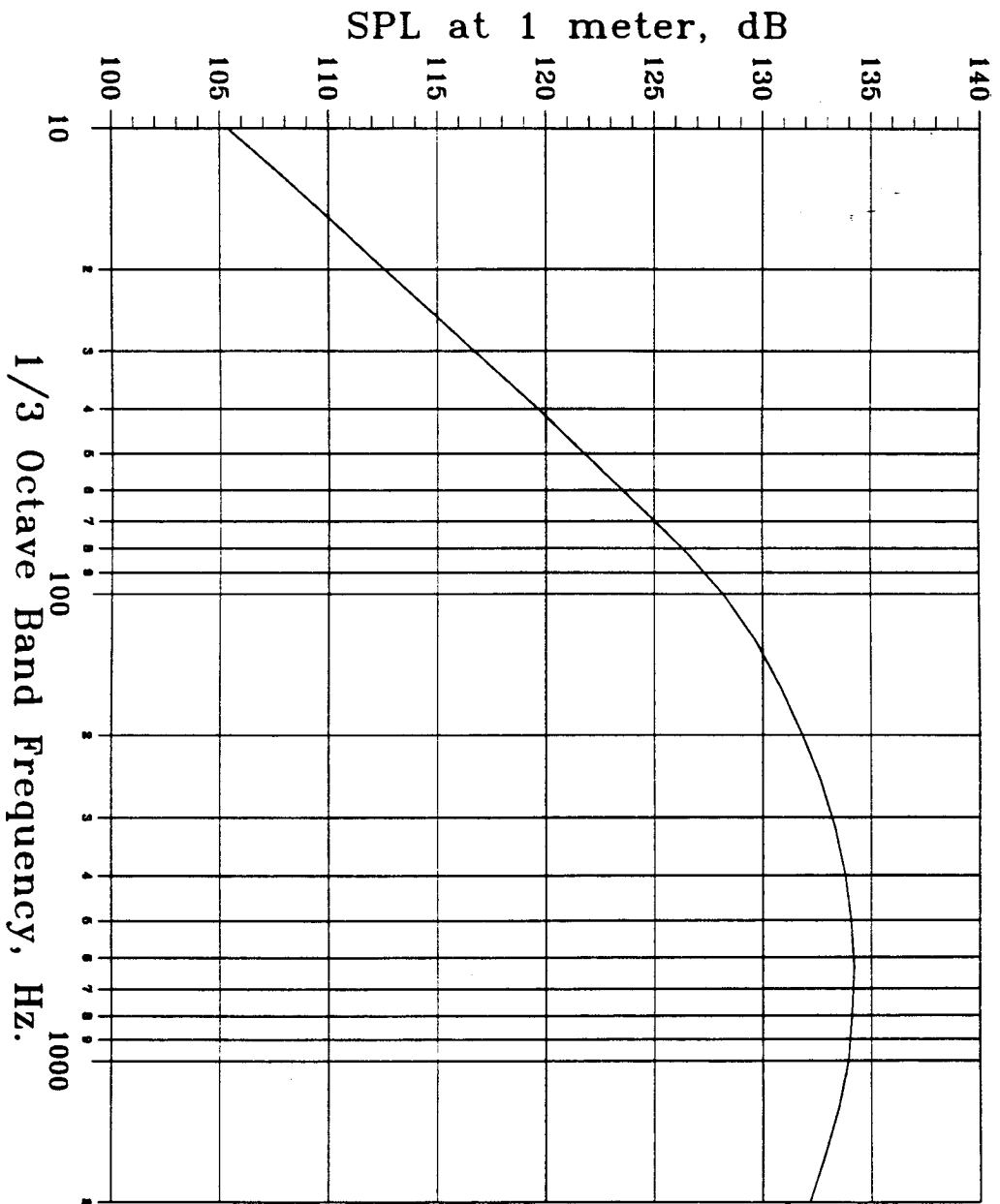
Figure 1   Jet noise spectrum for representative target aircraft for equivalent point source at 1 meter radius, for a radiation angle of 90 degrees to aircraft forward direction.
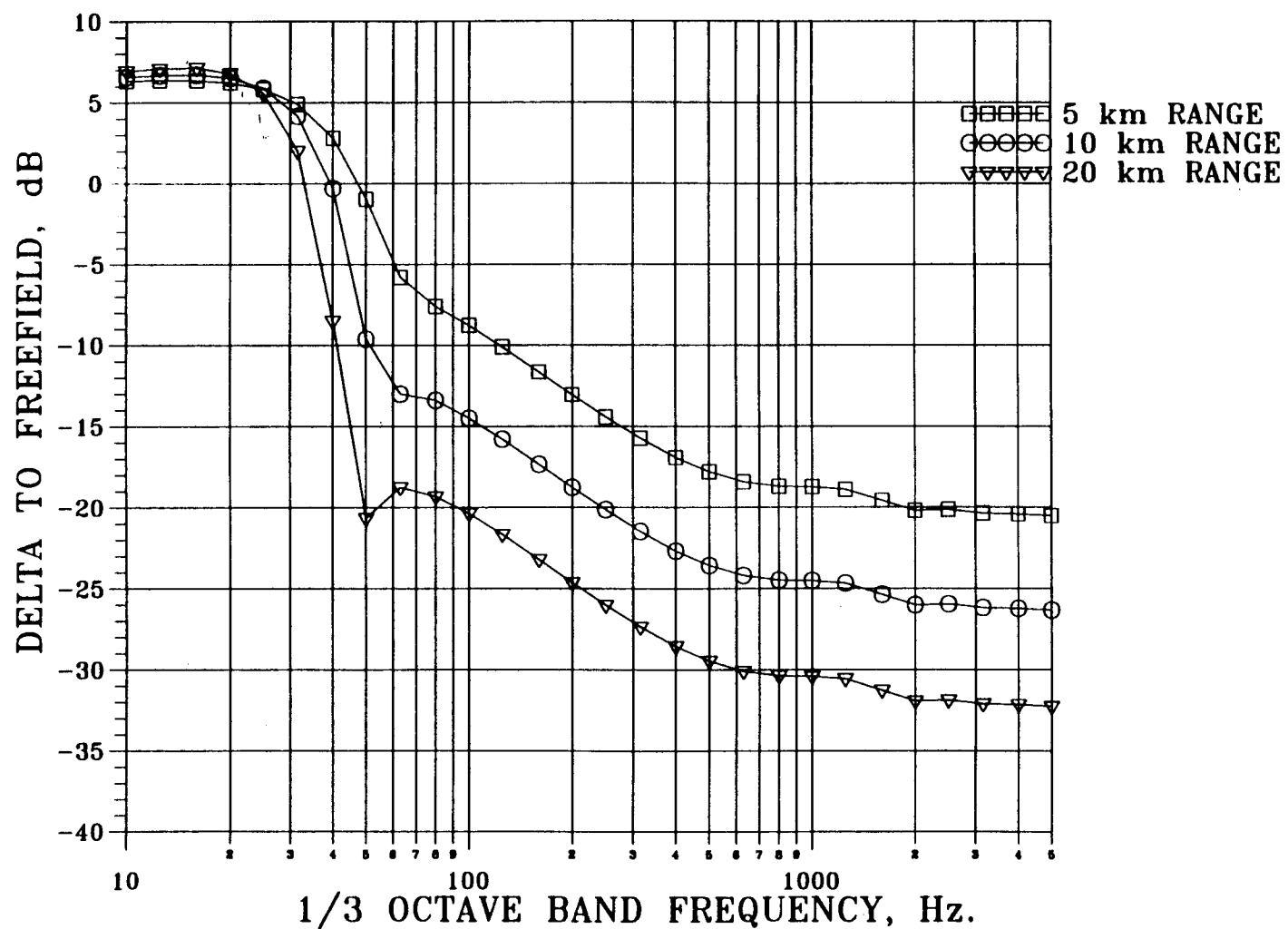
Figure 2   Prediction of ground attenuation using Chien and Soroka model. Source at 61m. altitude, receiver at 0 m., grass surface, various ranges (no spherical spreading).
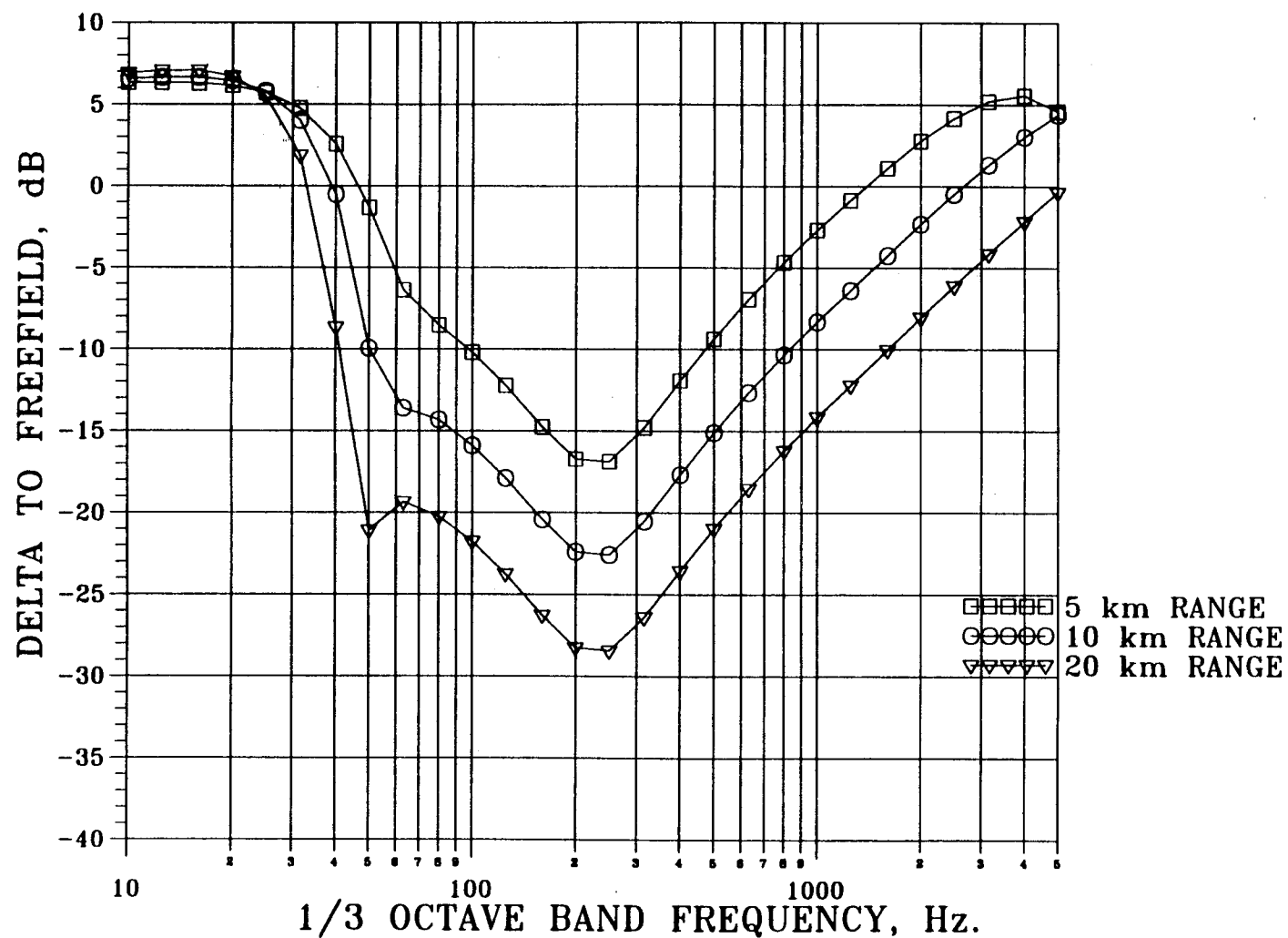
Figure 3   Prediction of ground attenuation using Chien and Soroka Model. Source altitude, 61 m., receiver at 1.8 m., grass surface, various ranges.
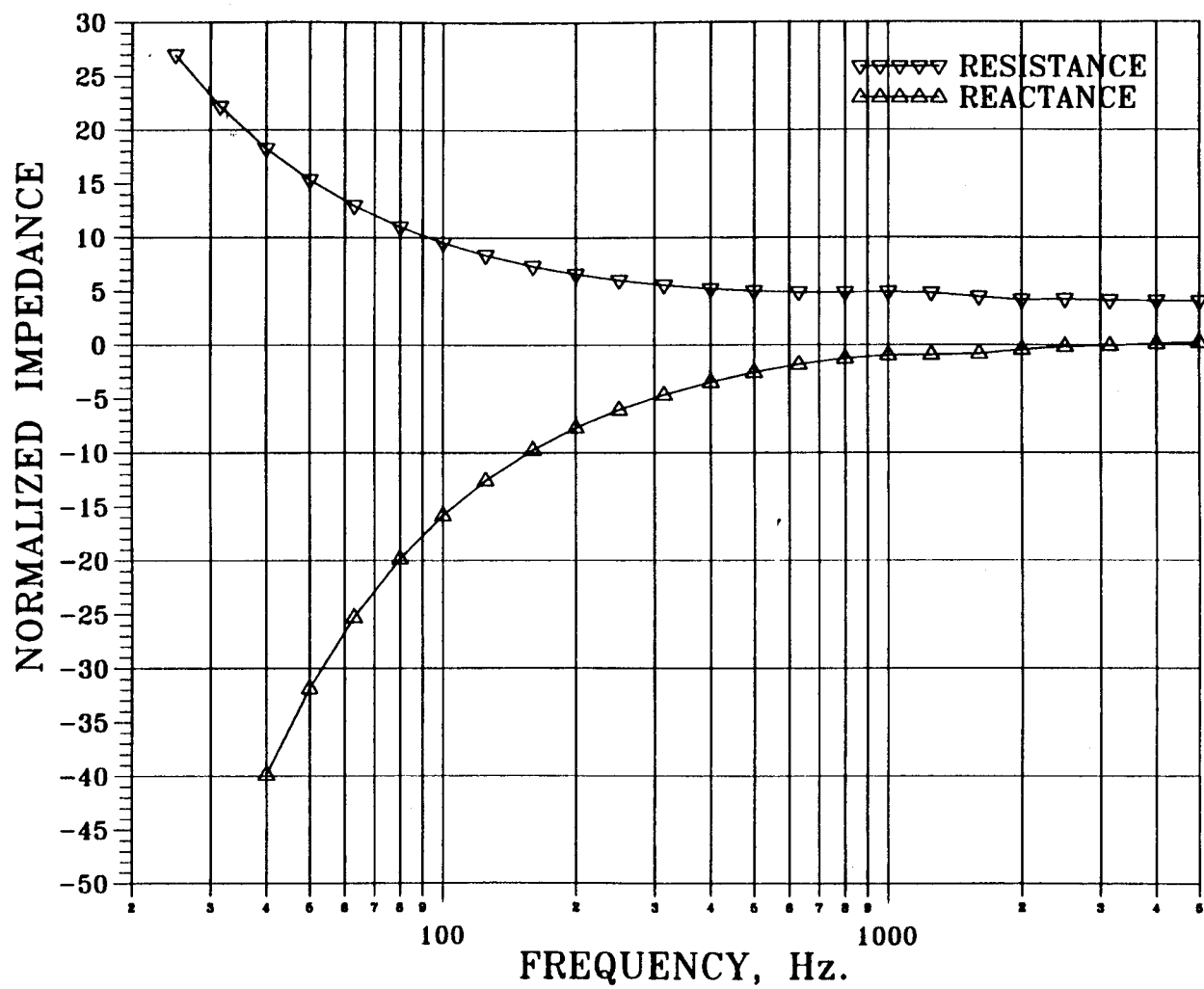
Figure 4   Ground acoustic impedance used for grass surface for ground effects calculations.
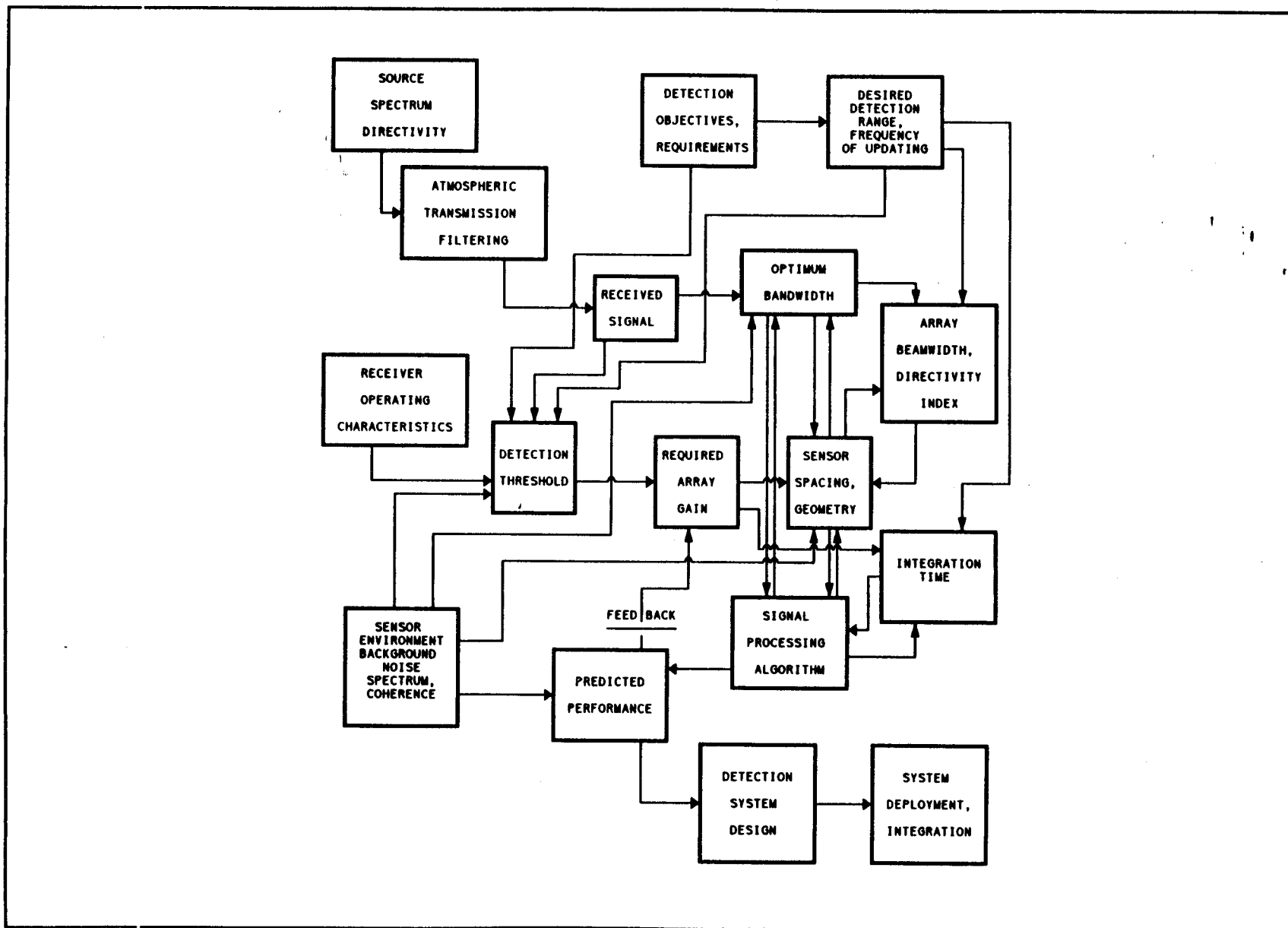
Figure 5   Flow chart illustrating complexity of acoustic detection system design process.

Mills Cross

Pentagon (Circular)

● **Sensor**

Figure 6   Mills Cross and Pentagon planar array geometry.
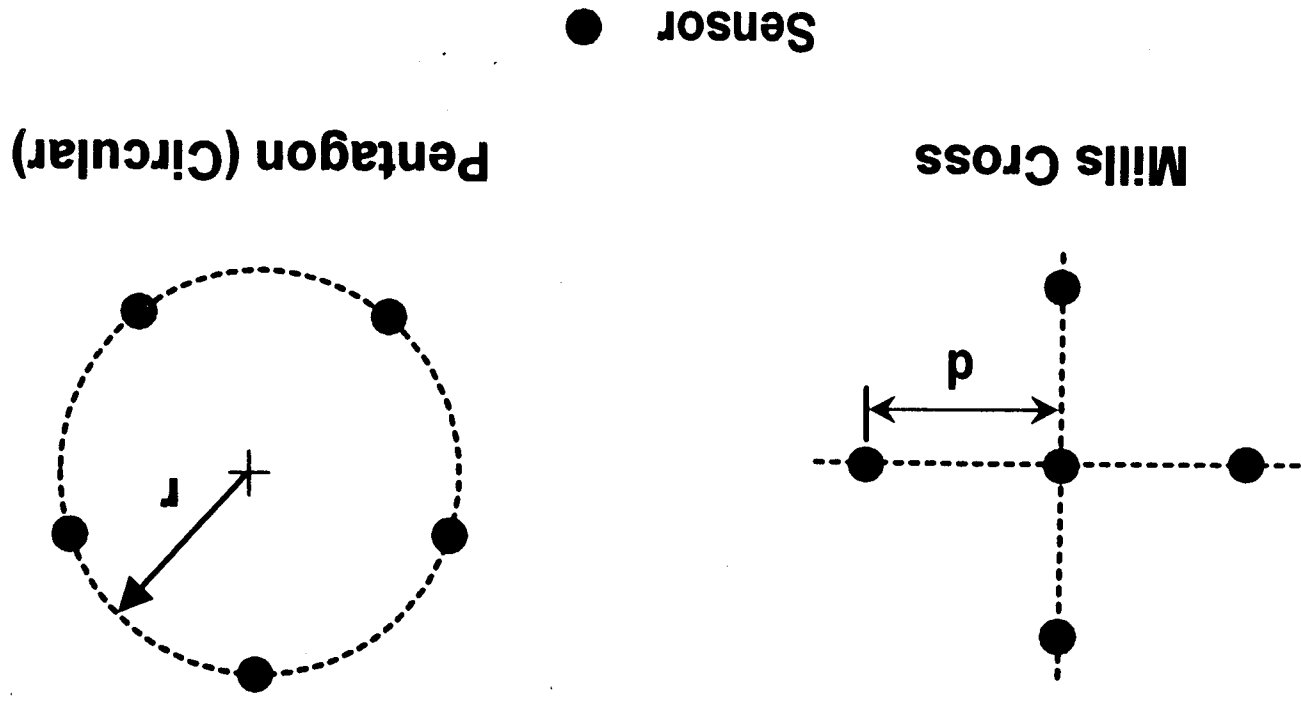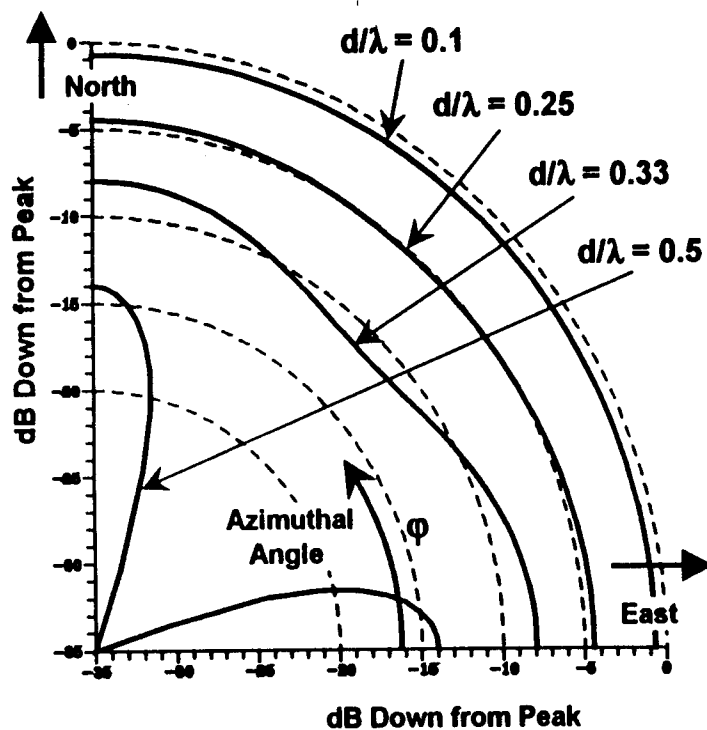
42
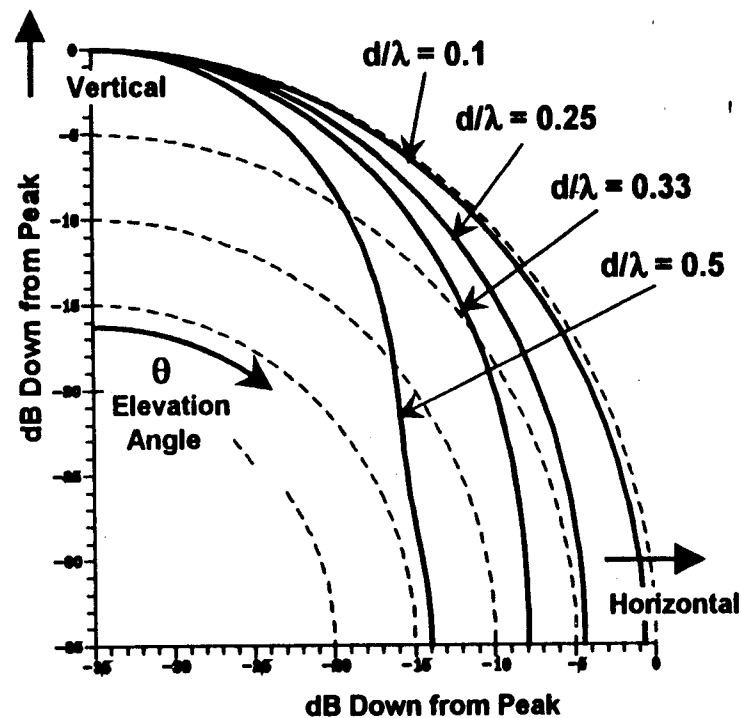
Figure 7   Vertical and horizontal directivity patterns for a Mills Cross planar array.
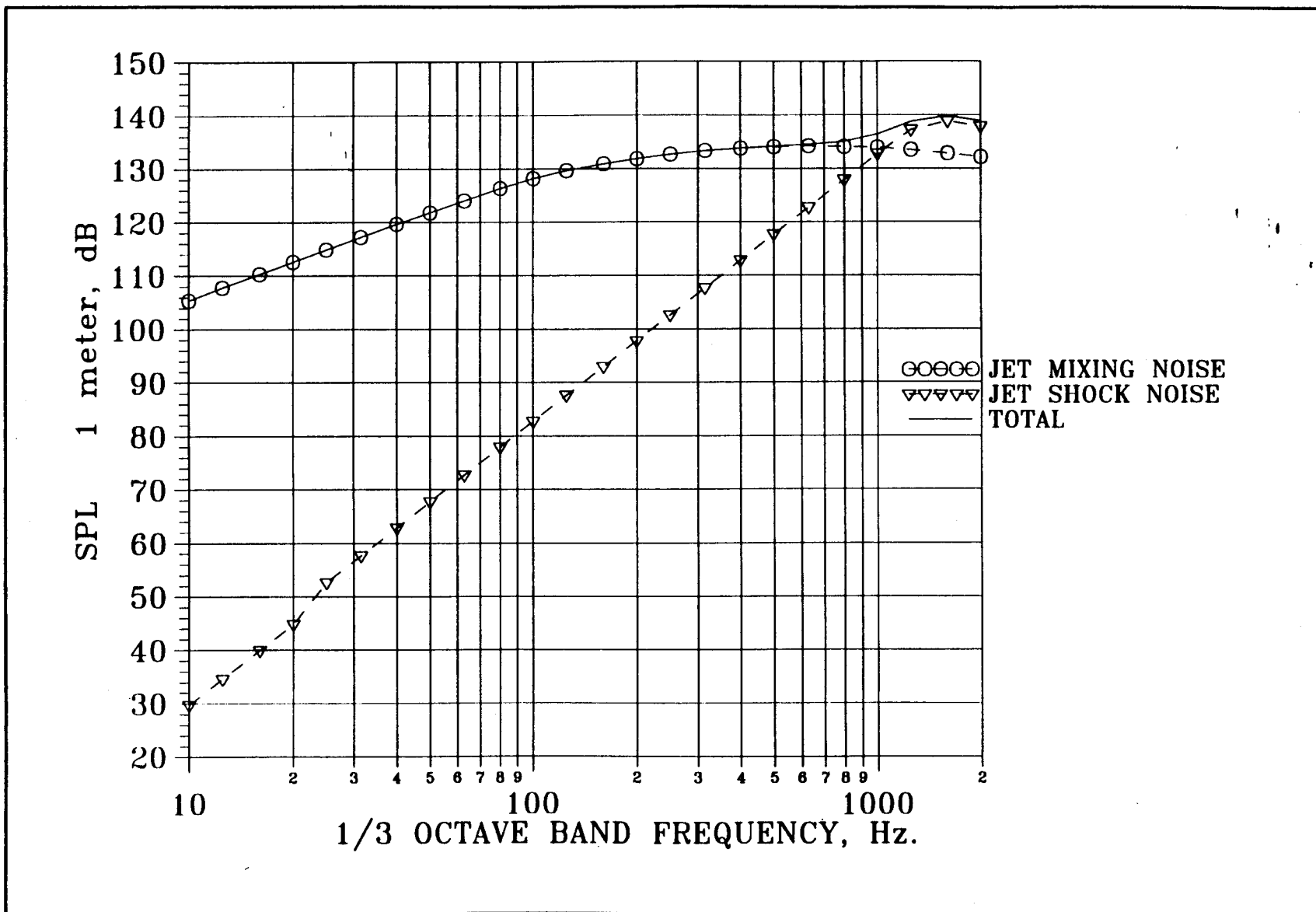
Figure 8   Jet mixing and shock noise source component spectra for aircraft, normalized to level for equivalent point source at one meter, as radiated at 90 degrees to the inlet.
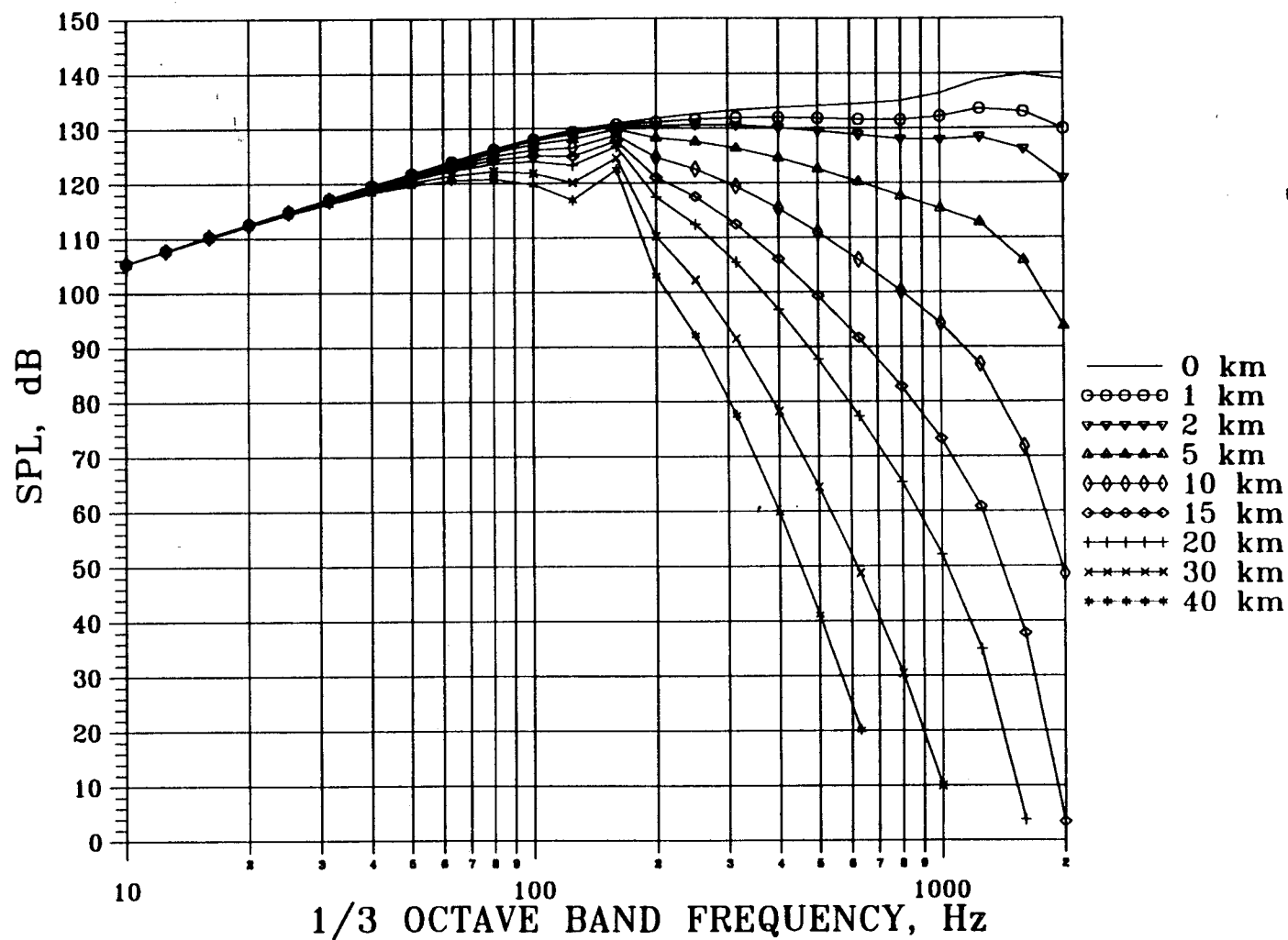
Figure 9   Filtering effect of atmospheric absorption on jet noise spectra for various propagation distances (spherical spreading effects not included).
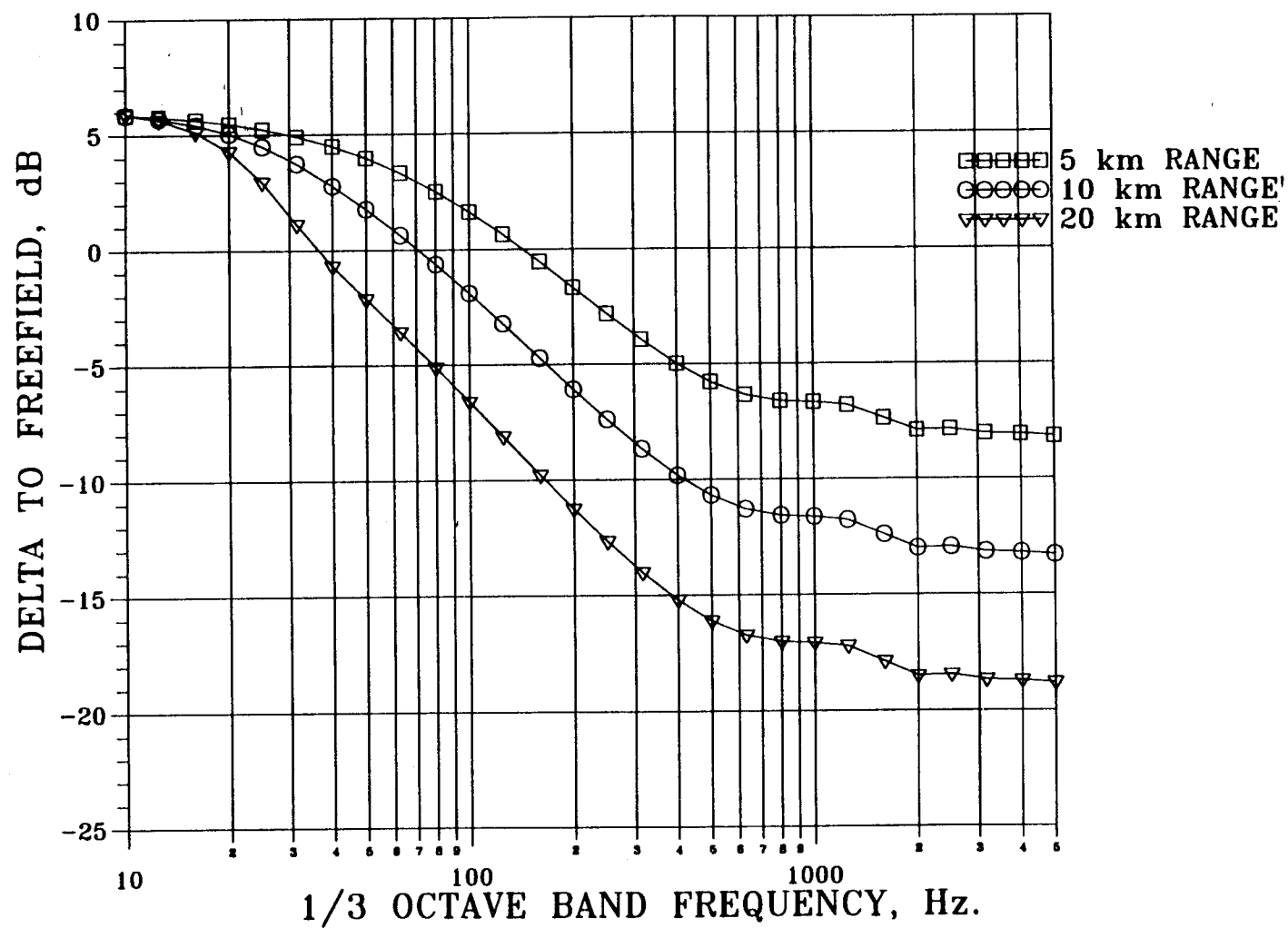
Figure 10   Ground propagation effect on signal attenuation for source height of 300 meters, receiver height of 0, grassland surface, for three ranges.
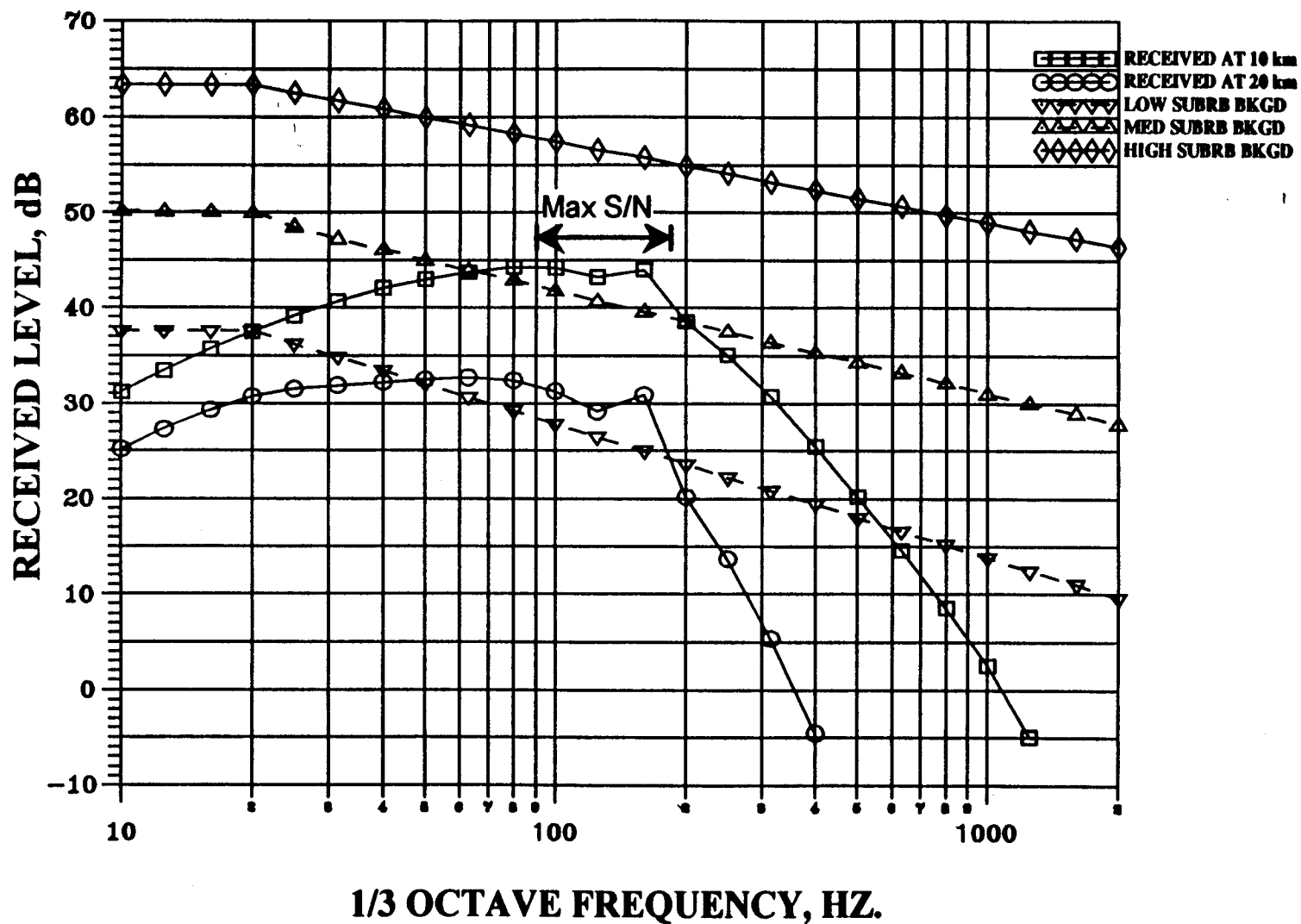
Figure 11   Received aircraft signal after transmission loss compared to three background levels. Aircraft at 300 meters altitude, Mach 0.8, azimuth angle of 90 degrees.
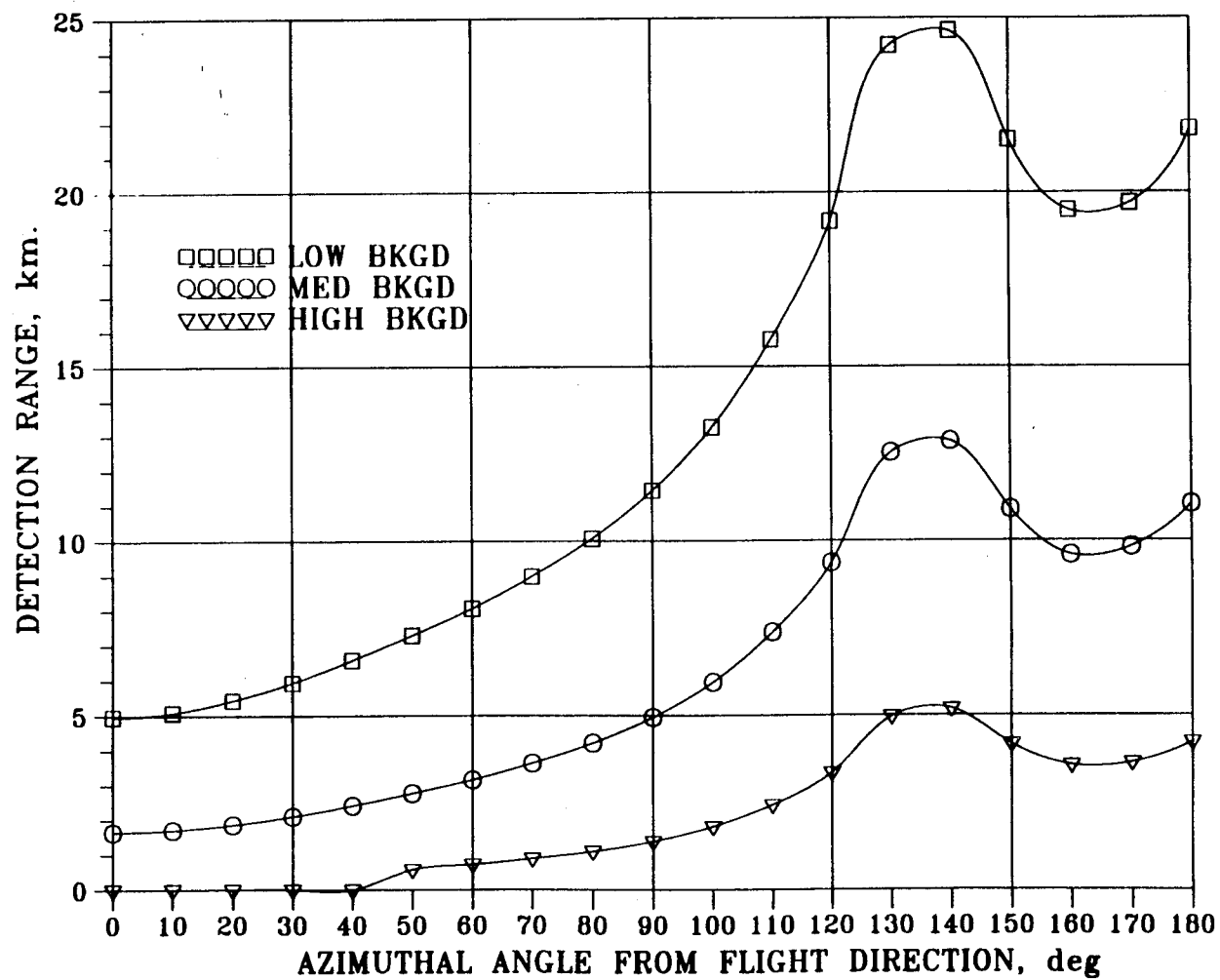
Figure 12   Detection range performance predictions for initial detector design, for three background levels.
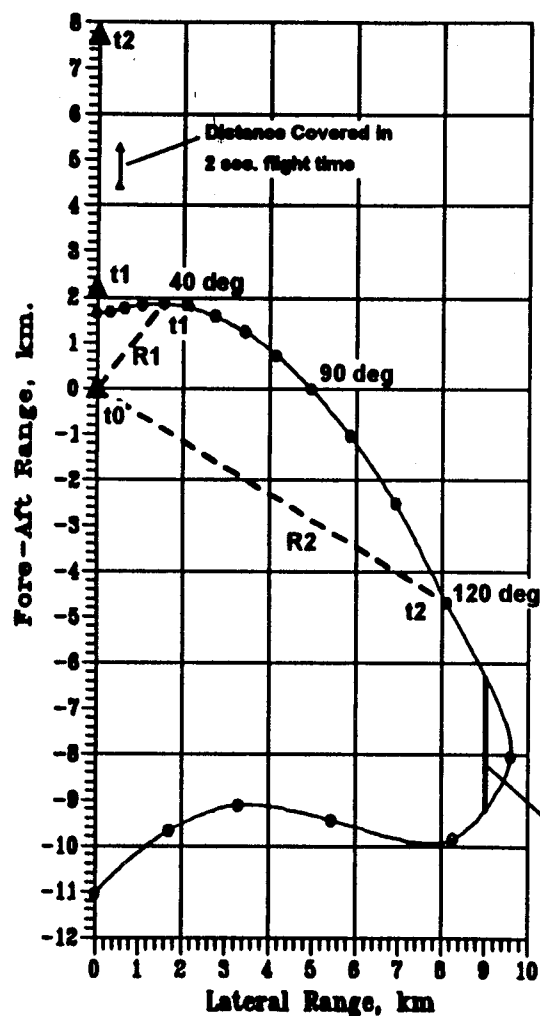
Median Suburban Background

c = 0.3404 km/sec
Va/c = 0.272 km/sec

At 40 deg emission azimuth

R1 = 2.42 km to detection edge
t1 = 7.11 sec. at arrival
(after emission)
Ra/c = 2.21 km at t1 + 1 sec.

At 120 deg emission azimuth

R2 = 9.37 km
t2 = 27.52 sec
Ra/c = 7.76 km at t2 + 1 sec

▲ Aircraft position at signal reception time

At 9 km lateral range, detectable
for duration of 10.48 seconds

Figure 13   Detection footprint analysis of initial detector design, median background level, showing aircraft position at signal reception for two emitted rays.
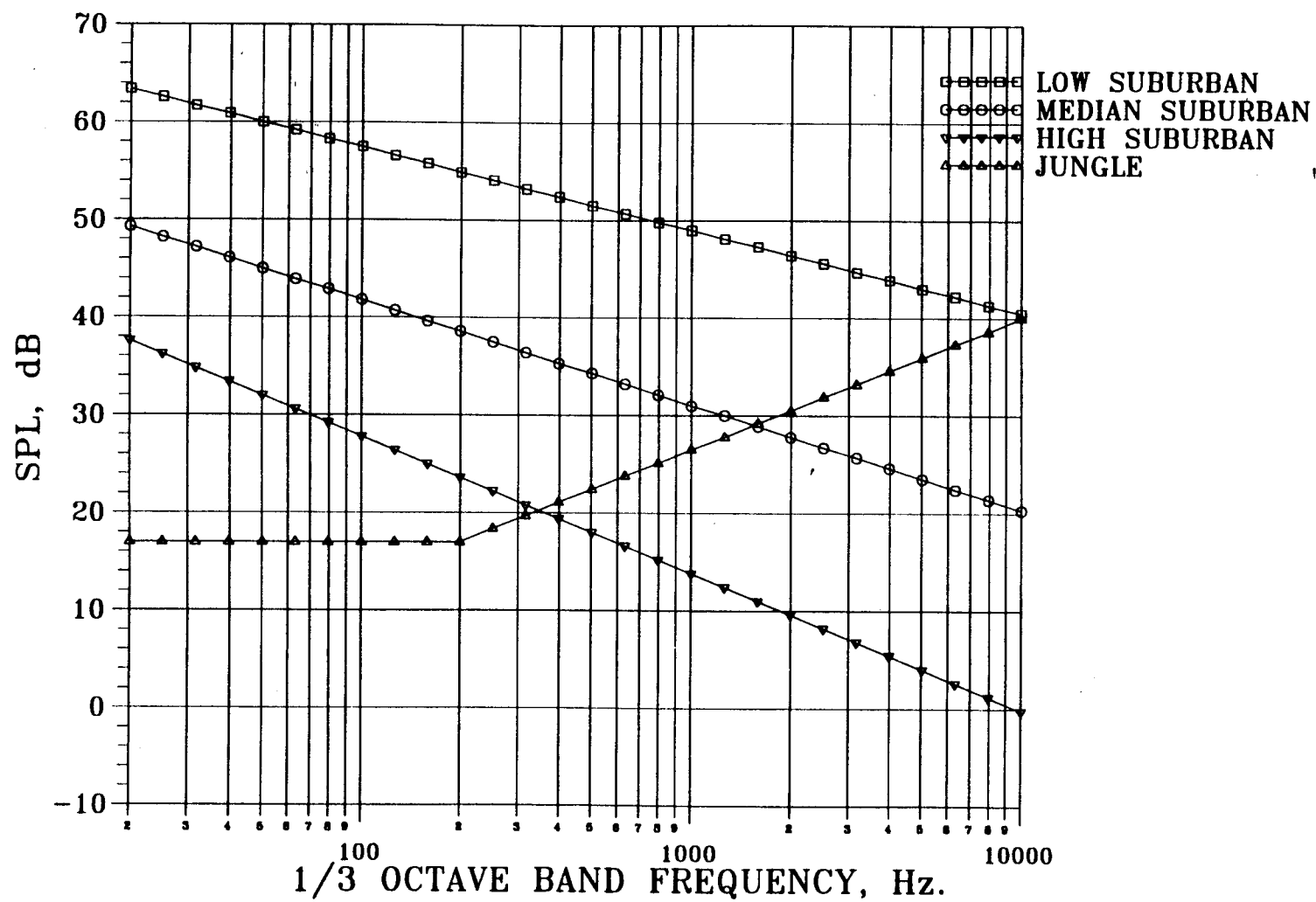
Figure 14   Third octave band background noise spectra from Lockheed report.
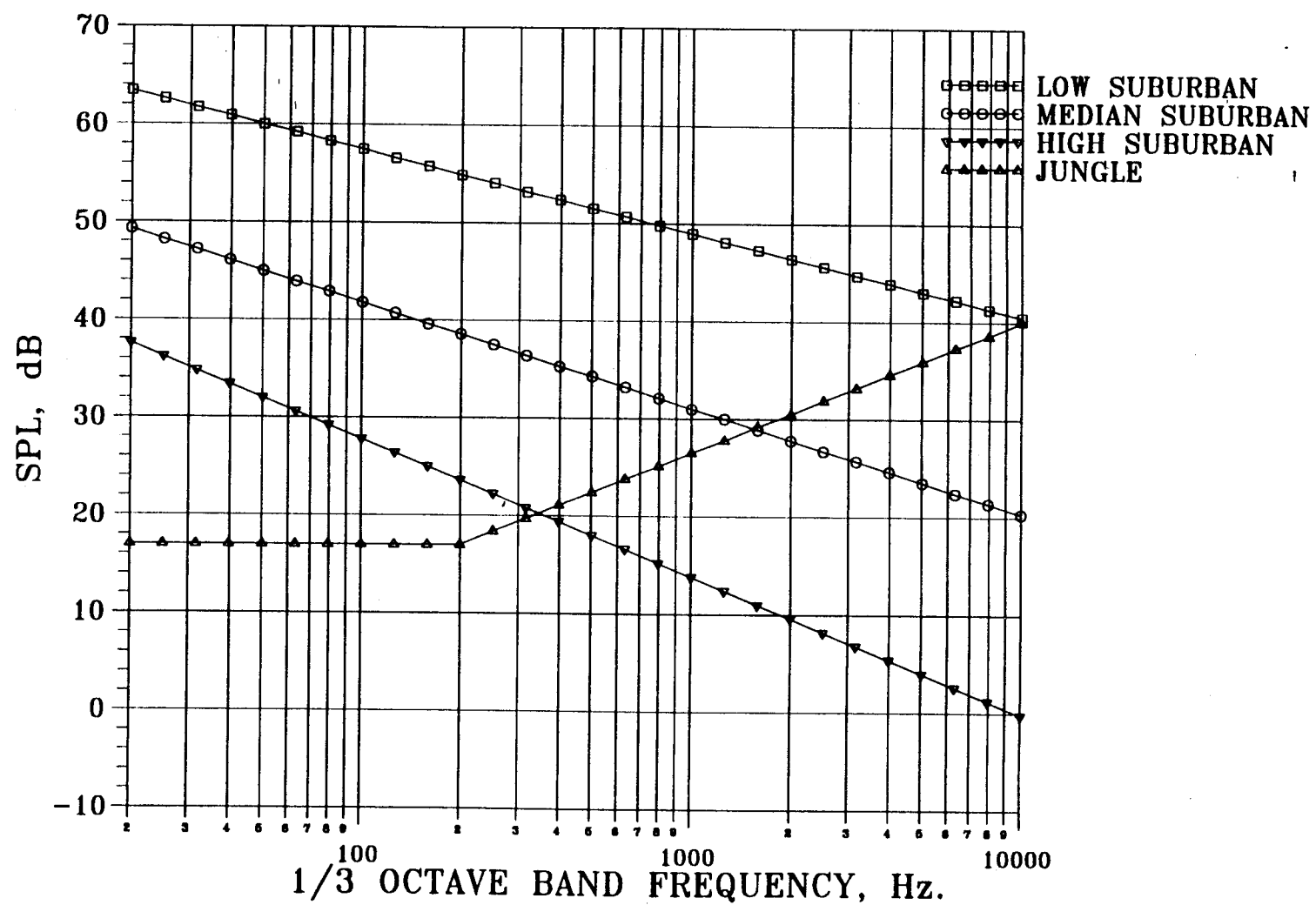
Figure 15   Third octave band background noise data provided by NASA Langley.

CASE #	100 HZ	125 HZ	160 HZ	200 HZ
1	52.0	51.5	51.0	50.0
2	49.0	47.5	47.5	47.5
3	45.5	45.0	42.0	39.0
4	28.0	27.0	26.0	26.0
5	59.0	59.5	59.5	58.5
6	55.0	53.5	50.0	46.0
7	46.5	46.0	46.0	45.0
8	44.5	43.0	40.0	35.0
9	37.0	37.0	36.0	35.0
10	52.5	52.0	46.0	44.0
11	45.0	46.5	46.5	46.5
12	43.5	45.0	40.0	37.0
13	38.0	38.0	36.0	34.5
14	43.5	45.0	40.0	36.5
15	57.0	57.0	53.0	50.0
16	46.0	43.0	40.0	38.0
17	40.0	40.0	35.0	30.0
18	20.0	21.0	21.0	21.5
19	57.0	55.0	49.0	48.0
20	45.5	45.0	37.5	38.0
21	52.0	52.5	51.0	49.0
22	49.0	47.5	44.0	40.0
23	44.0	43.5	38.0	37.0
24	48.0	47.0	44.0	43.0
25	53.0	53.0	52.5	52.0
26	41.0	41.0	40.0	39.0
27	44.0	43.0	42.0	41.0
28	35.5	35.0	36.0	36.5
29	43.5	42.0	40.0	38.5
30	15.6	14.5	13.5	13.0
31	46.0	45.0	43.0	43.5
32	49.5	48.5	48.0	48.0
33	51.5	50.5	50.5	50.5
34	48.5	47.5	47.0	48.0
35	40.0	48.0	38.0	46.0
36	50.5	49.5	48.0	48.0
37	50.0	50.5	47.5	48.0
38	51.0	51.0	47.5	47.5
AVERAGE	45.187	44.921	42.434	41.434
STDDEV	8.987	8.899	8.689	8.753

Figure 16   Statistical analysis of background noise data from multiple sources for four 1/3 octave bands.
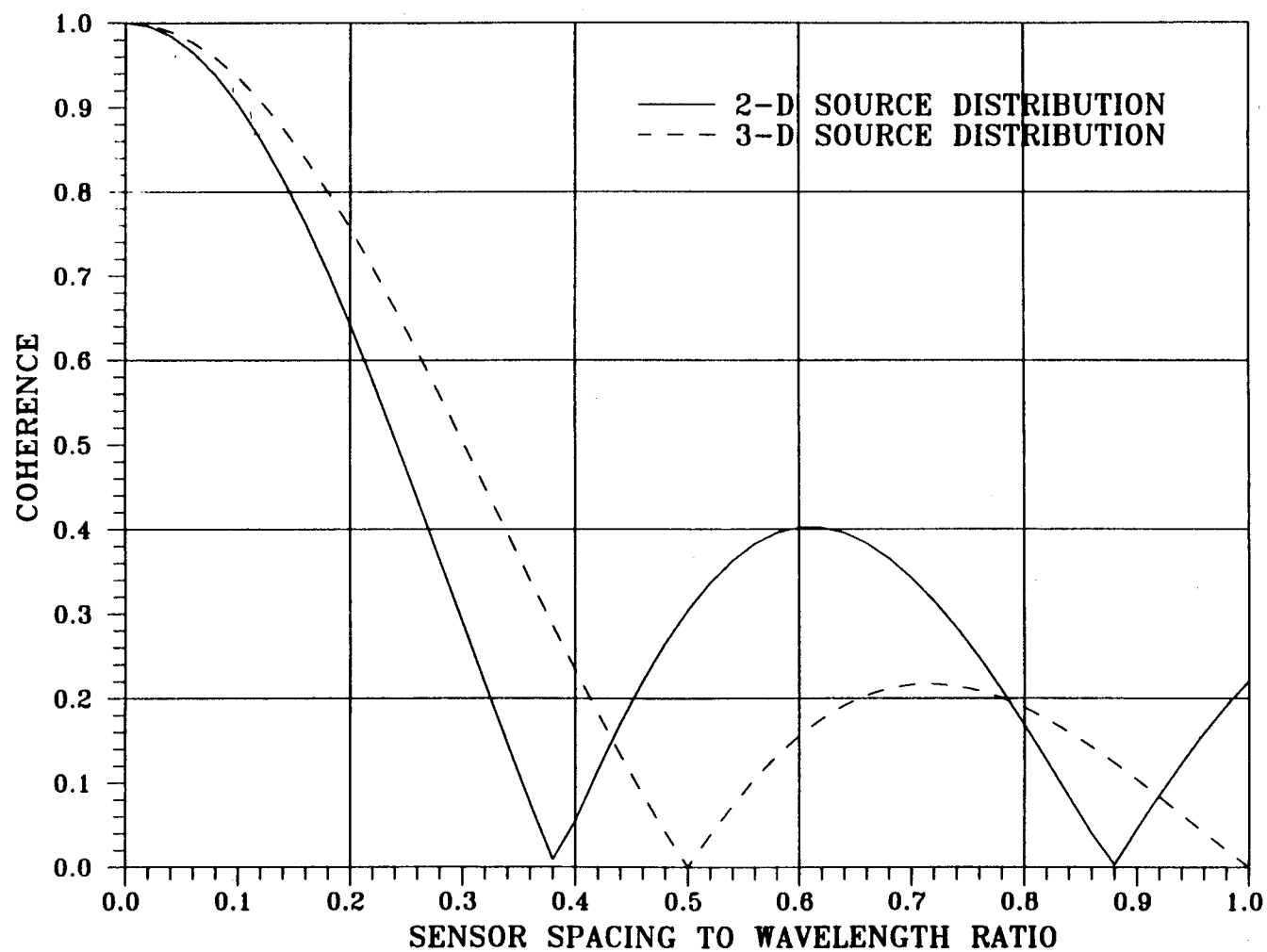
52

Figure 17   Two-sensor signal coherence as a function of array sensor spacing to wavelength ratio for two and three dimensional isotropic ambient noise fields.
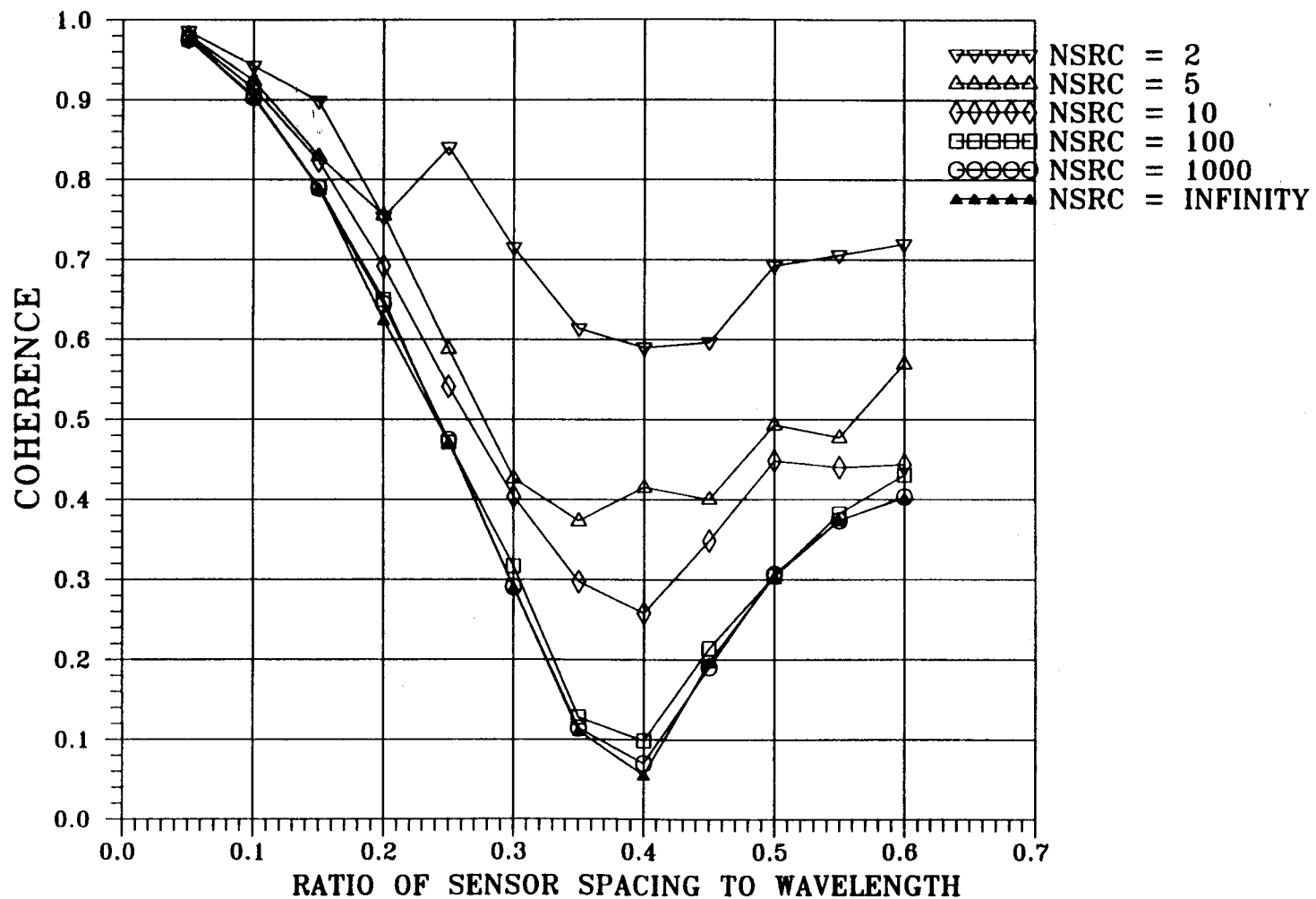
Figure 18   Variation of sensor-to-sensor ambient noise coherence with array d/λ for various number of sources, 30 averages taken to provide mean value.
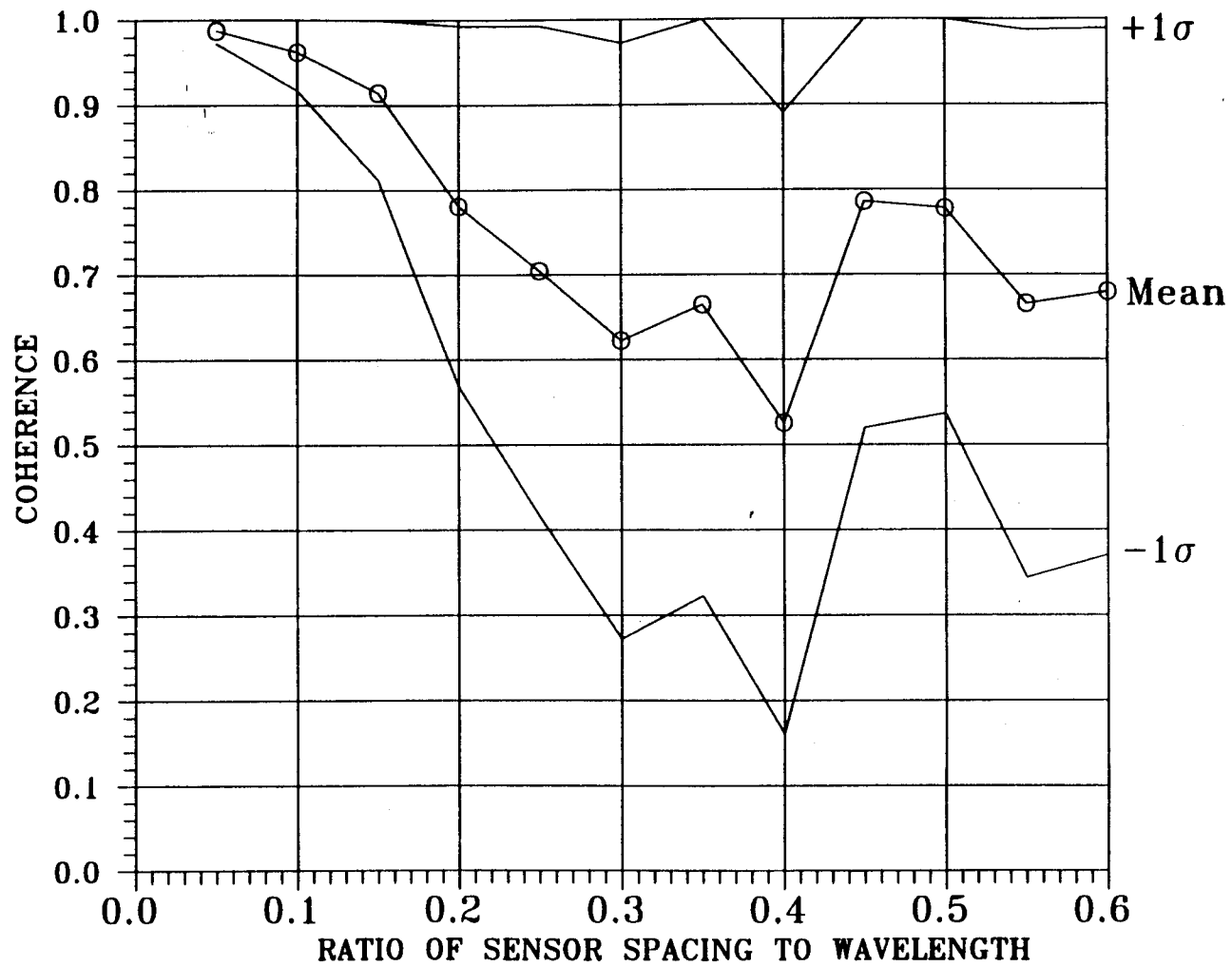
Figure 19　　　　Mean value and standard deviation of ambient noise coherence as a function of d/λ for 2 noise sources, average of 30 random samples.
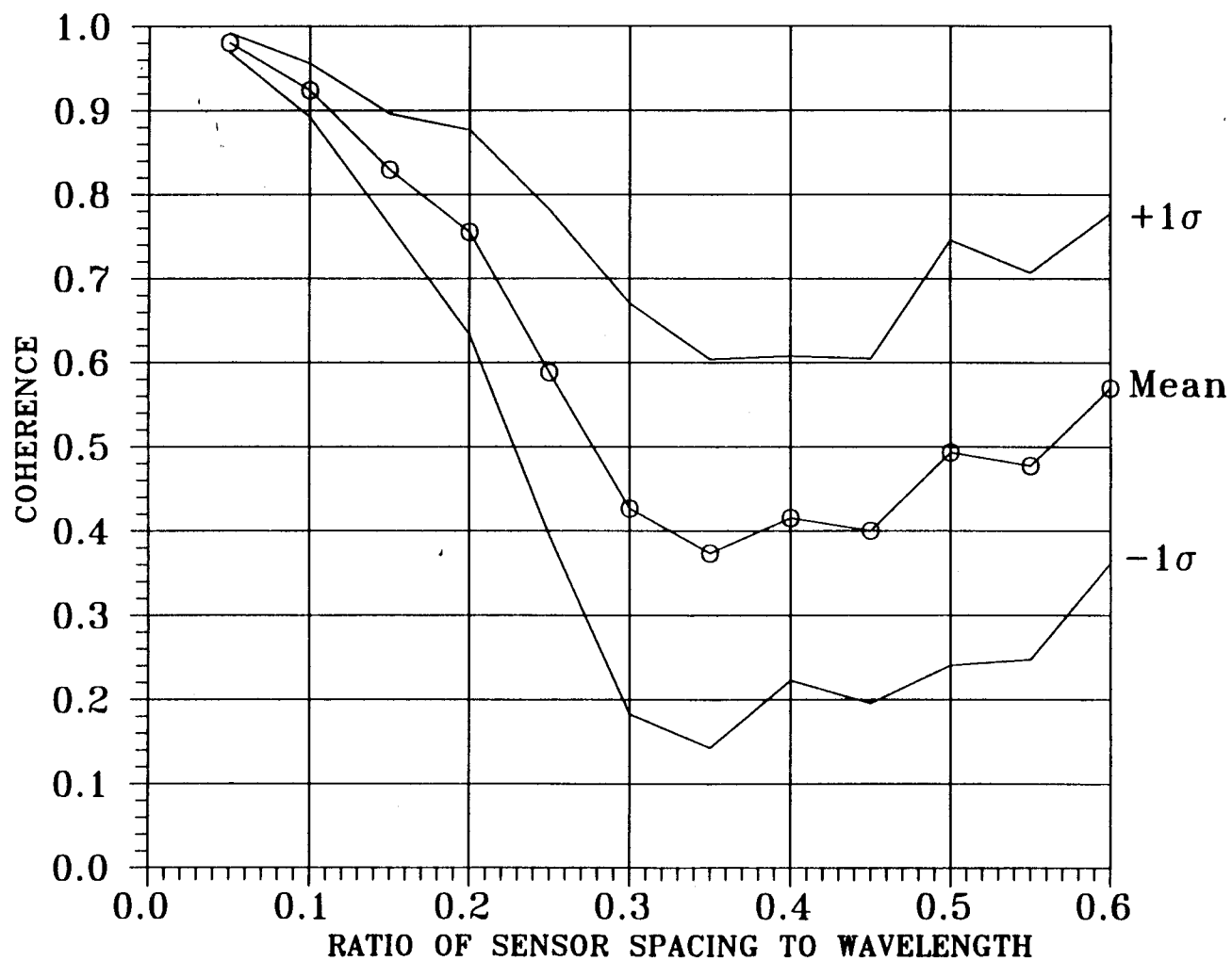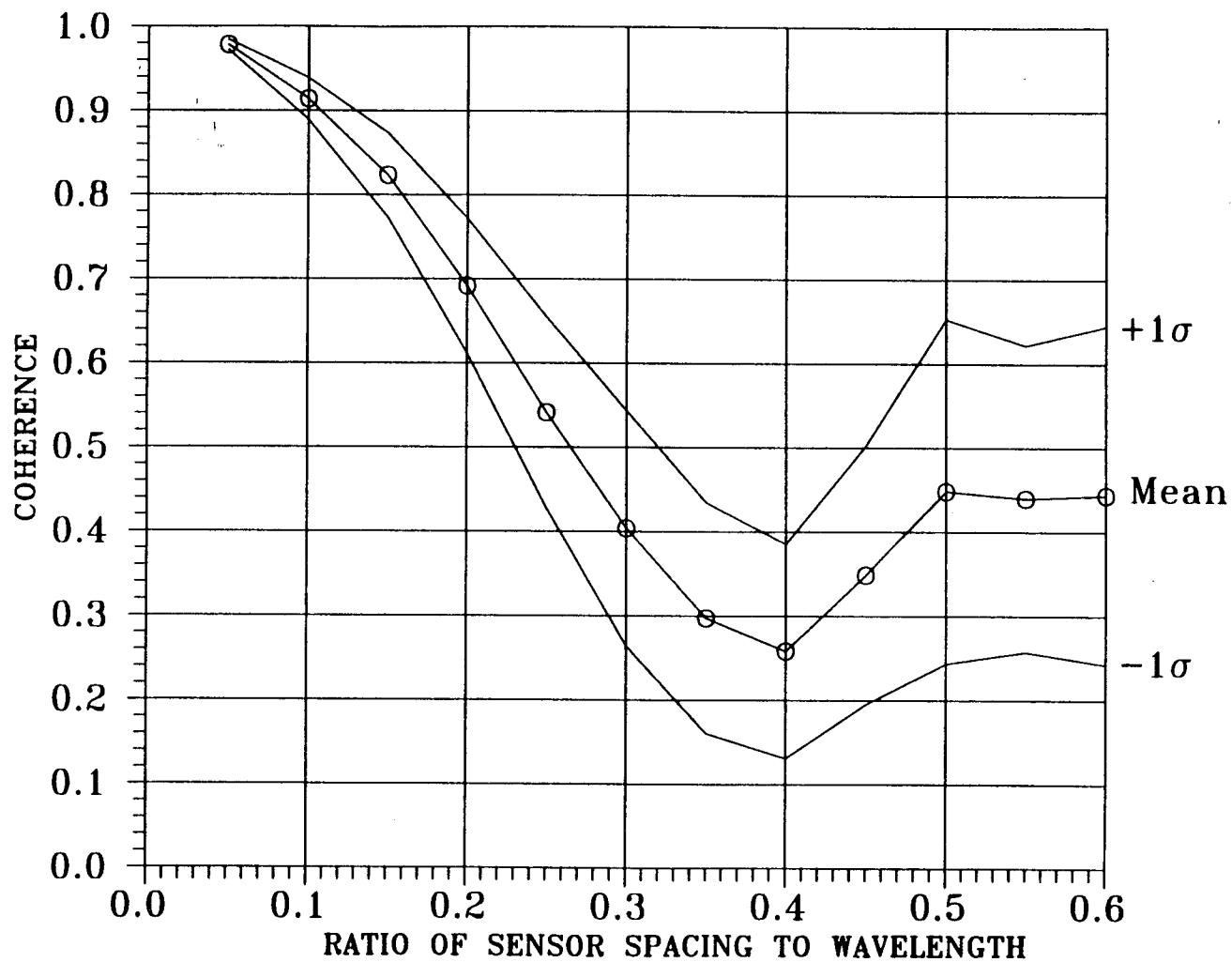
Figure 20   Mean value and standard deviation of ambient noise coherence as a function of d/λ for 5 noise sources, average of 30 random samples.

Figure 21   Mean value and standard deviation of ambient noise coherence as a function of d/λ for 10 noise sources, average of 30 random samples.
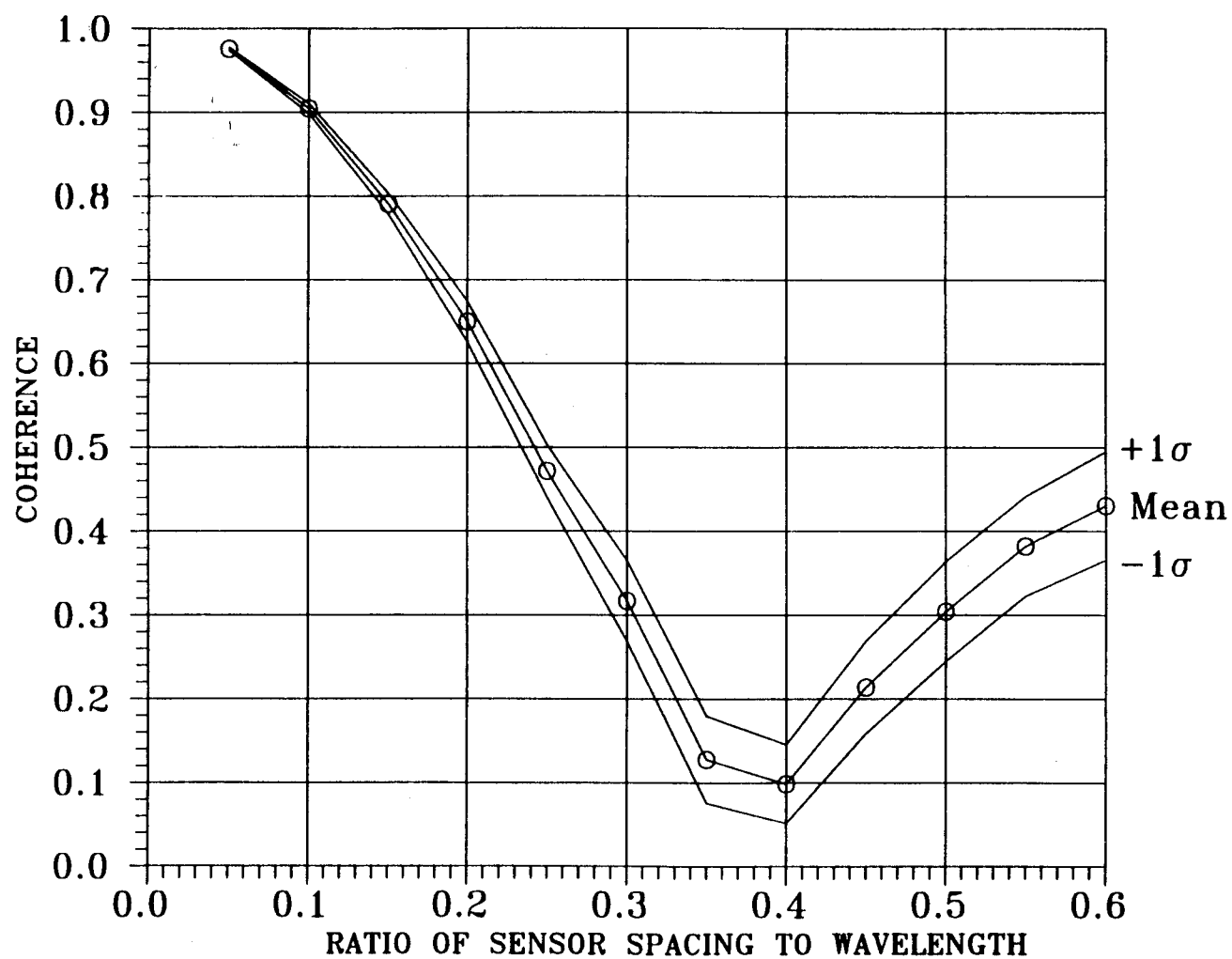
Figure 22   Mean value and standard deviation of ambient noise coherence as a function of d/λ for 100 noise sources, average for 30 random samples.
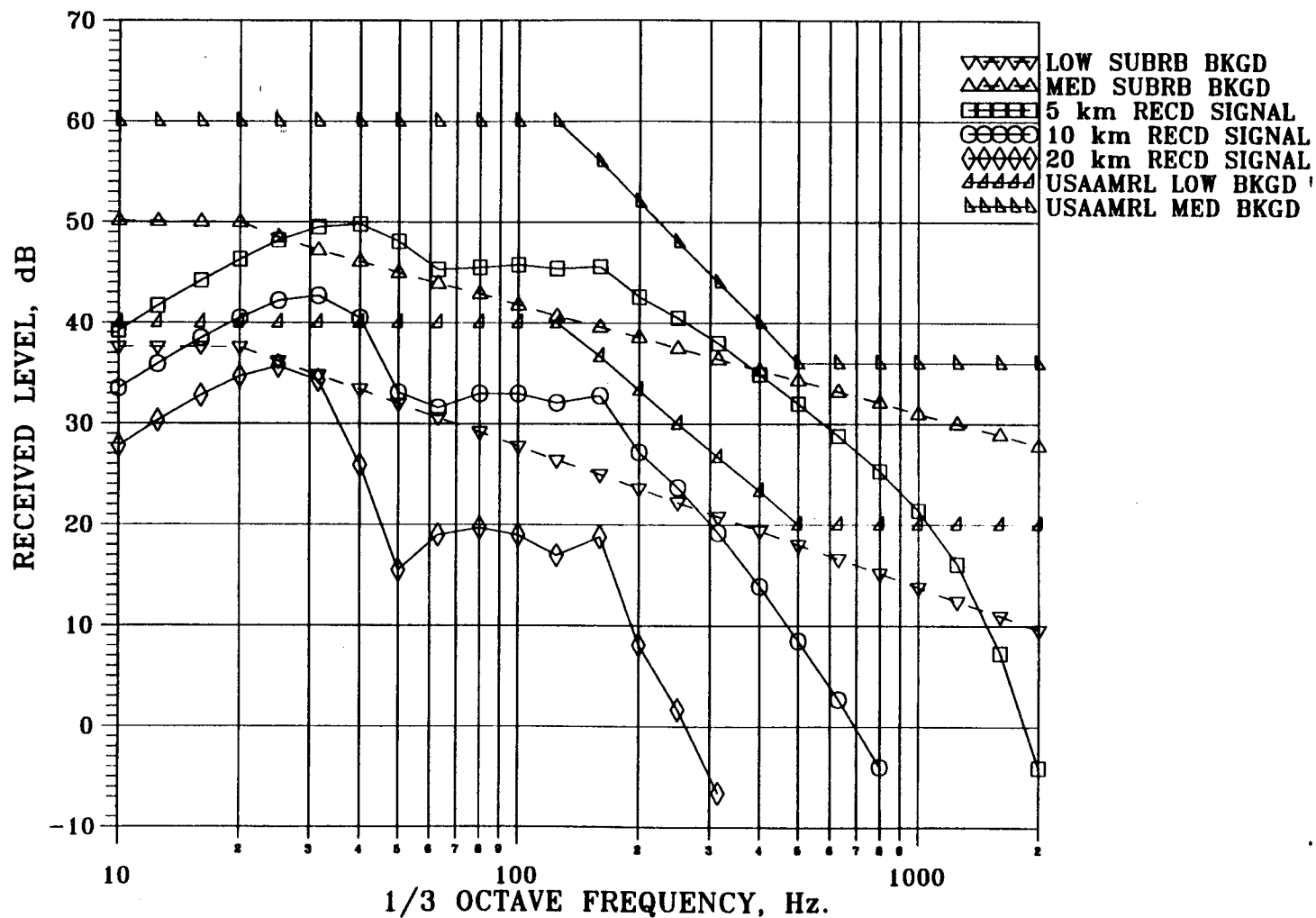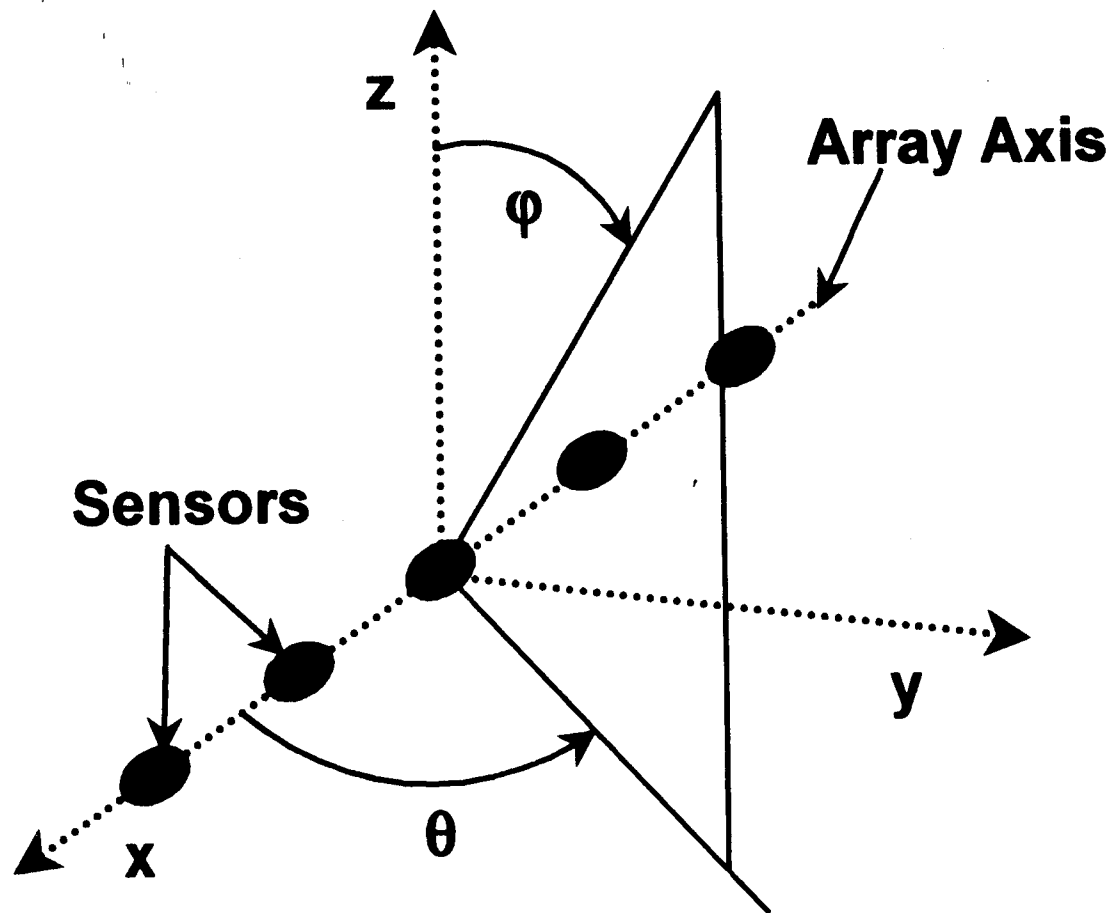
Figure 23   Received jet noise signal for revised jet noise source parameters for aircraft at 61 meters, compared to various background environments.

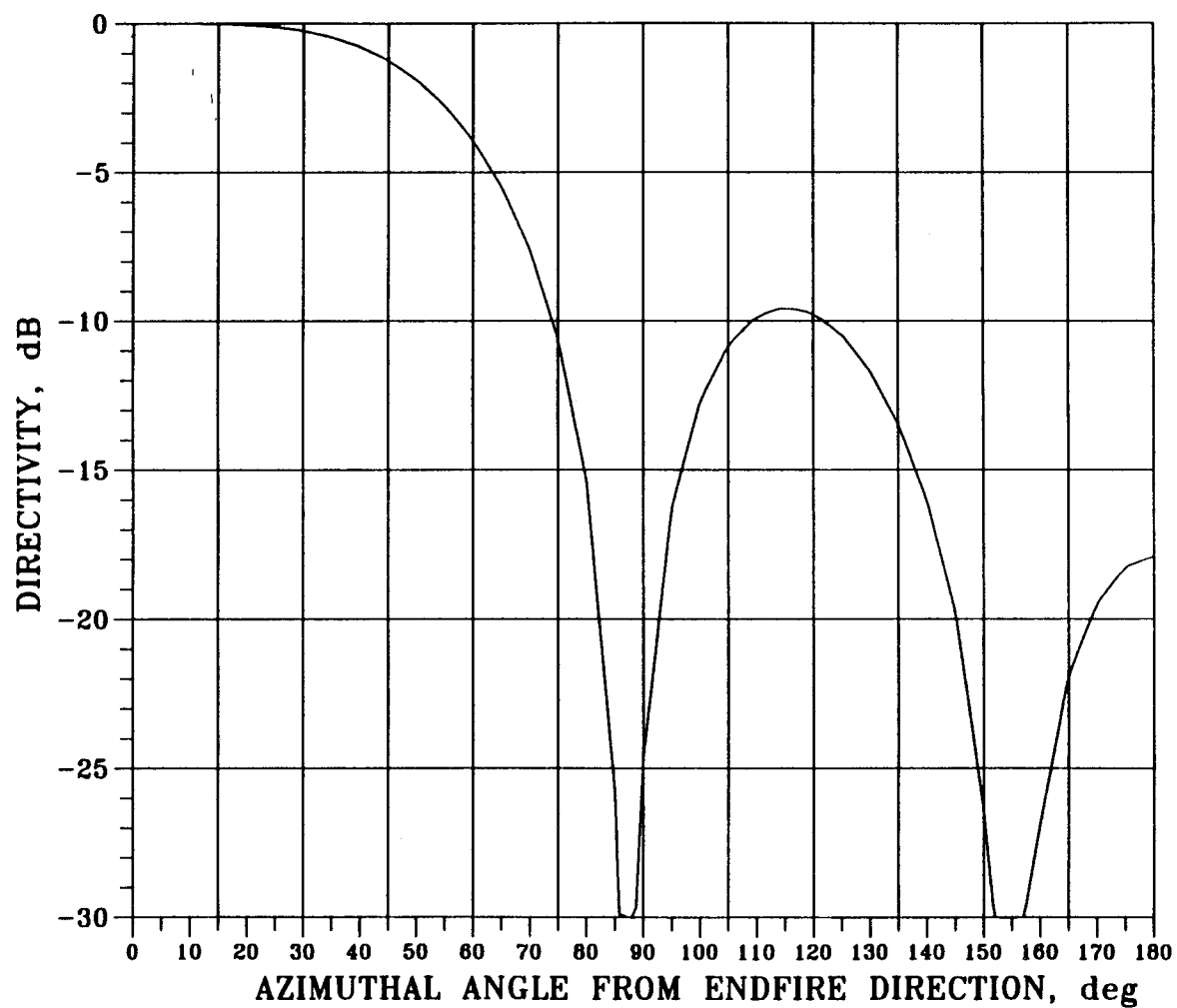Figure 24　　Geometry and coordinate system conventions for the linear endfire array.

Figure 25   Beam directivity pattern for three-sensor endfire array in the horizontal plane. Sensor spacing d/λ = 0.35.
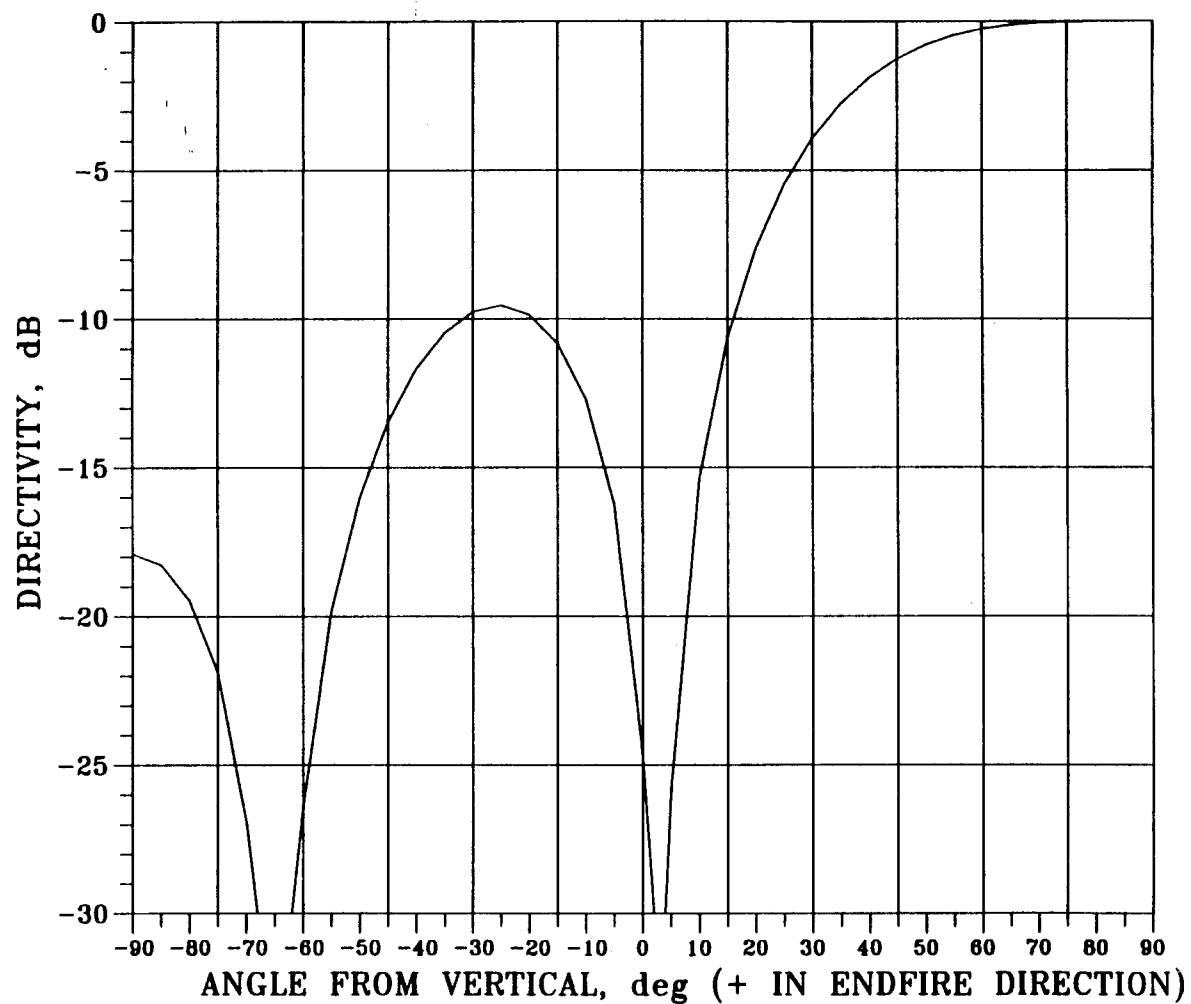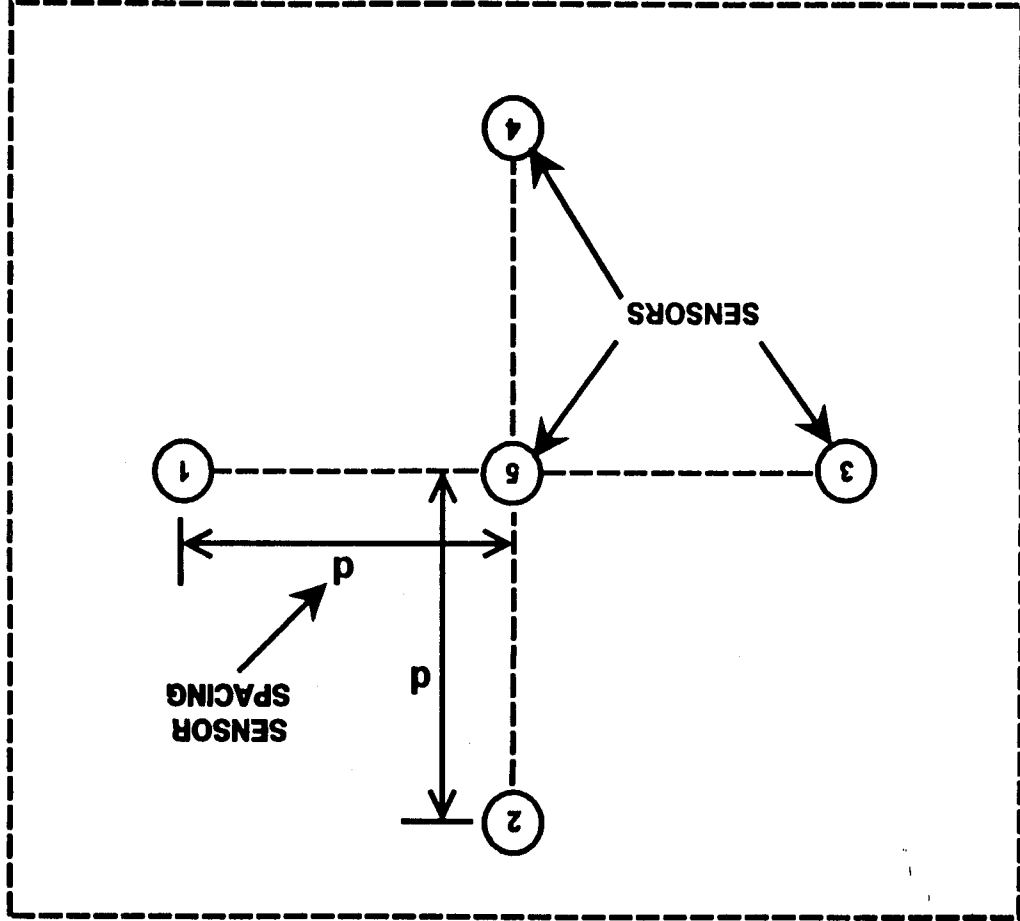
Figure 26   Beam directivity pattern for three sensor endfire array in a vertical plane aligned with the x- or the y-axis. Sensor spacing $d/\lambda = 0.35$.

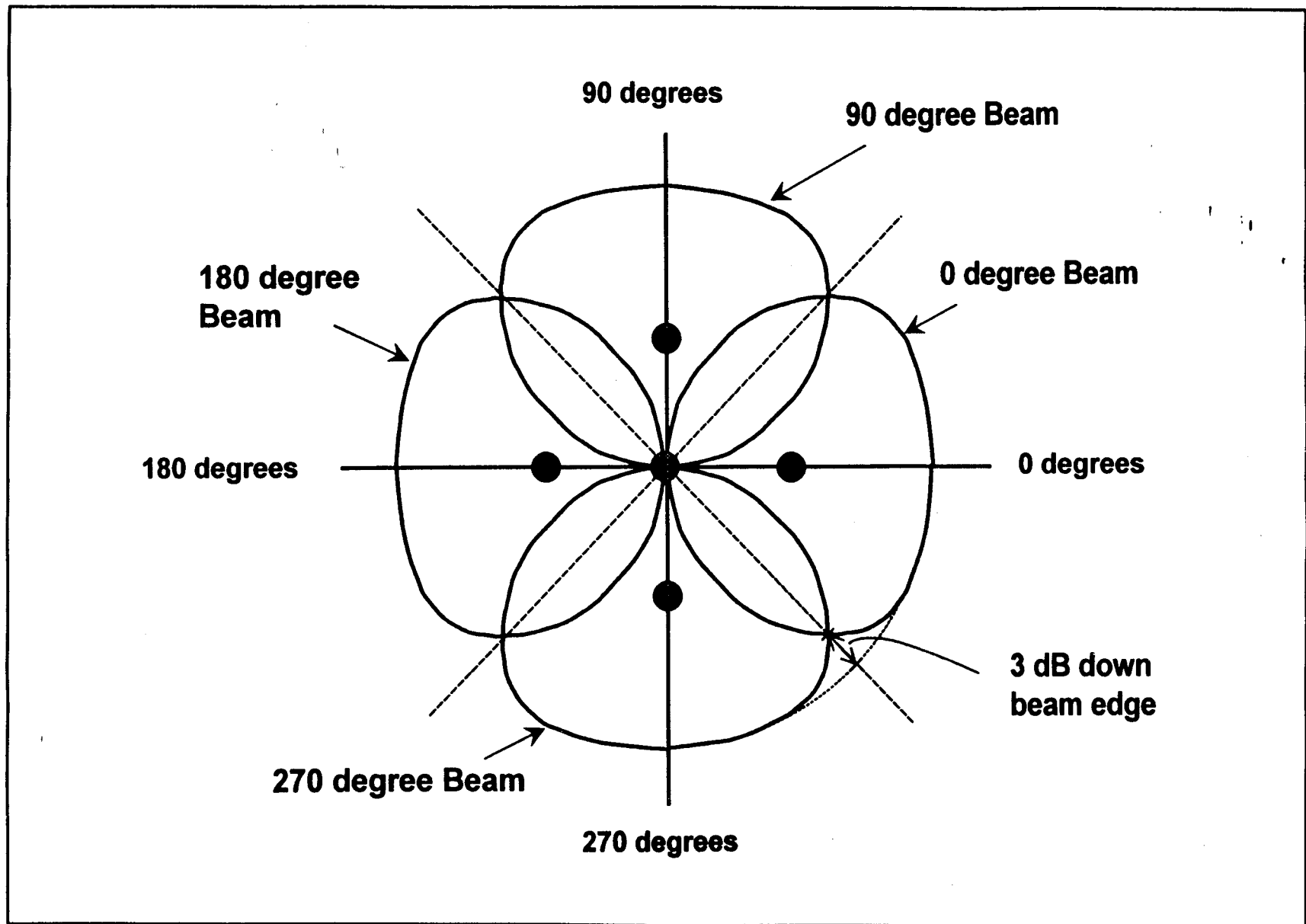Figure 27   Sensor geometric configuration of the crossed endfire array.

63

Figure 28   Illustration of overlapping beam patterns in the horizontal plane for the crossed endfire array.

**Vertical Beam
(Mills Cross)**

**Horizontal
Beam
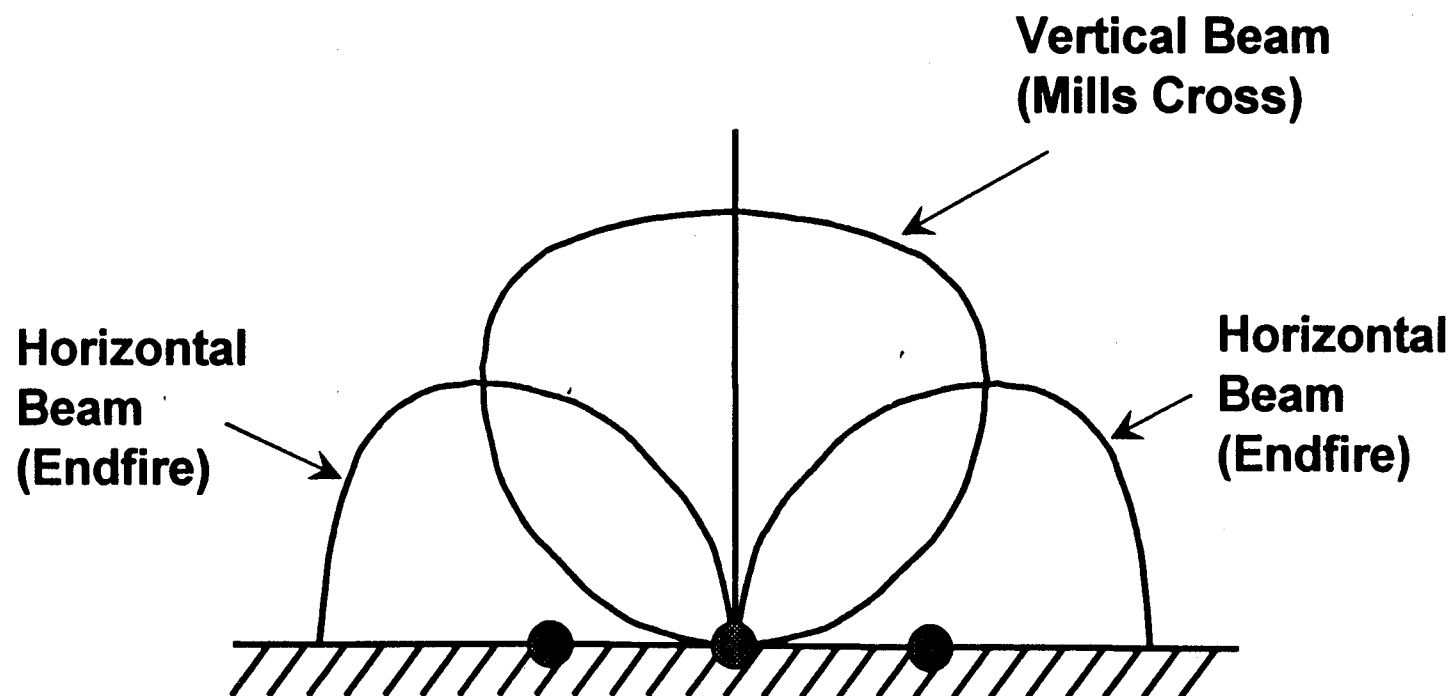(Endfire)**

**Horizontal
Beam
(Endfire)**

Figure 29   Illustration of overlapping beams in the vertical plane for combined Mills Cross and crossed endfire array.
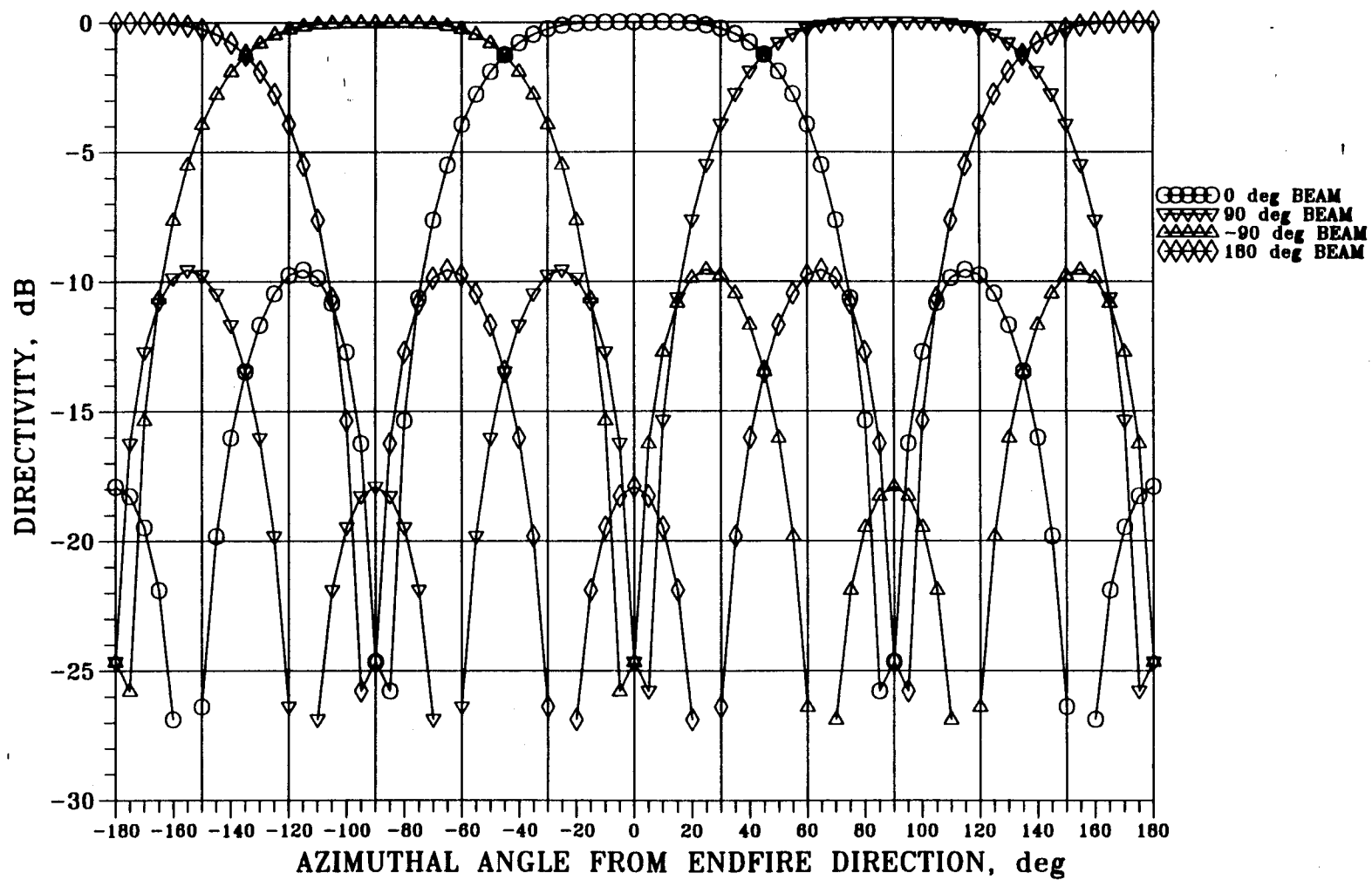
Figure 30   Crossed endfire array azimuthal directivity in the horizontal plane for predicted beam patterns.
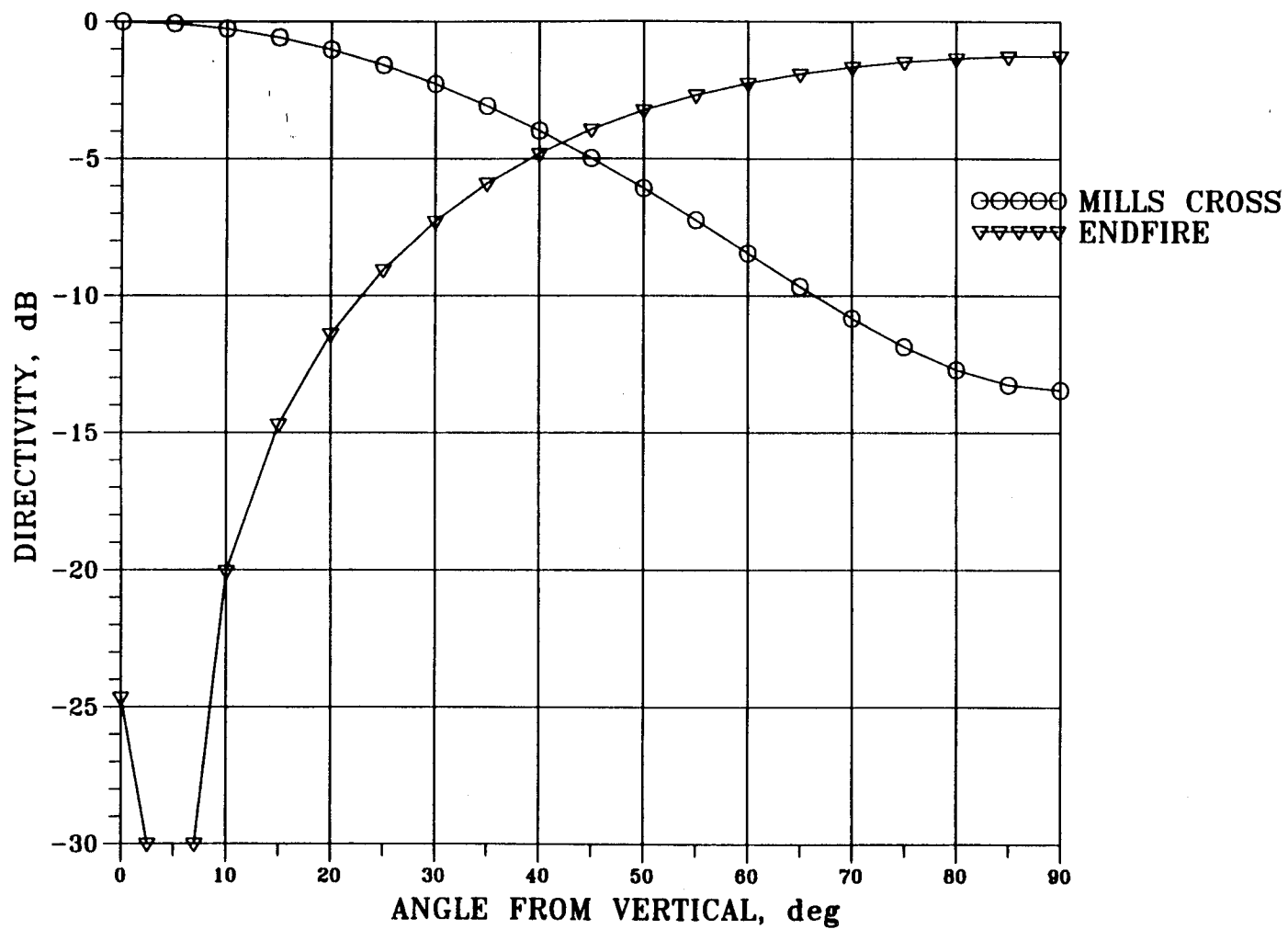
Figure 31   Vertical directivity for 5-sensor Mills Cross array beamed upward showing overlap with vertical beam pattern for 3-sensor endfire array.   Vertical cut at 45 degree azimuth angle.
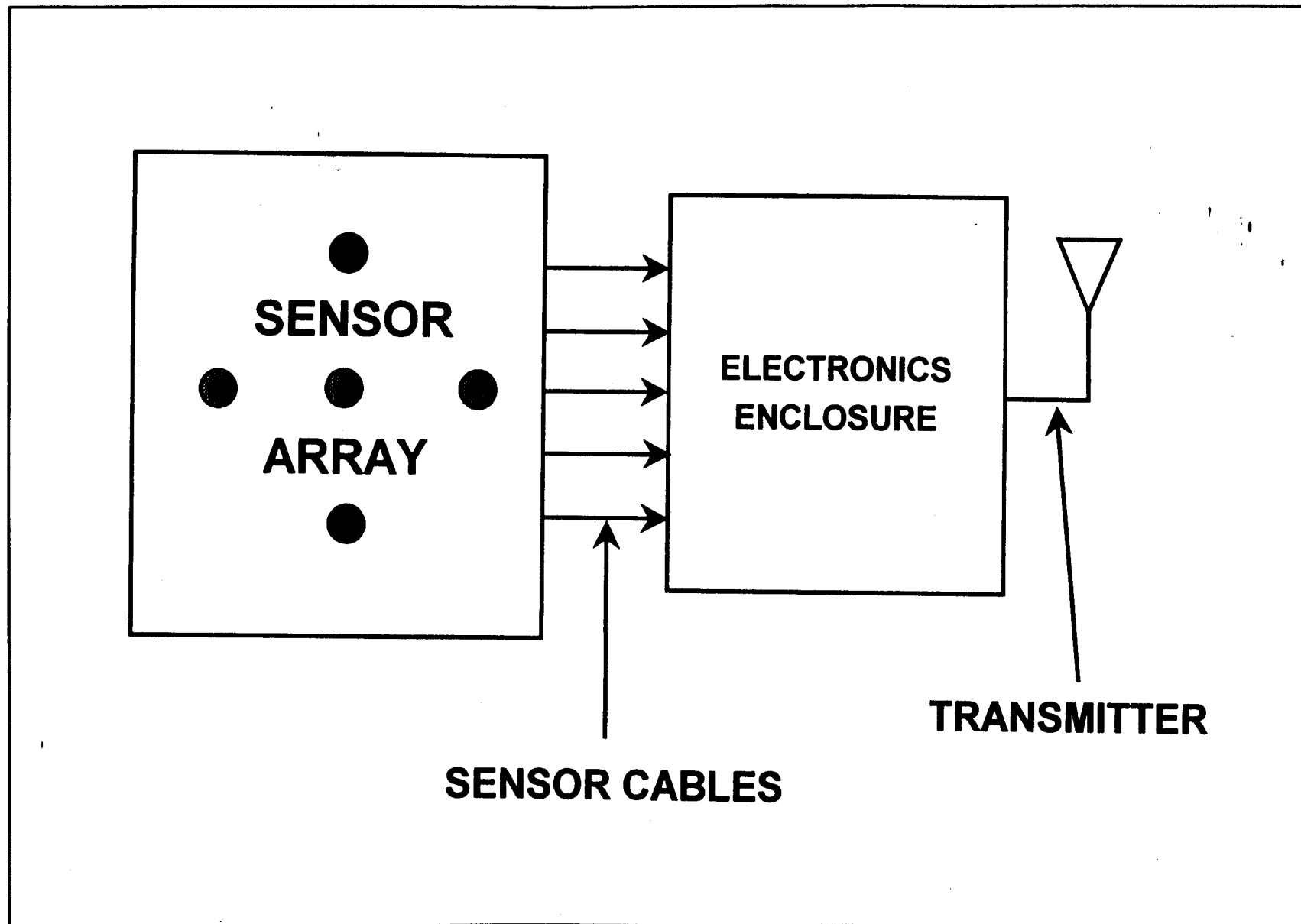
Figure 32   Components of acoustic array detection system.

ARRAY GEOMETRY

90°
②
180° ③ — ⑤ — ① 0°
④
270°

BEAMFORMER PROCESSOR

(S1) (S5) (S3) → AVERAGED 0 deg BEAM PHASE SHIFT AND SUM (ENDFIRE) → 0 deg. OUTPUT LEVEL → COMP. → DETECTION?
DETECTION THRESHOLD

(S2) (S5) (S4) → AVERAGED 90 deg BEAM PHASE SHIFT AND SUM (ENDFIRE) → 90 deg. OUTPUT LEVEL → COMP. → DETECTION?
DETECTION. THRESHOLD.

(S3) (S5) (S1) → AVERAGED 180 deg BEAM PHASE SHIFT AND SUM (ENDFIRE) → 180 deg. OUTPUT LEVEL → COMP. → DETECTION?
DETECTION THRESHOLD

(S4) (S5) (S2) → AVERAGED 270 deg BEAM PHASE SHIFT AND SUM (ENDFIRE) → 270 deg. OUTPUT LEVEL → COMP. → DETECTION?
DETECTION THRESHOLD

(S1) (S2) (S3) (S4) (S5) → AVERAGED VERTICAL BEAM PHASE SHIFT AND SUM (MILLS CROSS) → VERTICAL BEAM OUTPUT LEVEL → COMP. → DETECTION?
DETECTION. THRESHOLD.

DETECTION STATUS OUTPUT TRANSMIT POSITIVE DIFFERENCE, ALL BEAMS

DATA ACQUISITION AND SIGNAL PRE-PROCESSING

ACOUSTIC SIGNAL

SYNC

① → F1 → AD1 → B1 → W1 → FFT1 → (S1)
② → F2 → AD2 → B2 → W2 → FFT2 → (S2)
③ → F3 → AD3 → B3 → W3 → FFT3 → (S3)
④ → F4 → AD4 → B4 → W4 → FFT4 → (S4)
⑤ → F5 → AD5 → B5 → W5 → FFT5 → (S5)

F1-F5: Phase-matched analog bandpass parallel filters.
AD1-AD5: Synchronized parallel A-D converters.
B1-B5: Parallel digital data store and hold buffers.
W1-W5: Appropriate digital window functions.
FFT1-FFT5: Parallel FFT processors.
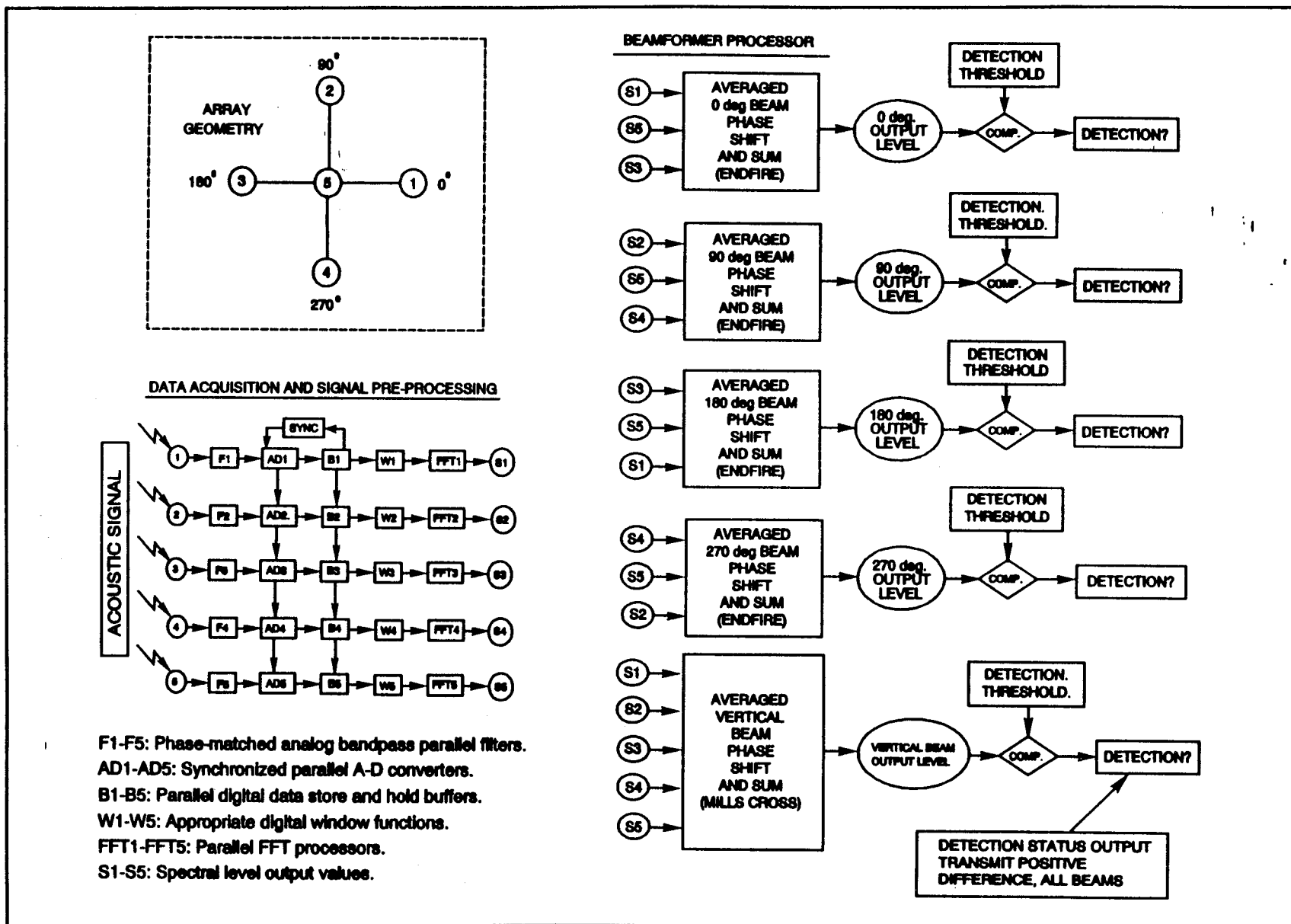S1-S5: Spectral level output values.

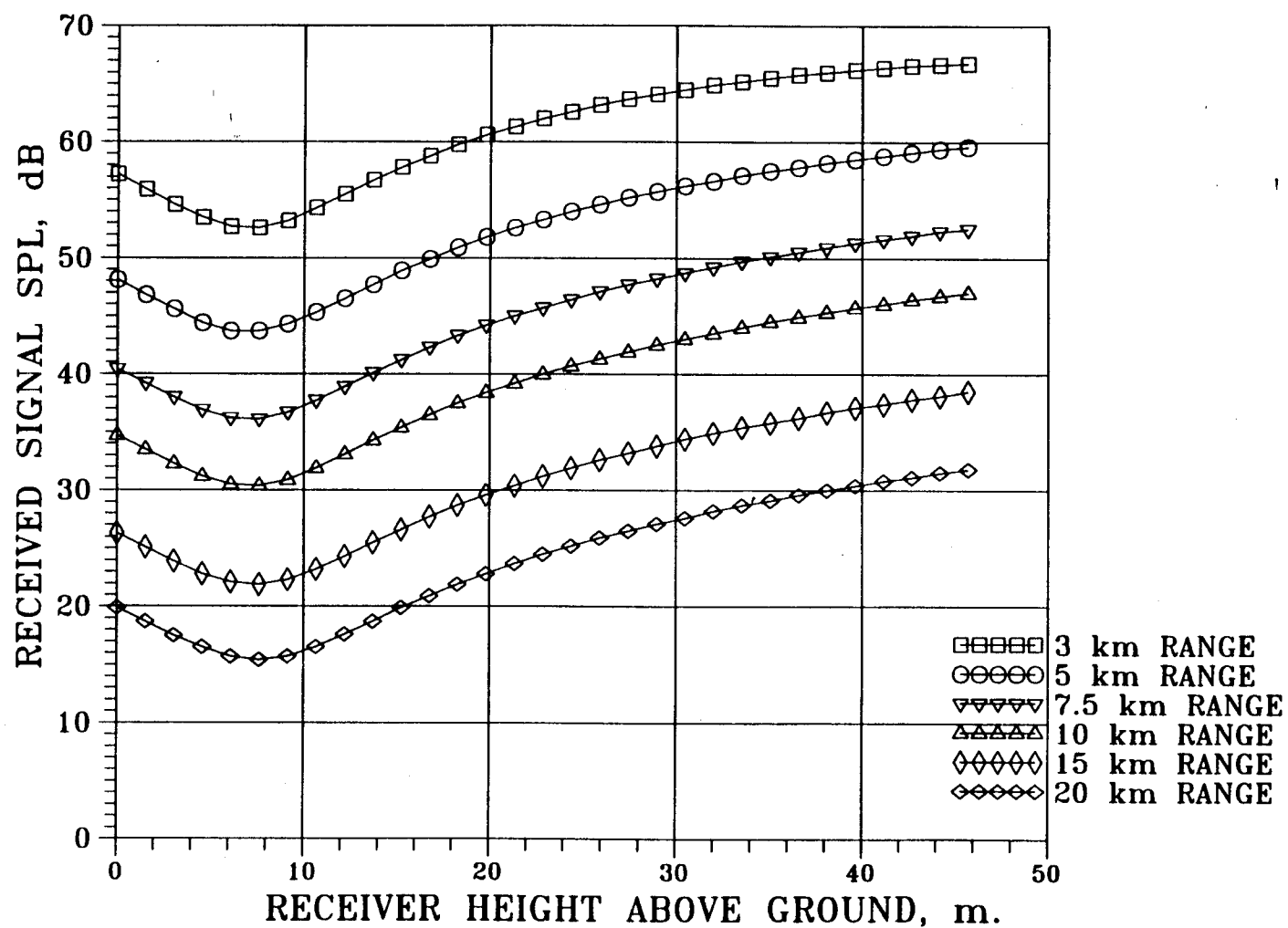Figure 33   Schematic of proposed acoustic array signal processing system.

Figure 34   Effect of receiver height above ground surface on level of received signal for several propagation ranges.
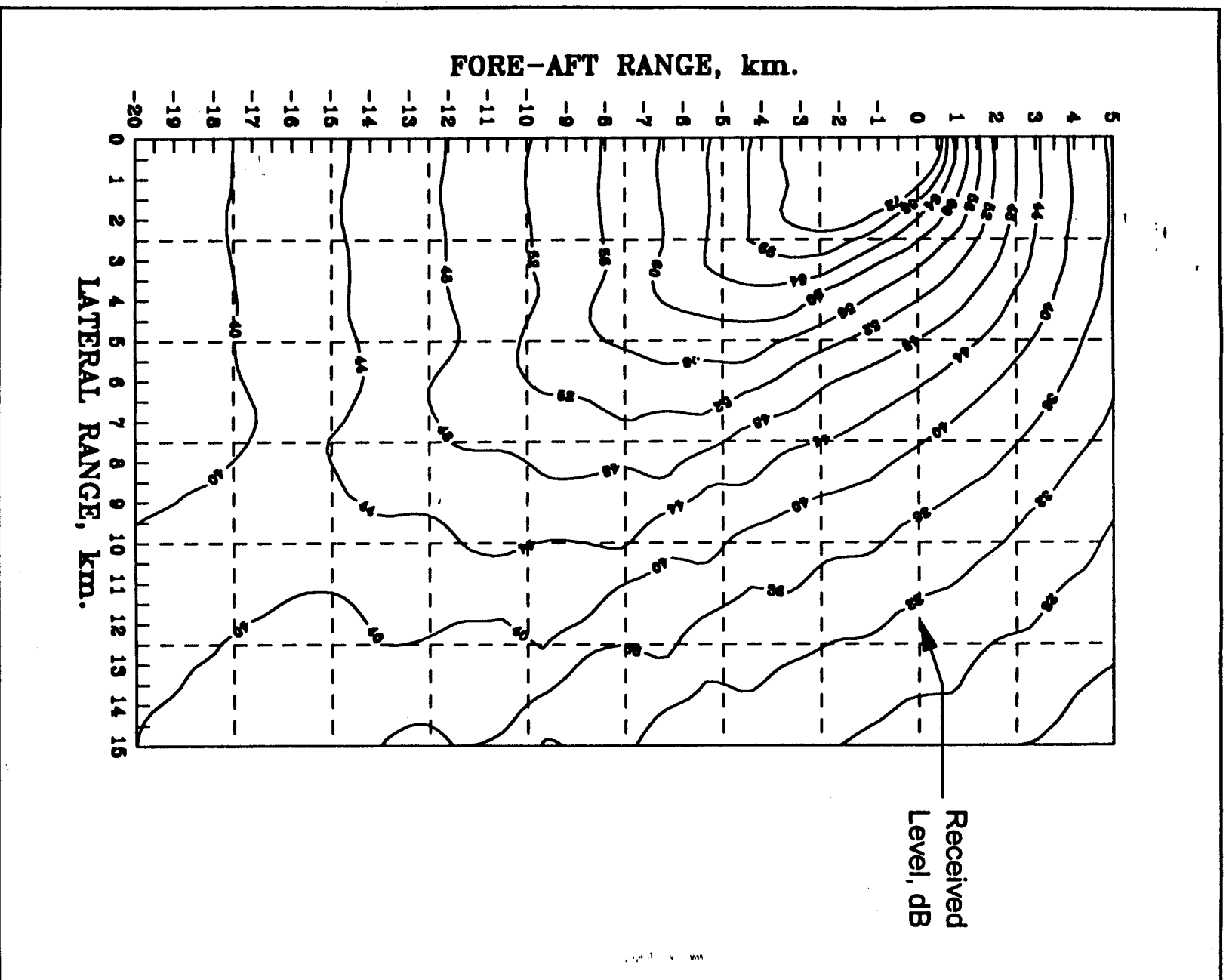
Figure 35   Contours of constant received level for aircraft source in horizontal plane.
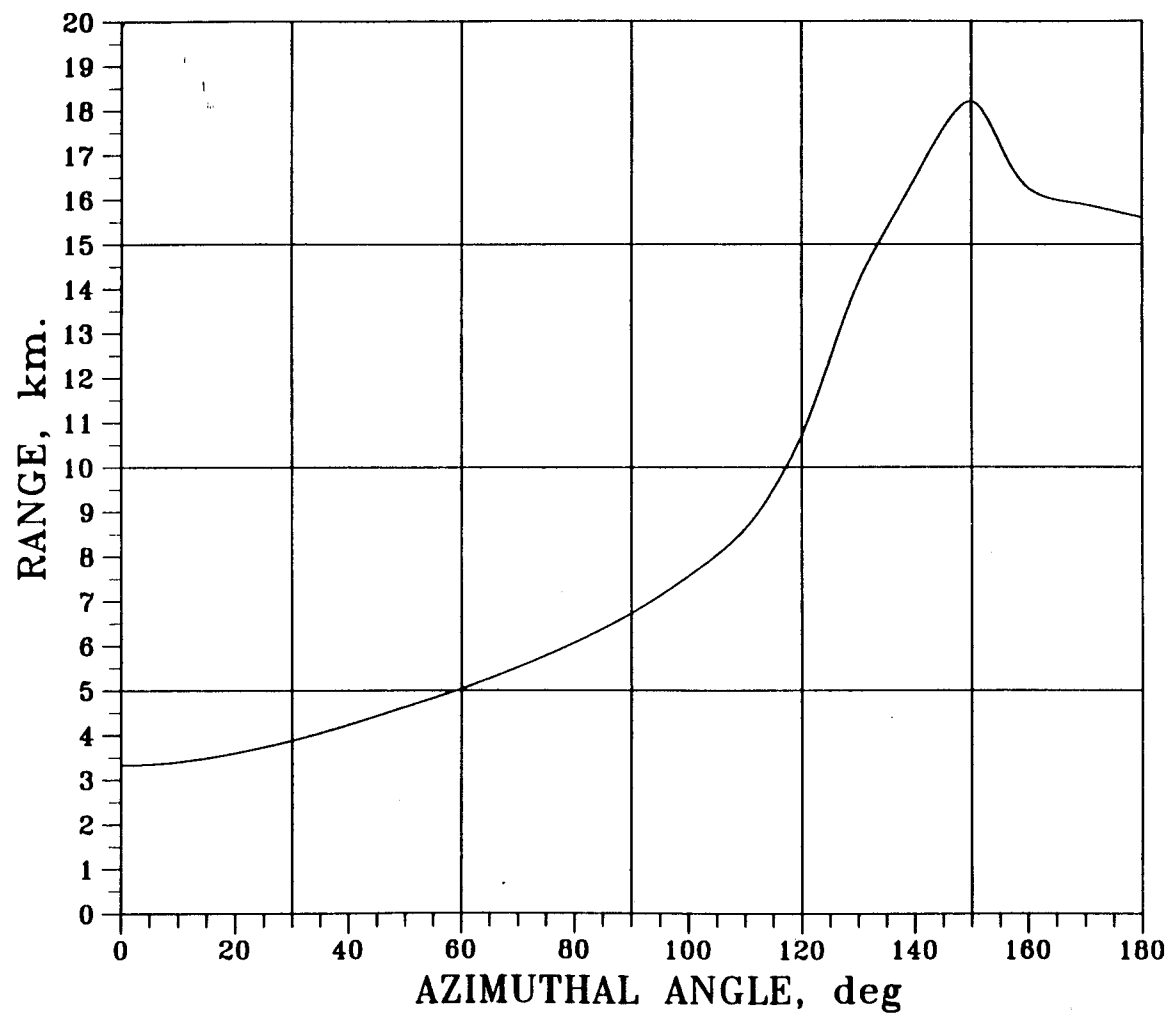
71

Figure 36   Predicted detection range for aircraft source in a median level background environment.
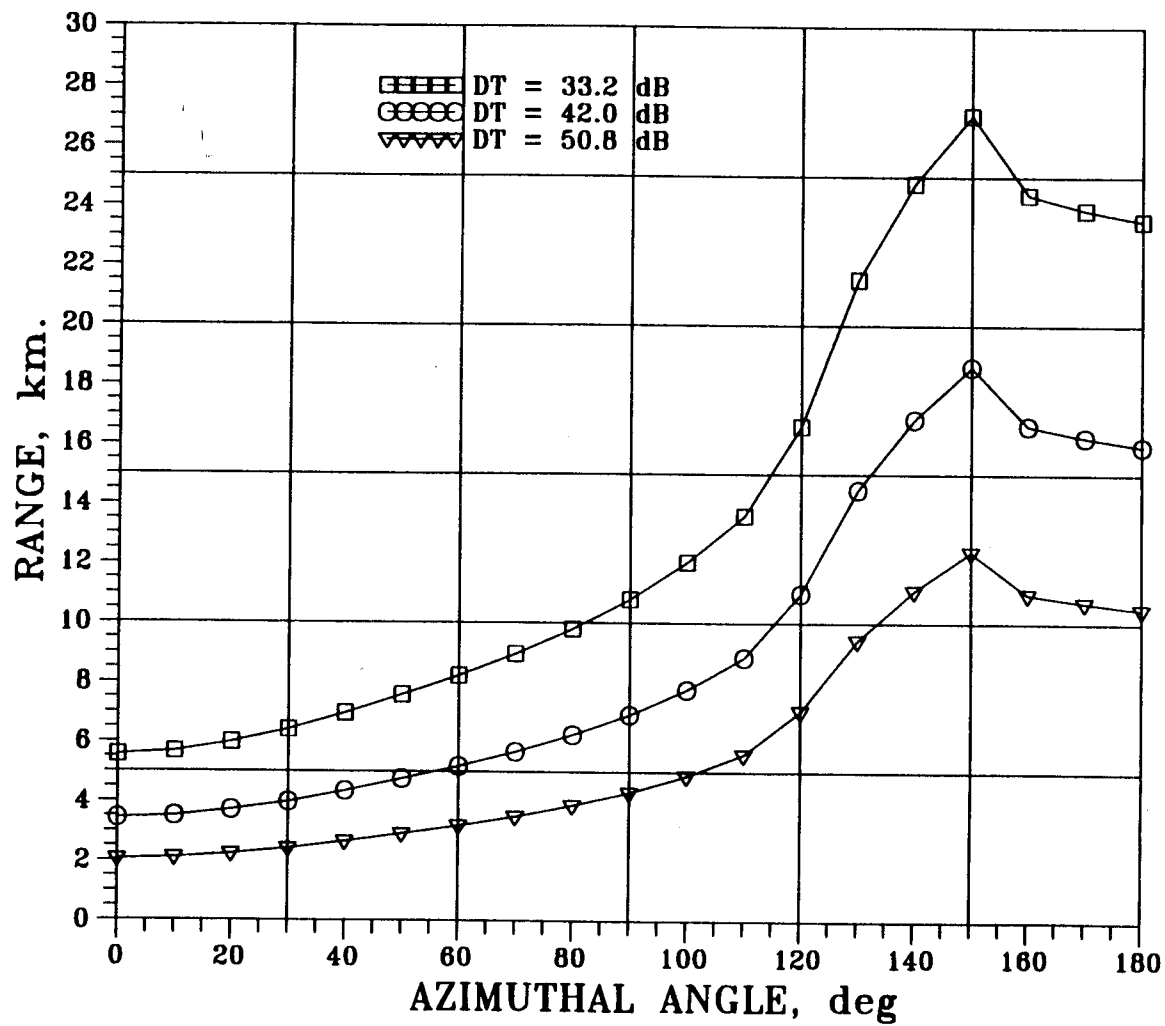
Figure 37 Predicted detection ranges for aircraft source for detection thresholds corresponding to low, median, and high background levels.
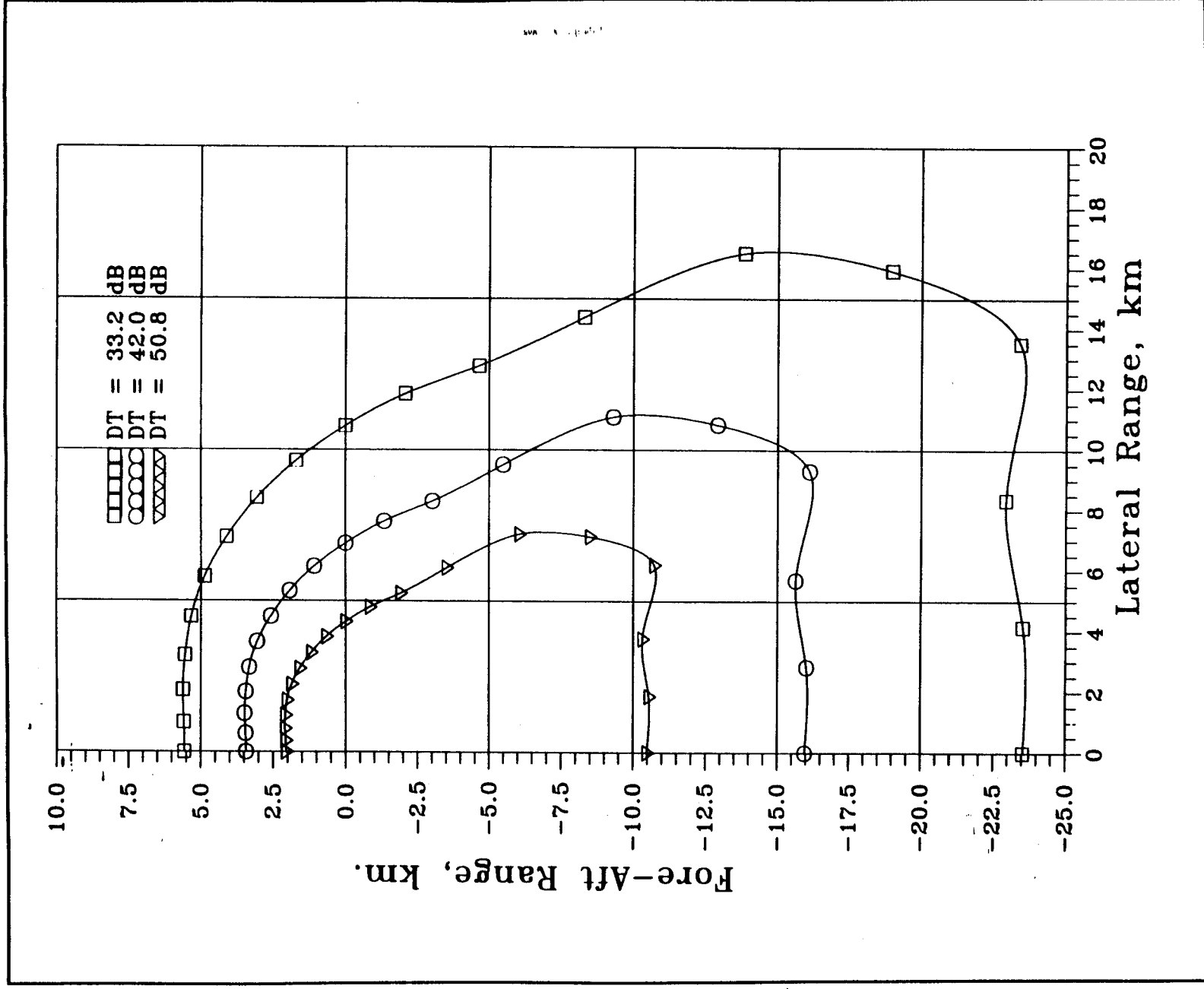
Figure 38   Predicted detection footprints for detection thresholds corresponding to low, median, and high background levels.
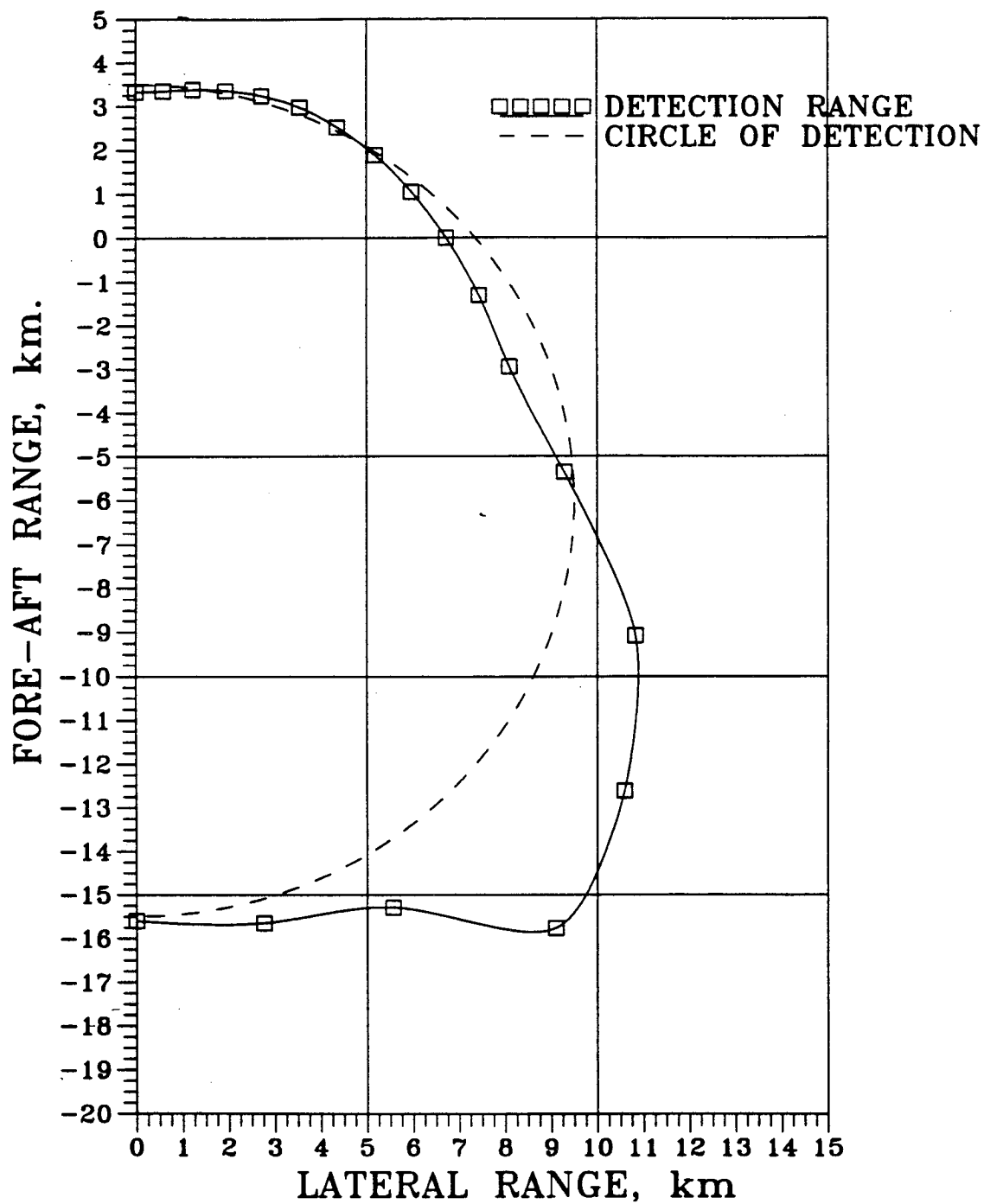
74

Figure 39   Circle of detection to be used for acoustic detection system site spacing based on predicted detection range in median level background noise.
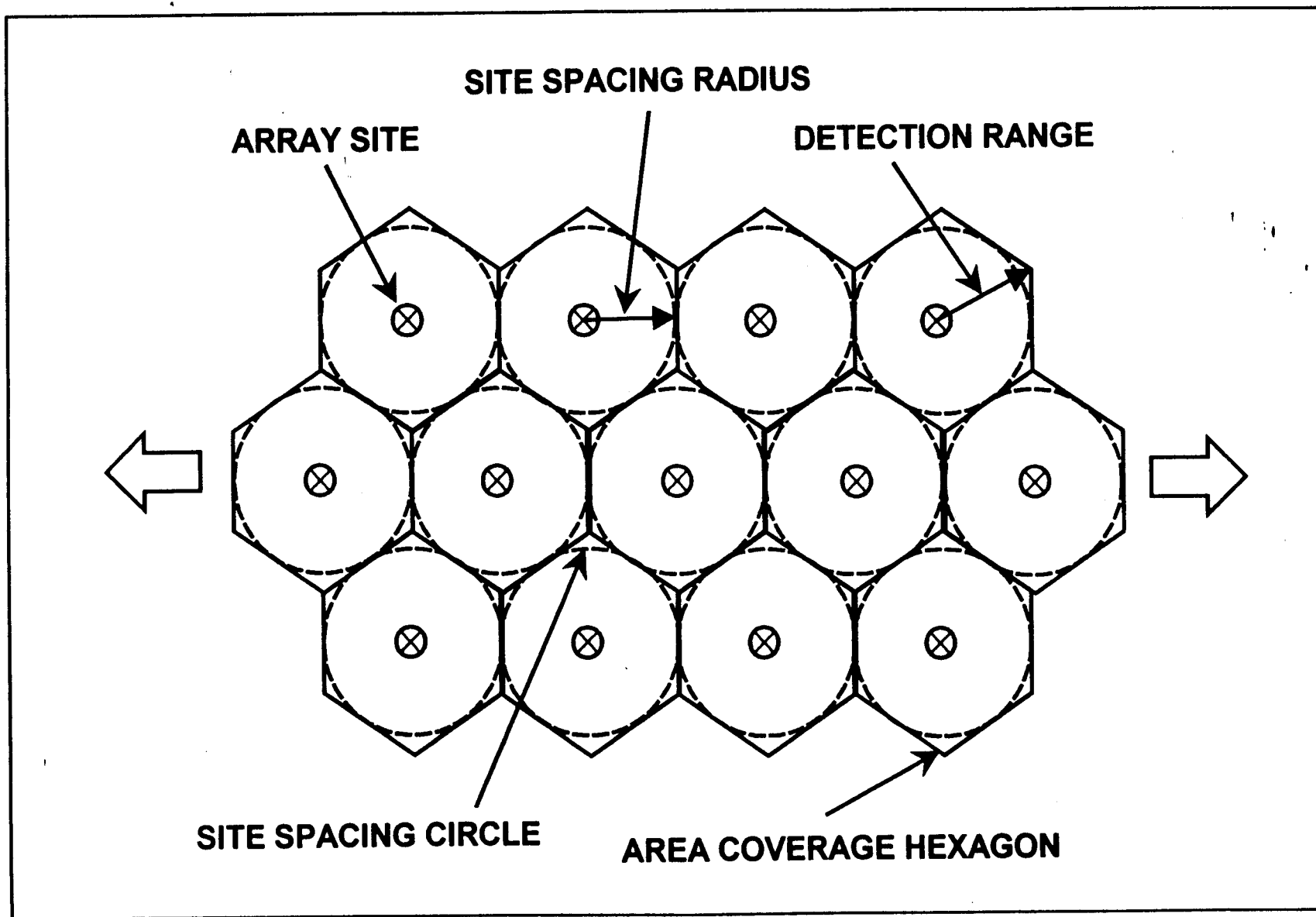
75

Figure 40   Illustration of a representative segment of closest packing deployment of sensor sites concept for acoustic detection full area coverage.

REPORT DOCUMENTATION PAGE

Public reporting burden for this collection of information is estimated to average 1 hour per response, including the time for reviewing instructions, searching existing data sources, gathering and maintaining the data needed, and completing and reviewing the collection of information. Send comments regarding this burden estimate or any other aspect of this collection of information, including suggestions for reducing this burden, to Washington Headquarters Services, Directorate for Information Operations and Reports, 1215 Jefferson Davis Highway, Suite 1204, Arlington, VA 22202-4302, and to the Office of Management and Budget, Paperwork Reduction Project (0704-0188), Washington, DC 20503.

1. AGENCY USE ONLY (Leave blank)	2. REPORT DATE December 1992	3. REPORT TYPE AND DATES COVERED Contractor Report	
4. TITLE AND SUBTITLE Aircraft IR/Acoustic Detection Evaluation - Volume 2 - Development of a Ground-Based Acoustic Sensor System for the Detection of Subsonic Jet-Powered Aircraft			**5. FUNDING NUMBERS** C NAS1-19060 WU 505-63-70-02
6. AUTHOR(S) Robert E. Kraft			

7. PERFORMING ORGANIZATION NAME(S) AND ADDRESS(ES)	8. PERFORMING ORGANIZATION REPORT NUMBER
McDonnell Douglas Corporation (Subcontractor) Douglas Aircraft Company General Electric 3855 Lakewood Boulevard Aircraft Engines Long Beach, CA 90846 Cincinnati, OH 45215	

9. SPONSORING/MONITORING AGENCY NAME(S) AND ADDRESS(ES)	10. SPONSORING/MONITORING AGENCY REPORT NUMBER
National Aeronautics and Space Administration Langley Research Center Hampton, VA 23681-0001	NASA CR-189705

11. SUPPLEMENTARY NOTES
Robert E. Kraft, General Electric Aircraft Engines, Cincinnati, OH 45215. This report was prepared by GEAE under Subcontract P.O. AS-25532-C to McDonnell Douglas Corporation. Langley Technical Monitor: David Chestnutt

12a. DISTRIBUTION/AVAILABILITY STATEMENT	12b. DISTRIBUTION CODE
▬▬▬▬▬▬▬▬▬ until December 31, 1994 Subject Category 71	

13. ABSTRACT (Maximum 200 words)

The design and performance of a ground-based acoustic sensor system for the detection of subsonic jet-powered aircraft is described and specified. The acoustic detection system performance criteria will subsequently be used to determine target detection ranges for the subject contract. Although the defined system has never been built and demonstrated in the field, the design parameters were chosen on the basis of achievable technology and overall system practicality. Areas where additional information is needed to substantiate the design are identified.

14. SUBJECT TERMS Military aircraft; Attack missions; Acoustic detection; Acoustic arrays; Detection systems; Acoustic propagation; Atmospheric acoustic environment			15. NUMBER OF PAGES 84
			16. PRICE CODE

17. SECURITY CLASSIFICATION OF REPORT Unclassified	18. SECURITY CLASSIFICATION OF THIS PAGE Unclassified	19. SECURITY CLASSIFICATION OF ABSTRACT Unclassified	20. LIMITATION OF ABSTRACT